

# Thesis\_GL\_draft.pdf

*by Sheharyar Ali*

---

**Submission date:** 24-Sep-2024 06:08PM (UTC+0200)

**Submission ID:** 2464180483

**File name:** Thesis\_GL\_draft.pdf (10.24M)

**Word count:** 31437

**Character count:** 149166

# Using VR Headsets for Helicopter Simulations

Analysing How Field-of-View In VR Headsets  
Affects Helicopter Pilot Performance

Sheharyar Ali



**TU**Delft

# Using VR Headsets for Helicopter Simulations

Analysing How Field-of-View In VR Headsets  
Affects Helicopter Pilot Performance

by

Sheharyar Ali

6  
Student Name    Student Number  
First Surname              1234567

Instructor: I. Surname  
Teaching Assistant: I. Surname  
Project Duration: Month, Year - Month, Year  
Faculty: Faculty of Aerospace Engineering, Delft

Cover: Canadarm 2 Robotic Arm Grapples SpaceX Dragon by NASA under CC BY-NC 2.0 (Modified)  
Style: TU Delft Report Style, with modifications by Daan Zwanenveld



# Preface

*A preface...*

*Sheharyar Ali  
Delft, September 2024*

## Summary

*A summary...*

# Contents

<b>Preface</b>	i
<b>Summary</b>	ii
<b>Nomenclature</b>	iv
<b>1 Introduction</b>	1
<b>2 Background</b>	3
2.1 Impact of Field of View (FoV) . . . . .	3
2.2 Experimental Methods . . . . .	10
2.3 Pilot Models . . . . .	11
2.4 Helicopter Model . . . . .	17
2.5 Conclusion . . . . .	19
<b>3 Visual model</b>	20
<b>4 Experiment Methodology</b>	28
4.1 Experiment Basics . . . . .	28
4.2 Model structure . . . . .	29
4.3 Forcing Function . . . . .	33
4.4 Experimental setup . . . . .	34
<b>5 Results and Discussion</b>	37
5.1 Subjective Results . . . . .	37
5.2 Objective Results . . . . .	37
5.3 Discussion . . . . .	39
5.4 Recommendations . . . . .	42
<b>6 Conclusion</b>	44
<b>References</b>	47
<b>A Alternate Visual Model</b>	50
A.1 Background . . . . .	50
A.2 Results . . . . .	54
A.2.1 Constant $\kappa$ . . . . .	54
A.2.2 Variable $\kappa$ . . . . .	57
A.3 Sensitivity Analysis . . . . .	61
A.4 Discussion . . . . .	63
<b>B Experiment Procedure</b>	65
B.1 General Procedure . . . . .	65
B.2 Terminating Experiment Due To Motion Sickness . . . . .	66
<b>C Experiment Matrix</b>	67
<b>D Human Research Ethics Committee Documents</b>	68
<b>E Analysing Effectiveness of VR Headsets to Jumpscare Participants</b>	72

# Nomenclature

If a nomenclature is required, a simple template can be found below for convenience. Feel free to use, adapt or completely remove.

## Abbreviations

Abbreviation	Definition
ISA	International Standard Atmosphere
...	

## Symbols

Symbol	Definition	Unit
V	Velocity	[m/s]
...		
$\rho$	Density	[kg/m <sup>3</sup> ]
...		

# 1

## Introduction

Flight simulators play a crucial role in providing a cheaper and safer alternative to real-world flight testing. Helicopter flight tests often involve pilots having to perform maneuvers in extreme conditions and often requiring the pilot to test the limits of the helicopter flight envelope [1]. This necessitates the use of very well trained pilots and top-of-the-line equipment and carries severe risks to pilot and equipment safety. Pilot-in-the-loop flight simulations offer a viable alternative to real-world flight testing by taking out the risk of pilot and equipment damage, while also being cheaper and being able to encompass a larger flight envelope [2]. They also reduce the environmental and noise impact of such testing, and can circumvent the logistics of setting up flight testing in a given airspace [1]. With a high enough fidelity, flight simulators can be used to certify helicopters and train pilots in such a way that the pilots can successfully transfer their training of flying a simulator into flying a real helicopter [3].

To achieve such goals however, requires the use of systems of a very high fidelity [1]. One example of such systems that hold incredible importance in a simulator, is the visual cueing system. Pilots rely extensively on the visual cues provided by the simulators to perform any basic maneuver, and the importance of providing high quality visual cues is imperative if extreme maneuvers need to be done in the simulator [4]. Traditionally, the visual cueing system of a flight simulator consists of a series of projectors projecting the out-of-window scene on a large screen. These methods, while effective, can often have limitations on aspects such as their Field of View, Resolution, Depth perception etc which can significantly lower the visual fidelity. These problems can be solved using higher quality equipment, but that adds extra costs and complexity to the whole mix [5]. A viable alternative to this, is the use of Virtual Reality (VR) headsets to replace the traditional projection systems. VR headsets allows a pilot to feel more immersed in the virtual world, and offers cheaper fixes to some of the aforementioned problems [1]. While VR technology has improved significantly in recent years, there is still very little research being done into using VR headsets as an alternative to current-gen projection systems [1].

The current research surrounding the use of VR headsets in the context of flight simulators has been squarely focused on understanding what effects it has on a pilot's ability to fly. This involves documenting the adverse effects of using VR headsets, such as motion sickness, and how to mitigate them, as well seeing how pilot performance changes overall [1][6]. While this does provide useful insights into positive and negative aspects of using VR headsets in this context, there is a clear gap in knowledge about why such performance changes can occur. As such, this study aims to understand and analyse how using VR headsets for visual cueing would affect pilot performance and why these changes are specifically happening. The goal is to create a visual model which can be used to explain why a pilot's perception is affected when aspects of the visual cues are changed in a VR headset, and use this to try and rationalise why the change in performance happens. To this end, the research objective for the thesis is: **How does using VR headsets to perform visual cueing affect the performance of Pilots flying a Helicopter Simulation.** To facilitate this objective, the focus was put on seeing what impact the Field of View has on pilot performance, when using VR headsets. The following research questions have been created to help achieve the research objective:

1. What manoeuvre is most impacted by changing Field of View (FoV)?

- 
2. What is the predicted pilot behaviour for the critical manoeuvre with changing FoV?
  3. ~~What~~<sup>51</sup> is the actual pilot behaviour for the critical manoeuvre with changing FoV?
  4. What is the overall effect of changing FoV on pilot performance?
  5. What strategies do pilots employ to overcome adverse effects of changing FoV?

# 2

## Background

This chapter details the literature study done to try and make a start on completing the research objective. Information about the impact of FoV on pilot behaviour, based on previous literature is shown in section 2.1. Information about the experimental methods used by other researchers is detailed in section 2.2, while information about the pilot models that can be created from said experimentation<sup>1</sup> methods is outlined in section 2.3. Information about creating a dynamic helicopter model is given in section 2.4 and finally, the main conclusions of this chapter are presented in section 2.5.

### 2.1. Impact of Field of View (FoV)

In any system where the goal is to create a simulation of a real-world vehicle, the importance of visual cues can not be understated. These cues can determine how realistic the simulation looks to the pilot and can determine how immersed they are in the scene. This means that visual cues play a big part in determining the fidelity of a simulator and this fidelity dictates how useful a simulator is for a given purpose [7]. Examples of important visual cues include:

- **Field of View (FoV):** This dictates how much of the scene the pilot can see at any given time [6] [8]
- **Resolution:** This dictates how clearly any object can be seen in the scene [6] [7]
- **Update rate:** This dictates the rate of change of the scene for any given movement within it [7].
- **Scene content:** This determines what there is to see in the scene and what forms of visual feedback the pilot can receive [7]

While all of these cues are important, the focus of this thesis is on the impact of the FoV only. The reason for this is because, in simulators that rely on projectors to project the view onto a fixed screen, the FoV is linked and restricted to the size of the screen and the settings used. This means that, if a pilot wishes to change the view envelope, they can only do so by translating or rotating the vehicle they are controlling. This essentially can lock pilots into the view envelope afforded to them by the limitations of the projection system and the FoV it can provide, i.e. they have a limited Field of Regard (FoR). The FoR is the total area that the pilot can see if the display system was able to move. In traditional flight simulators, this can only be done if high-resolution, expensive moving projectors are used and so, for most traditional simulators, their  $\text{FoV} = \text{FoR}$  [6]. In VR headsets however, this is not the case. Using VR headsets, a pilot can simply move their head around and the projected scenery will match. This means that a pilot can bypass the issues with having a restricted FoV by using VR headsets to perform the visual cueing in flight simulators. That is why the focus of this thesis is on evaluating how changes in FoV can impact pilot performance when using VR headsets, as this allows one to determine if the aforementioned benefit VR headsets have over traditional systems has any impact on how well a pilot does.

Previous research, done by Podzus et al, has already sought to investigate this to a certain extent. In this research, the focus was on trying to determine if the current technology for visual cueing used

in flight simulators is good enough to replace traditional compliance demonstration methods used to certify rotorcraft [6]. Traditional compliance demonstration procedures require large amounts of flight testing which can be dangerous and costly, especially for high risk manoeuvres. Thus, Podzus et al set about to find out if current-gen flight simulators are of a high enough fidelity to replace this flight testing, specifically for a category-A rejected take-off (CAT-A RTO). This maneuver involved the pilot taking-off as normal and then maintaining a pre-determined glideslope as they ascend backwards to a pre-determined Take-off Decision Point (TDP) height. Once this is achieved, the pilot must decide if they wish to reject take-off or continue take-off, based on whether or not an engine failure was triggered in the simulation. After the pilot has made a decision, they must then perform the required flight maneuver for that decision, as dictated by their training.

To test the cueing fidelity of modern simulators, this maneuver was carried out by trained pilots in two separate testing campaigns. The first campaign involved making use of the Air Vehicle Simulator (AVES) at the German Aerospace Center (DLR). For this campaign, the setup of AVES was altered to perform the test with four FoV conditions. The second campaign was carried out at the Helicopter Pilot Station (HPS) at the Royal Netherlands Aerospace Center (NLR) and involved the use of two VR headsets, instead of the standard projection methods. The two headsets were the Varjo XR-3 and the Pimax 8K-X. The FoVs tested for each campaign are outlined in Table 2.1

**Table 2.1:** Table showing the simulator settings used throughout the two campaigns [6]

Setting	Horizontal FoV [°]	Vertical FoV [°] (up/down)
AVES [DLR Campaign]	240	93 (+35 [°] / -58 [°])
Rotorcraft Certification by Simulation (RoCS) Sim [DLR Campaign]	220	78 (+20 [°] / -58 [°])
Full Flight Simulator Level D (FFS-D) [DLR Campaign]	180	60 (+24 [°] / -36 [°])
Full Flight Simulator Level C (FFS-C) [DLR Campaign]	150	40 (+13 [°] / -27 [°])
Varjo XR-3 [NLR Campaign]	88	65
Pimax 8K-X [NLR Campaign]	140	90

The RoCS Sim setting is the FoV used by the engineering simulator made by the RoCS project, while the FFS settings represent the minimum FoV needed to achieve the level D and level C certification for a flight simulator.

To analyse how pilots performed with the different testing conditions, the researchers made use of both objective and subjective rating techniques to measure performance. The subjective methods involved the pilots giving comments on how they feel like they did with the different FoVs, and what specific issues they encountered with each of the tested setups. The objective analysis was done by looking at the simulator data and evaluating it against certain criteria imposed on different parts of the flight. These are shown in Table 2.2:

	Desired	Adequate
Take-Off Rate Of Climb (ROC)	$350 \pm 50$ ft/min	$350 \pm 100$ ft/min
Take-Off Glide-slope (GS)	4-5 knots	3-6 knots
Touchdown Rate Of Descent (ROD)	<400 ft/min	<500 ft/min
Touchdown GS	<5 knots	<10 knots
Touchdown Point	On X (32x32 ft)	On concrete (43x43 ft)

**Table 2.2:** Table showing the performance tolerances used for the objective analysis [6]

The DLR test campaign provided some interesting results with regards to the FoV needed to adequately perform the tasks. The subjective results showed that significantly lowering the FoV did indeed hinder the participants. The pilots did find FoVs lower than 220 [°] to be objectionable as, according to their comments, lower FoVs did not allow pilots to accurately estimate their flight path. The pilots claim that, for the FFS Level D and Level C settings, they were not able to maintain sight of the helipad for their entire flight and thus, had to use their instruments to complete the maneuver. This made the

pilots feel uncomfortable and insecure while flying backwards. This is also somewhat echoed in the objective results where there were minor performance differences between the AVES, FFS Level D and RoCS Sim settings. However, for the FFS Level C setting, none of the pilots were able to meet the GS and ROC 'adequate' targets, as outlined in Table 2.2. The researchers compiled the objective and subjective results from the DLR test campaign and concluded that a minimum horizontal FoV of 190 $^{\circ}$  must be provided for the pilots to accurately perform the CAT-A RTO maneuver. This is because this FoV ensures that the pilots' peripheral vision is not obstructed and thus, the pilots are not distracted. For the NLR test campaign, the pilots preferred the VR projection systems over the standard ones. The pilots claimed that the larger view provided by the VR headsets allowed them to always maintain sight of the helipad. Additionally, the pilots preferred the Pimax headset over the Varjo since the Pimax offered a larger FoV in general. This is despite the fact that the boundaries of the FoV were blurry in the Pimax but regardless, having a larger FoV made the pilots feel more comfortable. In terms of objective results of the campaign, the performance data for the pilots across the different projection system could not really be compared against one another. This is due to the fact that the different projection systems were used with different parameter settings, tolerances and procedures, which were all iterated and refined for different pilots. This is why the researchers used the objective results of one pilot's performance to draw their conclusions. They claim that the performance across the projection systems was relatively similar for this pilot, with the exception of the pilot's GS during descent. The researchers observed that the pilot had a much shallower approach when they were using the Varjo headset, which they claim is due to the fact that the pilot struggled to see the forward movement and height ground cues. The researchers theorise that this could be a result of the limited FoV offered by the Varjo since the pilots' GS using all other projection systems was in the adequate region of the tolerances. Regardless, the researchers' main conclusion is the fact that the VR headsets are indeed a superior projection method compared to the standard one, and that, despite the Varjo having a higher resolution, the Pimax was the superior headset due to its higher FoV.

Another research project that wanted to see how changing FoV affects the fidelity of flight simulators, is that done by Atencio Jr. In this research, Atencio Jr sought to evaluate how NASA's Ames Vertical Simulator compared to the real world case of a UH-60 A helicopter in flight [9]. The research revolved around asking pilots to perform certain tasks in both an actual UH-60A helicopter and in the simulator and see how their performance compared for both. Due to logistical reasons, two different types of simulators were used for this project, which are referred here and in the original paper as the F-Cab and the N-Cab. The main difference, of relevance to this project, between the F-Cab and the N-Cab is the fact that the N-Cab has a higher horizontal FoV than the F-Cab. The Horizontal FoV of the N-Cab is 140 $^{\circ}$  as compared to the 120 $^{\circ}$  in the F-Cab. The Hammer plots, which show how the out-of-window view is distributed for each configuration, are shown in Figure 2.1 and Figure 2.2 respectively:

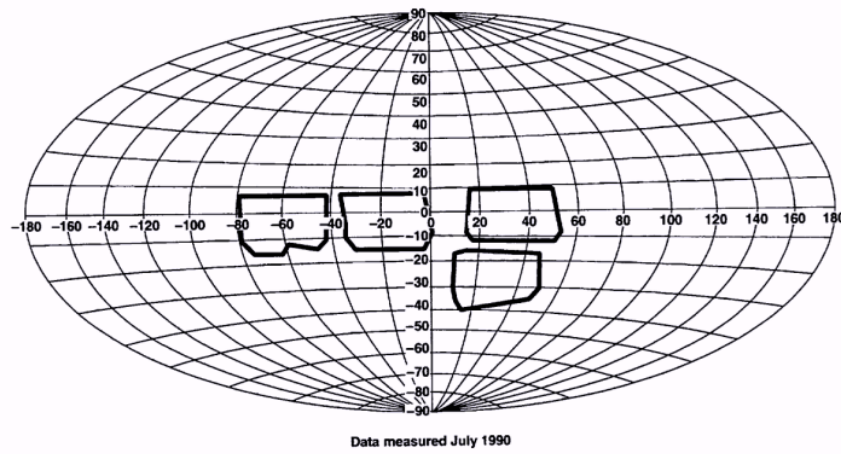


Figure 2.1: Figure showing the FoV provided by the N-Cab simulator [9]

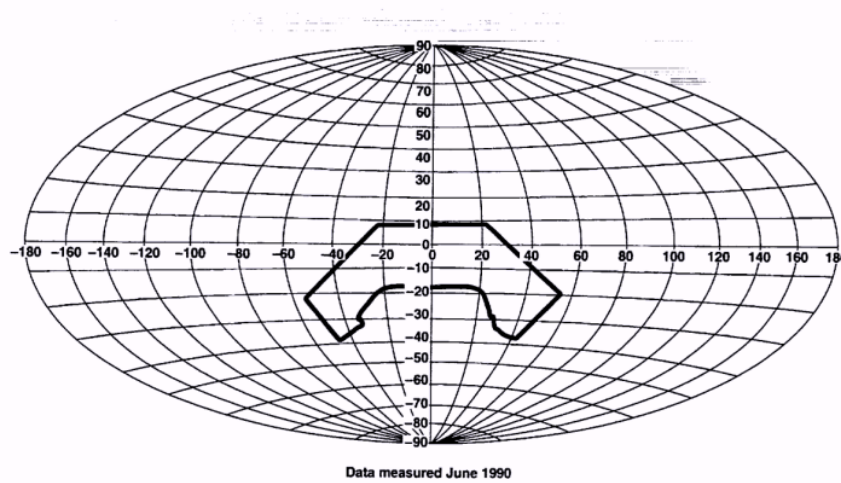
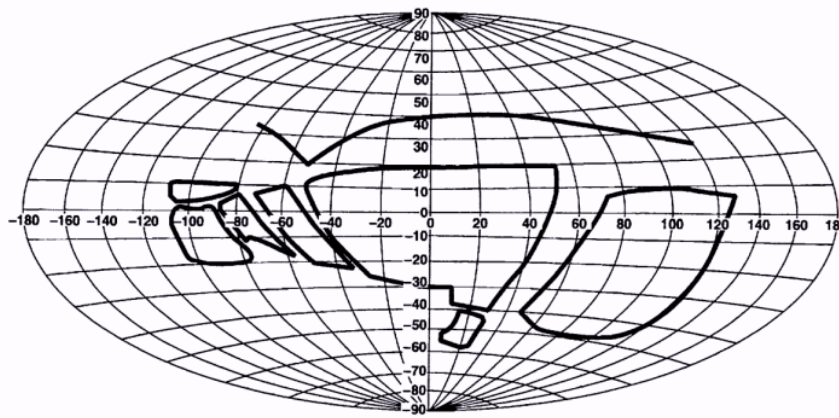


Figure 2.2: Figure showing the FoV provided by the F-Cab simulator [9]

If one compares this to the Hammer plot of the actual helicopter, pictured in Figure 2.3, it is clear that the simulators have a lower overall FoV than the actual helicopter.



19

Figure 2.3: Figure showing the FoV of the actual UH-60A helicopter [9]

Some of the main differences between the simulators and the actual helicopter are:

1. The actual helicopter has an approximately 10 [°] larger up-view and about 15-20 [°] larger down-view as compared to the F-Cab
2. The F-cab does not have the chin window, right-side window and left-side window that the actual helicopter does
3. There is a gap of approximately 15 [°] between the centre and right-windows of the N-Cab, which does not exist in the actual helicopter
4. The actual helicopter has an approximately 10 [°] larger up-view and about 15 [°] larger down-view as compared to the N-Cab
5. The N-Cab lacks the chin window, right-side window and the overhead window that the actual helicopter has.

Because of these deficiencies, one can analyse the pilot comments regarding their performance in both the actual helicopter and the simulators to see what effect a degraded FoV has. The pilots were asked to perform three different tasks in the simulators and the helicopter, which are detailed below:

1. **Bob-up Maneuver:** The pilot has to start from a hover and quickly "bob-up" 40 [ft] to the target, and then stabilise. After a 5 [s], the pilot has to descend back down to the original position and stabilise
2. **Side-Step Maneuver:** The pilot has to start from a hover and quickly translate 40 [ft] to the right <sup>81</sup> and stabilise. This is followed by translating back to the original position and stabilising.
3. **Dash/Clock-Stop Maneuver:** The pilot starts from a hover and quickly accelerates to 60 [kts]. This is followed by a rapid deceleration back to a hover.

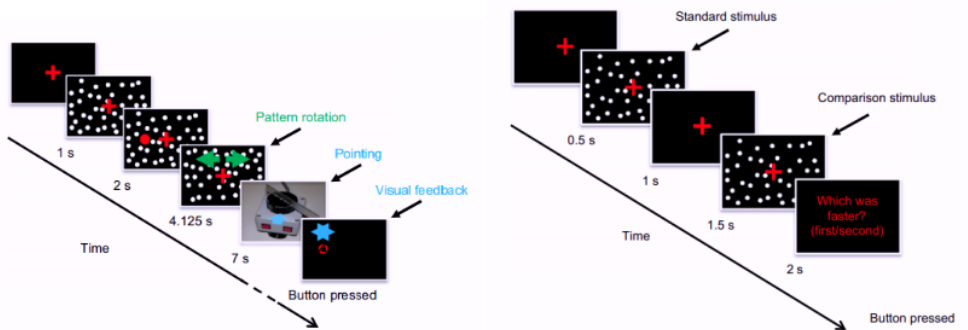
The restricted FoVs of the simulators meant that the pilots encountered much difficulty during their runs. For the first task, the pilots had trouble seeing or anticipating the lower hover targets when they were at the top target. This meant that they often overshot the targets and/or had to make more abrupt movements to try and stop. This often affected their ability to stabilise at the end of the maneuver. This problem was also encountered for the side-step maneuver where pilots could not effectively see their stopping points. For the third task, the pilots could not see the references for spatial position when they pitched up or down due to the restrictive FoVs. This meant that they had to use the radar altimeter to find out what their height was, instead of using out-of-window visual cues, and only used the visual

cues to confirm if the maneuver had been completed successfully. This converted the task from a visual-reference task, as it would be in real-life, to an instrument-monitoring task. This is similar to the conclusions reached by Podzus et al whereby it was apparent that pilots had to rely heavily on their instruments. In both cases, the pilots had to go against their instincts to use out-of-window visual cues which raised their overall workload and lowered performance.

Similar work was done by Chung et al, whereby their goal was to evaluate the effect of three visual parameters of simulators, namely the FoV, Colimation and Resolution [7]. The experiment setup made use of the R-Cab and N-Cab simulator setups mentioned previously. To see the effect of FoV, the researchers used a wide and a narrow FoV to test the participants. To create equivalent FoVs in each Cab, and to change the FoV from a wide to a narrow one, they made use of masks to block off certain windows in the Cabs. The experiment involved participants controlling a four degree-of-freedom simulation of a UH-60A helicopter and trying to keep their longitudinal and lateral position constant, in the face of a disturbance. Data was then collected on their position error. The results showed that the wider FoV resulted in better velocity control and thus, smaller position errors. The researchers link this to the idea that the improved velocity control performance provided by the wider FoV increases damping in the closed loop system. They theorise, that this is a result of the improved peripheral vision one gets from a wider FoV. Additionally, when the pilots were asked which FoV they preferred, the pilots chose the wider FoV as their perception of roll attitude control and longitudinal velocity control was much better.

The idea that roll control may be affected by the FoV was also tested in the research done by Kenyon et al [10]. They did a variety of experiments [79] the most relevant experiment to this project is the critical tracking experiment, where the objective was to keep the visual scene at a roll angle of 0 [ $^{\circ}$ ]. This had to be done for FoVs of 10 [ $^{\circ}$ ], 20 [ $^{\circ}$ ], 40 [ $^{\circ}$ ], 80 [ $^{\circ}$ ] and 120 [ $^{\circ}$ ]. The researchers measured the effective time delay of all the participants and used that as a metric to draw up their conclusions. The researchers found that the decrease in effective time delay was exponential as FoV was increased, with most participants reaching their minimum value with an FoV of 20 [ $^{\circ}$ ], and the rest reaching it with an FoV of 40 [ $^{\circ}$ ]. They theorise that an FoV of 40 [ $^{\circ}$ ] already contains enough of a "peripheral view" to do the experiment effectively. For a roll tracking task, they theorise that most of the work is done by the participants' central view and the peripheral view only enhances the performance slightly. Regardless, they also suggest that an FoV of something as small as 10 [ $^{\circ}$ ] is wholly insufficient to do such a task, as some peripheral vision is still needed. These results can be useful in coming up with FoVs that can be tested in the experiment phase of this project.

The last two research projects are a departure from the analysis of FoV for the use of simulators, but nonetheless they provide key insights into what happens when FoV changes. These concern research projects done by Pretto et al and Duh et al. The goal of the research by Pretto et al is to see how changing FoV affects (i) perceived amplitude of rotations about the body vertical axis, and (ii) the perceived speed of forward translations. To test the first condition, the experiment conducted by the researcher was as follows. Participants were seated in front of a large panoramic screen and were shown a cross right in the front of the screen. They were instructed to keep their eye on the cross at all times. They were then shown a pattern of white dots scattered around the screen and a target circle, located 5 [ $^{\circ}$ ] left of the cross. When the experiment starts, the red dot disappears and the white dots rotate with a given amplitude, depending on the testing condition, and the participants job is to determine how far they think the red dot has moved, depending on the flow presented by the white dots. This is repeated for a multitude of different rotation speeds and three different FoVs; namely 30 [ $^{\circ}$ ], 60 [ $^{\circ}$ ] and 230 [ $^{\circ}$ ]. The second experiment involved a random scattering of white dots on the same screen setup. These dots provided two stimuli; the first one was the standard stimulus which moved the dots towards the participants at a speed of 5 [m/s], and the second stimulus moved the dots towards the participants at a speed that varied with the experimental condition tested. The participants had to tell the researchers which stimulus was the faster one. A visual representation of the two experiments is presented in Figure 2.4



(a) Figure showing the procedure for the first FoV experiment done by Pretto et al [11]

[19]

by Pretto et al [11]

**Figure 2.4:** Figure showing the procedure for the two FoV experiments done by Pretto et al [11]

This experiment was done with two types of FoV conditions. The first one was a central FoV condition where the peripheral parts of the screen were occluded and no dots were shown there. The second was the peripheral FoV condition whereby the central part of the screen is occluded and dots were only shown in the peripheries. The difference between the conditions can be seen in Figure 2.5

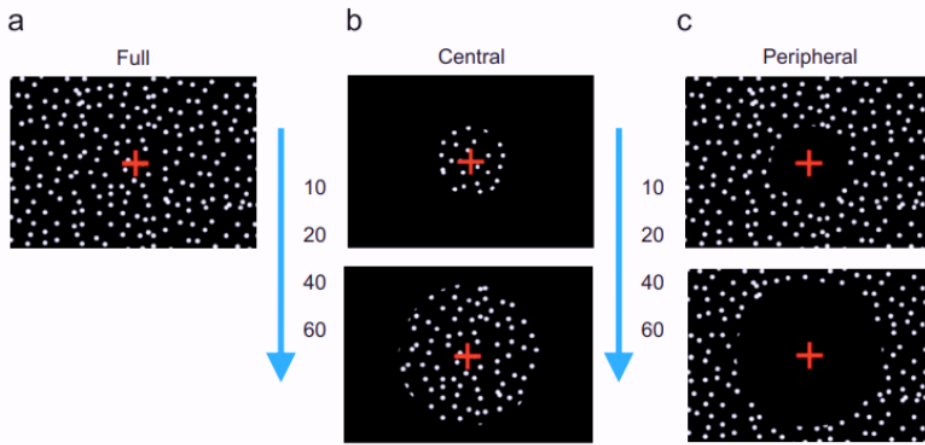


**Figure 2.5:** Figure showing the (a) Full FoV Condition, (b) the Central FoV condition, with FoV changing from 10 [°] (top) to 60 [°] (bottom) and (c) the Peripheral FoV condition, with FoV changing from 10 [°] (top) to 60 [°] (bottom) [11]

33

The results of the first experiment led the researchers to the conclusion that increasing the FoV beyond 30 [°] does not impact the average performance of the participants. However, it does decrease the variance of the results slightly. The results of the second experiment seem to show that, for central FoVs smaller than 60 [°], the participants underestimate the visual speed. If the participants were only using their peripheral vision, the participants tended to overestimate the visual speed.

The goal of the research, by Duh et al, was to investigate the relationship between FoV and scene content on the postural stability of participants [12]. The study revolves around the fact that the more immersed a participant is in the scene, the easier it is to inducevection. Vection is when a person believes that they are moving, even though they are not. Hoh et al sought to investigate if changing the FoV and the scene content of a simulation where the participant is shown to be rotating, can affect a participant's postural stability. To this end, the participants were shown two separate scenes, one a city scene and one a simple radial pattern, and the scenes were changed such that the participant felt

like they were rotating around in the scene. The participant's job was to try and maintain their stance throughout the simulation and data was collected on how long it took for the participants' stance to break and how hard the participants found it maintain their stance. The working theory here is that the more immersed a participant is in the scene, the more likely they are to experiencevection, which would cause them to lose their balance. The scenes were presented at six different FoVs and it was found that the participants showed more dispersion and found it harder to keep balance as FoV increased. The researchers concluded that by receiving more information in their peripheral vision, the participants had greater self-motion perception.

Based on all this research, some key conclusions can be reached about the impact of FoV on pilot control. Due to a lack of motion cues received in the peripheral region of the retina (caused by a narrow FoV), the pilot feels less immersed and tends to underestimate their own speed [11] [12]. It is also worth noting that if motion is solely perceived using one's peripheral vision, i.e. they only have their peripheral vision and nothing else, then they generally tend to significantly overestimate their speed [11]. Conversely, if the FoV is smaller than 60°, the pilot will underestimate their speed [11]. If pilots incorrectly estimate their velocities in such tasks, their damping in the closed loop system is lowered and their positional control becomes worse [7]. Additionally, while the crossover frequency of the pilot does not change due to a reduced FoV, their effective time delay increases and their phase margin decreases [10]. Degraded out-of-window visual cues can cause a lot of problems in a scenario where a pilot needs to accurately and precisely judge their position and velocity. The maneuver that would be most impacted by degradation of out-of-window cues would be a near-ground hover since pilots use the surroundings to provide them with cues pertaining to their velocity and position. Therefore, it is wise to assess the impact of FoV on pilot behaviour in the case of a pilot performing some sort of maneuver close to the ground, while hovering.

While the research done does a good job in pointing out what happens when FoV degrades, there is a significant gap in knowledge about why this ends up happening. The general consensus is that a lack of activity in the peripheral region of a pilot's vision leads to worse performance, but nothing has as-of-yet sought to explain why that is. The key piece missing, which this thesis aims to provide, is what information is being lost in the peripheral vision of a pilot as their FoV degrades, and how that can be modelled and used to predict pilot performance. Having reached a good understanding of the theory to test and develop, three key things are still missing. These are, namely, knowledge on how to set up and carry out an experiment to test any hypotheses developed, knowledge on how to create a working simulation of a helicopter to do the experiments in and, knowledge on how the outputs of the experiments can be analysed and linked to a pilot model. These aspects are discussed in full, in the proceeding sections

## 2.2. Experimental Methods

As one would expect, the methods used in the experimentation stage of the research depended heavily on what the goal of the research was. For research that was focused on evaluating impacts of visual cues in a realistic setting, the emphasis was on having an experiment setup of the highest possible fidelity. This means that the experiment would be done in either an actual helicopter, as was the case in research done by Baron et al [8] and Hoh et al [13], or by having a highly detailed simulation, as was the case in research done by Podzus et al [6], [2], H.M. Baker [14], L. Iseler [15] and Erazo et al [16]. For the simulations, the fidelity of the different aspects of the simulation varied depending on what the overall goal of the research is. For research projects which revolve around testing the fidelity of the simulators, as compared to the real-world case, particular attention is paid to ensure that the experience of the simulation is almost identical to a real world scenario. This involves factors such as:

- Using a highly detailed (six or four degrees-of-freedom) helicopter model to simulate the dynamics [6] [8]
- Ensuring that the layout of the various instruments and Heads-Up Display (HUD) elements resemble those of an actual helicopter [14]
- Using highly trained participants such as trained helicopter or aircraft pilots [6][8][14]
- Testing participants in tasks that they would perform in their normal routine in a real-life helicopter (such as a CAT-A RTO). [6]

Most experiments relevant to this topic, focus solely on the impact of specific visual cues on the pilot, instead of comparing the visual cues of simulators with a real-world example. Such research will often involve either augmenting or degrading visual cues and evaluating how pilot performance changes [10] [11] [17] [18] [19]. The experiment tasks that the participants have <sup>145</sup> perform are limited to simple disturbance rejection tasks or velocity (or position) tracking tasks. A disturbance rejection task involves the pilot trying to negate a perturbing forcing function, such that they keep velocity, or position constant. The tracking tasks involve the participants trying to match their velocity or position with that of a particular target signal. The researchers will then make use of the time traces of the participants' output signals to see how their performance changes over time. This performance can then be compared against the different testing conditions, such that the researchers can get a basic understanding of how the participants were affected by the testing conditions. How this data is analysed, or indeed what type of data is even collected, depends heavily on the type of pilot model the researchers want to create. This is elaborated upon in section 2.3.

### 2.3. Pilot Models

One of the most widely used pilot models for such investigations is the Crossover Model created by McRuer and Krendel [20]. This model suggests that human pilots follow a set of adjustment rules for compensatory tracking tasks. Such tracking tasks involve pilots trying to minimize the error between a controlled element and a reference signal. The feedback loop for such a task is shown in Figure 2.6:

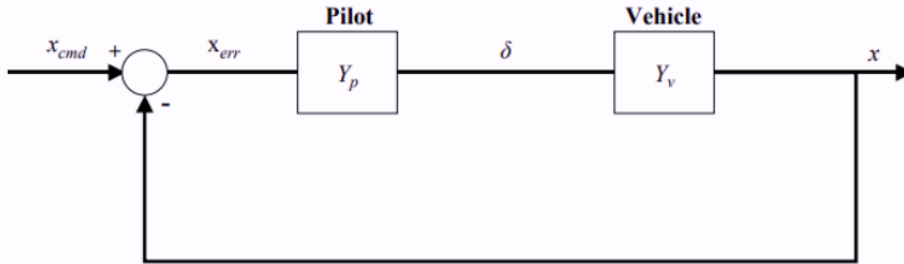


Figure 2.6: Figure showing the feedback loop for a simple compensatory tracking task [18]

The Crossover Model states that a pilot will change their dynamics,  $Y_p$ , such that the open loop dynamics,  $Y_p Y_c$ , resemble Equation 2.1:

$$Y_p Y_c = \frac{\omega_c e^{-\tau s}}{s} \quad (2.1)$$

where  $\omega_c$  is the crossover frequency and  $\tau$  is the pilot delay. The crossover frequency represents the transition frequency beyond which, the pilot is unable to effectively perform closed loop tracking and the system acts as open loop. The pilot delay is there to represent delays caused by pilot perception, interpretation and neuromuscular actuation. To achieve the open loop dynamics of Equation 2.1, the pilot dynamics,  $Y_p$  will take the form of:

$$Y_p(s) = K_p \frac{(1 + T_L s)}{(1 + T_I s)} e^{-\tau s} \quad (2.2)$$

where  $K_p$  is the pilot gain,  $T_L$  is the lead constant and  $T_I$  is the lag constant. The lag and lead constants are thus chosen to provide the open loop dynamics depending on the dynamics of the controlled elements. The goal would then be to calculate these pilot parameters for the different testing conditions in an experiment to see how pilot behaviour and dynamics change.

While this model is widely used, it does have a very simplistic representation of the pilot's dynamics [21]. Thus, one can supplement the Crossover model with more realistic representation of pilots' sen-

sory and neuromuscular aspects, as is done in the Cybernetic model [22][23]. A visual representation of this model is given in Figure 2.7:

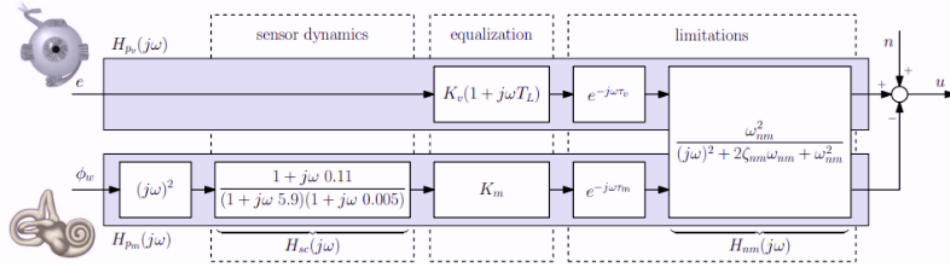
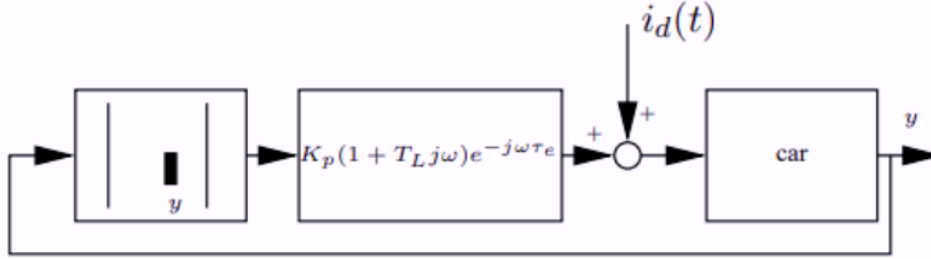


Figure 2.7: Figure showing the multi-modal cybernetic pilot model [22]

116

As can be seen in Figure 2.7, the pilot model is now split into two distinct modes; the visual (top) and the vestibular (bottom) mode. For both modes, the entire model is split into sensor dynamics, equalisation terms and pilot limitations. The limitations part now contains the delays associated with both modes of perception as well as the term for neuromuscular limitations, given by  $H_{nm}$  in Figure 2.7. For the visual model, the sensor dynamics are usually modeled as a Unity gain [23]. The equalisation term in the visual mode in Figure 2.7 does not contain a lag term because the controlled dynamics in the cited experiment only had a lead term [22]. It is also worth noting that in this model, the equalisation for the lag and/or lead in the controlled dynamics is done solely via the visual mode and thus, the vestibular equalisation only contains a gain term. The sensor dynamics for the vestibular mode,  $H_{sc}$  correspond to the dynamics of the semicircular canals found in human ears which are used for velocity perception [22] [23]. The main free parameters for this model are the equalization parameters (visual gain  $K_v$ , visual lead constant  $T_L$ , visual lag constant  $T_I$  and the motion gain  $K_m$ ) and the visual and motion reaction delays  $\tau_v$  and  $\tau_m$ , respectively. [22]. The free parameters can be calculated using various parameter estimation techniques, such as Fourier transforms, and the parameters obtained are in the frequency domain. Frequency domain parameter estimation models have the issue that they are a two-step process; the first step involves obtaining a non-parametric pilot describing functions in the frequency domain and the second step involves optimising the parameters. This is an issue because there are biases involved in both steps and they compound to have a major effect on the final result [24]. To alleviate this, one may need to use more complex techniques, like a Maximum Likelihood Estimator (MLE), which may make the final analysis of the result much harder. Another issue stems from the fact that a human controllers' remnant means that all signals in the loop are stochastic, and power in all frequencies. Therefore, the forcing function has to be designed such that it has a signal-to-noise ratio over certain frequencies that the researcher wants to test. The problem however, is that the Crossover model is only applicable over a certain range of frequencies, called the crossover region, so the forcing function can not be made up of frequencies beyond this region. Additionally, if one wishes to use the multi-modal cybernetic model, multiple forcing functions are needed such that one can quantify the participants' responses to the visual and motion cue separately [23]. That means that the forcing functions and the cues have to be significantly different from one another.

One of the biggest challenges with the model however, is ensuring that the cues a participant receives, match up with the model design. As an example, take a situation where a human has to control the lateral position of a car on a straight road and one wishes to fit the model shown in Figure 2.8 to the human:



180

Figure 2.8: Figure showing an example model for a human controlling the lateral position of a car [25]

73

He<sub>129</sub> the human gets the lateral position of the car as the only feedback (i.e. the first block<sub>193</sub>) and then, based on the dynamics of the car (i.e. the third block), applies the proper equalisation (i.e. the second block). However, if the human is able to see the heading of the car, as they would in a realistic environment, then the control becomes a closure of two loops. This means that the model<sub>191</sub> of Figure 2.8 is no longer applicable to the situation and instead, one has to use the model shown in Figure 2.9.

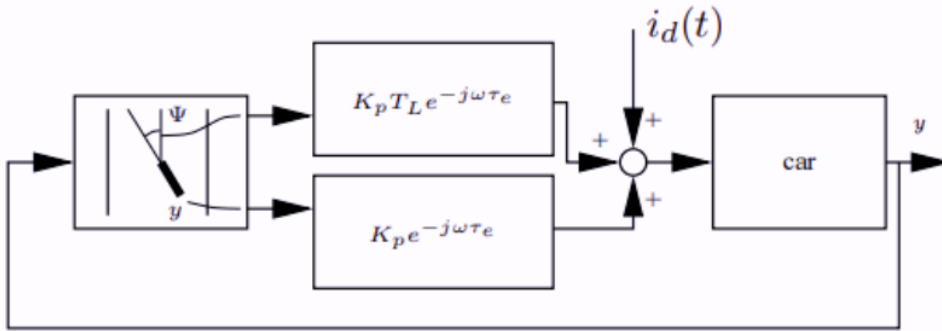


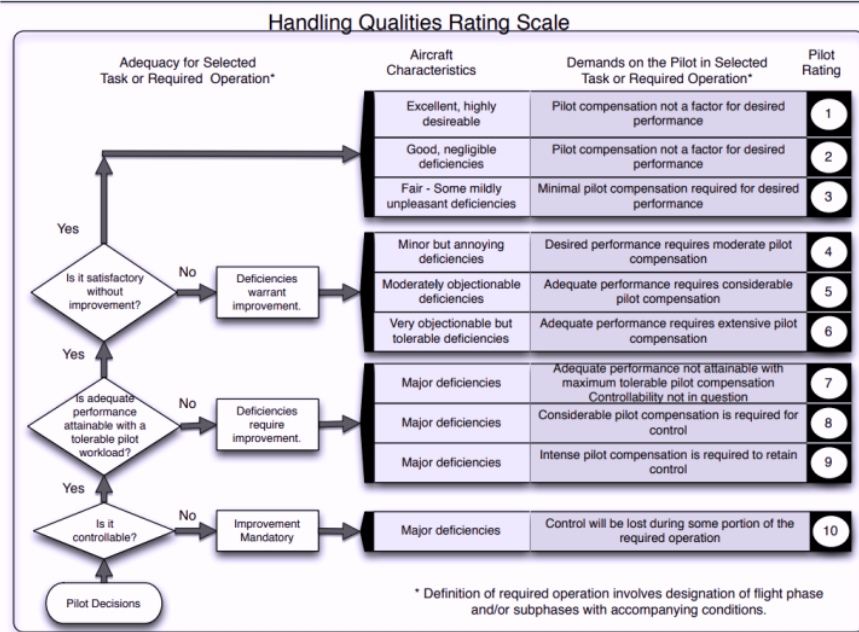
Figure 2.9: Figure showing the model that would be applicable for a human controlling the lateral position of a car with the heading angle and lateral position as feedback [25]

This highlights the inherent issue with trying to apply a cybernetic model to a realistic simulation; the fact that the researcher has to meticulously design the simulation such that the pilot only receives cues that the researcher wants them to. This can become difficult in highly detailed simulations since a pilot can just pick any emergent or invariant feature in the view and use that as a basis for their control inputs. This can result in the applicable cybernetic model, for this particular participant, having multiple loops and feedback channels that the researcher did not anticipate [25]. This is why, while this is a widely popular method of creating a pilot model in Human Machine Systems, the experiment design and analysis techniques required to create it can often be too complicated for what the research requires.

That is why a simpler technique often involves using the output data of the experiment directly and doing some kind of statistical test on it to determine how the pilot performance changes with respect to the experiment design. An example of this can be seen in the performance metrics used by Baron et al and by Podzus et al, which are shown in Table 2.2 [6] [8]. In these examples, the output data from the experiments is simply compared against each other rather than being used to build up a complex pilot model. This can often be supplemented by techniques like the Analysis of Variance (ANOVA)

test which aims to see if there was any significant trend emerging in the data for the different testing conditions [24].

One disadvantage of such methods, as compared to the Cybernetic model, is the fact that it does not give much insight into why the pilot behaviour changes; these methods merely point out how the performance changes. One method to remedy this is by using subjective methods to see how the pilots believe the conditions have changed and how they adapted to them. Three of the most widely used subjective assessment techniques are the Cooper-Harper Handling Qualities Rating Scale (HQR), the Bedford Rating Scale and the Visual Cue Rating (VCR) scale. The HQR is shown in Figure 2.10:



<sup>24</sup>  
**Figure 2.10:** Figure showing the Cooper-Harper Handling Qualities Rating Scale [26]

The main use-case for this scale is when one needs to evaluate the additional effort a pilot needs to make (above the nominal task workload) to achieve a given level of performance, in the face of some sort of control augmentation [19] [26]. This scale is widely used in research in which the participants are trained pilots, since they can easily judge if the workload they are experiencing is something they would normally experience, or if it is due to the experimental condition being tested [7] [9]. The Bedford Rating scale, shown in Figure 2.11, has the same working principle as the HQR.

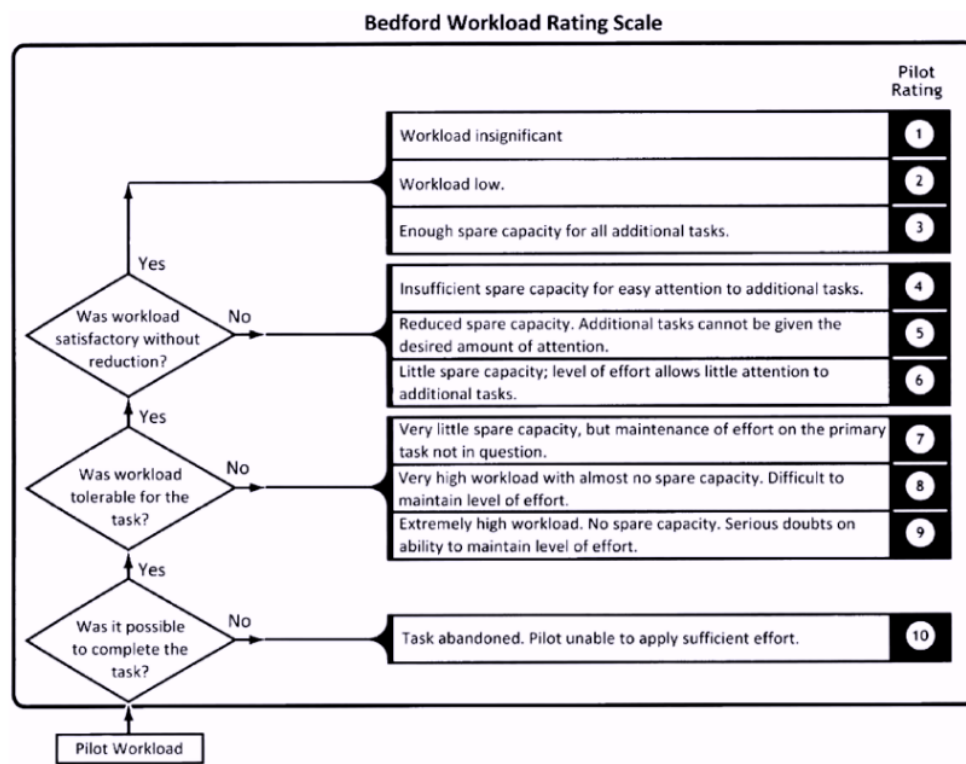


Figure 2.11: Figure showing the Bedford rating scale [27]

The final subjective assessment method worth discussing is the Visual Cue Rating Scale (VCR). Using a VCR scale involves the pilot giving a score of 1-5 based on how precise and aggressive they could be when controlling attitude and translational rates of a vehicle. The scale itself can be seen in Figure 2.12

VISUAL CUE RATING'S (VCR's)	
PILOT RATES	
<b>Ability to be:</b> <ul style="list-style-type: none"> <li>- Precise</li> <li>- Aggressive</li> </ul> <b>In controlling:</b> <ul style="list-style-type: none"> <li>- Attitude</li> <li>- Horizontal translational rate</li> <li>- Vertical translational rate</li> </ul>	<b>1 - GOOD</b> → can make aggressive and precise corrections with confidence and precision is good <b>2</b> → <b>3 - FAIR</b> → can make limited corrections with confidence and precision is only fair <b>4</b> → <b>5 - POOR</b> → only small and gentle corrections possible and consistent precision is not attainable

Figure 2.12: Figure showing the VCR scale [6]

In the research done by Podzus et al, the participants gave VCR scores for the translational rate and attitude, and this was then plotted together to give an intuitive visualisation of visual fidelity. The

combined average VCRs for all the conditions tested in this research (shown in Table 2.1) are shown in Figure 2.13

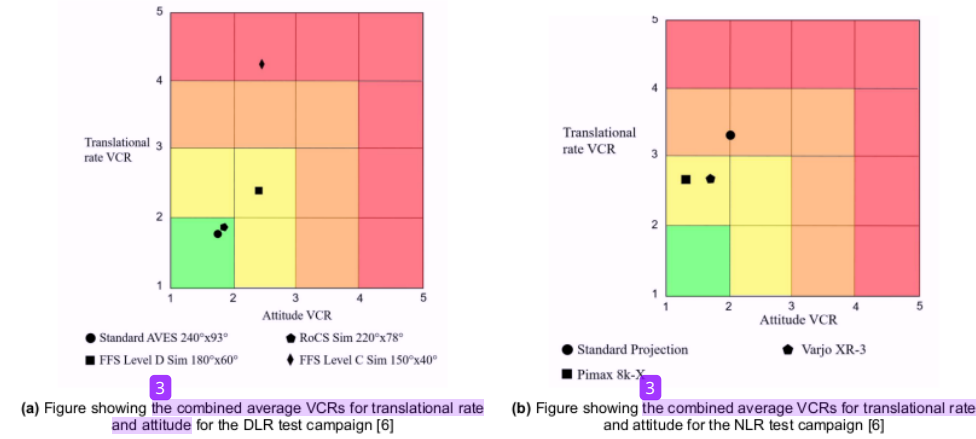


Figure 2.13: Figure showing the combined average VCRs for the different testing conditions in research done by Podzus et al [6]

As can be seen from the figures above, the combined VCR scale provides an intuitive way of comparing the different conditions against each other. However, this also highlights the issues with using such subjective rating scales; the training required to do so. Indeed, the reason why studies that choose to use such scales use trained pilots as test subjects is because those pilots have been trained in the nuances of using such subjective methods. As an example, take Pilot Rating 5 and 6 on the HQR in Figure 2.10. An average person would not be able to figure out the difference between a system that has "moderately objectionable differences" and one that has "very objectionable but tolerable differences". This knowledge comes with training and experience that only pilots will likely have. Therefore, if the researcher expects to not have access to a lot of trained pilots for their experiments, as is the case for this thesis project, then the use of such scales can make the subjective results unreliable and inaccurate. In such a case, the researcher is better off asking more general and open-ended questions to gather subjective results. This means that one should not hope to use these subjective comments to objective scores (like the Pilot Ratings).

The main conclusion that can be drawn for this part is the fact that the pilot model one uses depends heavily on what type of experimentation will be carried out. Detailed and complex models, like the Cybernetic model, can offer a lot of objective insight into how pilot performance and behaviour change, but require complex analysis techniques and precise experiment design. Additionally, if the structure of the model contains multiple control loops, then the analysis becomes more complicated in order to decouple the results of the multiple loops. This, of course, means that the experiment design and the experiment outputs must also be designed in such a way that enough information is available to decouple the results for the control loops. Simple models which compare variances in the objective pilot performance can easily quantify and explain the change in pilot performance, but struggle to explain why the changes in pilot behaviour occur. These can be supplemented with subjective ratings, like the HQR or the Bedford Scale, but those have their own disadvantages. The biggest disadvantage is the fact that they require a lot of training for participants to efficiently use as an untrained participant will not know how to effectively discern the subtleties between the different ratings. Ultimately, what this research shows, is that one needs to ensure that they have a good understanding of what type of participants will do the experiment, and what the experiment will look like, before they choose to apply a pilot model to the results. The time-frame of this thesis means that it is not reasonable to expect that enough trained pilots will be available to do the experiments. This means that the use of the complex subjective rating scales is unlikely. Additionally, the results of the visual model developed will dictate what the experiment will need to look like. This will then influence what type of pilot model can be created.

## 2.4. Helicopter Model

The fidelity of the helicopter dynamics model depends heavily on the research being done. As an example, for the research done by Bachelder, the goal was to investigate how Night-Vision Devices (NVD) can be used to give the pilot of a rotor-craft some synthetic cues, and how their perception is affected [18]. This means that, for the purposes of the research, the helicopter model used in the experiments did not need to have a very fidelity since the focus was on more of cueing of the NVD and on pilot behaviour. This is why, Bachelder used a simple model, shown in Figure 2.14:

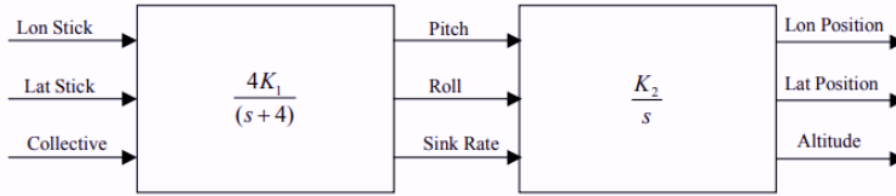


Figure 2.14: Figure showing the helicopter dynamics model for [18]

As can be seen from Figure 2.14, the dynamics consist of a simple integrator with lag to go from the control input [29] the attitude angles and a simple integrator to go from the attitude to position. Generally, however, the dynamics model used is derived from a six degrees-of-freedom model, whose state space representation is outlined as such [14] [17] [28]:

$$\dot{\mathbf{x}}(t) = A\mathbf{x}(t) + B\mathbf{u}(t) \quad (2.3)$$

where

$$\begin{aligned} \mathbf{x} &= \{u, v, w, p, q, r, \theta, \phi, \psi\} \\ \mathbf{u} &= \{\theta_0, \theta_{1s}, \theta_{1c}, \theta_{0T}\} \end{aligned} \quad (2.4)$$

The components of the state vector,  $\mathbf{x}(t)$  in Equation 2.4 are [28]:

- $u$ : Horizontal velocity component in the body-fixed x-direction (m/s).
- $v$ : Horizontal velocity component in the body-fixed y-direction (m/s).
- $w$ : Vertical velocity component in the body-fixed z-direction (m/s).
- $p$ : Angular velocity around the body-fixed x-axis (rad/s).
- $q$ : Angular velocity around the body-fixed y-axis (rad/s).
- $r$ : Angular velocity around the body-fixed z-axis (rad/s).
- $\theta$ : Pitch angle (rad).
- $\phi$ : Roll angle (rad).
- $\psi$ : Yaw angle (rad).

and the components of the input vector,  $\mathbf{u}(t)$  are [28]:

- $\theta_0$ : Collective pitch angle (rad).
- $\theta_{1s}$ : Swashplate servo pitch angle (rad).
- $\theta_{1c}$ : Swashplate servo roll angle (rad).
- $\theta_{0T}$ : Tail rotor collective pitch angle (rad).

For the system given by Equation 2.3 and Equation 2.4, the A and B matrices for the linearised system are given by:

$$\mathbf{A} = \begin{bmatrix} X_u & X_w - Q_e & X_q - W_e & -g \cos \Theta_e & X_v + R_e & X_p & -g \sin \Phi_e \cos \Theta_e & X_r + V_e \\ Z_u + Q_e & Z_w & Z_q + U_e & -g \cos \Phi_e \sin \Theta_e & Z_v - P_e & Z_p - V_e & 0 & Z_r \\ M_u & M_w & M_q & 0 & M_v & M_p - 2P_e I_{xz} I_{yy} & -\Omega_a \cos \Theta_e & M_r + 2R_e I_{xz} I_{yy} \\ 0 & 0 & 0 & 0 & 0 & 0 & 0 & -P_e (I_{23} I_{zz}) I_{yy} \\ Y_u - R_e & Y_w + P_e & \cos \Phi_e & -g \sin \Phi_e \sin \Theta_e & Y_v & Y_p + W_e & -g \cos \Phi_e \cos \Theta_e & Y_r + U_e \\ L'_u & L'_w & L'_q + k_1 P_e - k_2 R_e & 0 & L'_v & L'_p + k_1 Q_e & 0 & L'_r + k_2 Q_e \\ 0 & 0 & \sin \Phi_e \tan \Theta_e & \Omega_a \sec \Theta_e & 0 & 1 & 0 & N'_r + k_3 Q_e \\ N'_u & N'_w & N'_q - k_1 R_e - k_3 P_e & 0 & N'_v & N'_p + k_3 Q_e & 0 & N'_r + k_1 Q_e \end{bmatrix} \quad (2.5)$$

$$\mathbf{B} = \begin{bmatrix} X_{\theta_0} & X_{\theta_{1s}} & X_{\theta_{1c}} & X_{\theta_{0T}} \\ Z_{\theta_0} & Z_{\theta_{1s}} & Z_{\theta_{1c}} & Z_{\theta_{0T}} \\ M_{\theta_0} & M_{\theta_{1s}} & M_{\theta_{1c}} & M_{\theta_{0T}} \\ 0 & 0 & 0 & 0 \\ Y_{\theta_0} & Y_{\theta_{1s}} & Y_{\theta_{1c}} & Y_{\theta_{0T}} \\ L'_{\theta_0} & L'_{\theta_{1s}} & L'_{\theta_{1c}} & L'_{\theta_{0T}} \\ 0 & 0 & 0 & 0 \\ N'_{\theta_0} & N'_{\theta_{1s}} & N'_{\theta_{1c}} & N'_{\theta_{0T}} \end{bmatrix} \quad (2.6)$$

where terms like  $X_u$  and  $X_{\theta_0}$  are the various stability derivatives,  $U_e$ ,  $V_e$  and  $W_e$  are the velocity components,  $P_e$ ,  $Q_e$  and  $R_e$  are the angular rates and  $\Theta_e$ ,  $\Phi_e$  and  $\Psi_e$  are the attitude angles [28]. Keen readers will notice that the A matrix in Equation 2.5 is an 8x8 matrix while the state vector  $x$  has a size of nine. For the A matrix, the yaw angle,  $\psi$  has been omitted since the yaw angle has no effect on the aerodynamic or dynamic forces and moments [28]. Therefore, that would mean the last column was a column of zeros and that has been omitted such that the rest of the equation was readable on the page. This particular model is also a more simplified version of the actual helicopter dynamics since it neglects the coupling between the rotor and the fuselage, but this is still an excellent representation of the helicopter dynamics [17] [28]. It is worth noting that the input vector,  $u(t)$ , can be changed to suit the experiment being done. As an example, in the research done by Moon et al, the input vector consists of pilot inputs instead of attitude angles [17]:

$$u(t) = [\delta_c \quad \delta_{lon} \quad \delta_{lat} \quad \delta_p] \quad (2.7)$$

where:

- $\delta_c$ : Control input representing collective pitch angle.
- $\delta_{lon}$ : Control input representing longitudinal control.
- $\delta_{lat}$ : Control input representing lateral control.
- $\delta_p$ : Control input representing tail rotor pitch angle.

Here the pilot inputs are mapped onto the attitude angles (much like the left block in Figure 2.14) using the following transfer function:

$$G_{act}(s) = \frac{30^2}{s^2 + 2(0.75)30s + 30^2} \quad (2.8)$$

This means that the rate commanded dynamics are, again, identical in all axis.

In conclusion, the best way to model the helicopter dynamics for this research would be to start with the six degrees-of-freedom system given in Equation 2.3 and Equation 2.4. Then, one needs to simplify it by removing all degrees-of-freedom which will not be used for the experiment and deciding what the input to the system will be. If the inputs are control inputs, then there needs to be a transformation block that converts those to attitude angles which can then be used to calculate the associated translations and rotations.

## 2.5. Conclusion

The goal of this literature study was to create research questions that complete the research objective: "How does using VR headsets, to perform visual cueing, affect the performance of Pilots flying a Helicopter Simulation". As such, the literature reviewed focused on finding out the answer to three main aspects of the research objective, namely:

1. What kinds of visual cues are crucial for pilots in helicopter flight?
2. What goes into creating a pilot and helicopter model that can be used in simulation and experiments?
3. How is pilot performance tested and evaluated?

The reviewed research revealed that the most important visual cues for pilots vary depending on what task they are performing. The most important task in a normal flight envelope would be a near-ground hover since it requires precise velocity and position control. As such, for this maneuver, the most important visual cues are the Field of View (FoV) provided by the visual cueing system. Since the FoV of the view dictates how well the pilot can see all other visual cues, it can be deemed to be of the highest importance. If the FoV degrades significantly, the pilot will start to underestimate or overestimate how fast they are flying and will be prone to errors in maintaining their position. For a near-ground maneuver, this can be extremely dangerous, thus, maintaining a proper FoV is crucial for such a flight case. Additionally, the pilots will need to rely more on their instruments instead of the out-of-window cues which goes against their instincts, and that raises their workload.

Research into the types of pilot and helicopter models, as well as the experimental methods, used in literature also revealed some interesting results. The highest fidelity pilot model one can create is the Cybernetic model, which allows one to calculate performance parameters like the crossover frequency and effective time delay of the pilot. However, to build up such a model, the experimental methods one needs to use are quite expensive. One needs to ensure that the pilot receives proper visual (and if applicable, vestibular) cues in the actual experiment, the forcing function is designed such that the required system identification techniques can be applied effectively and, in case of a multi-loop model, the experiment itself has the correct outputs such that the multiple loops can be disentangled. The system identification techniques themselves can get extremely complicated, especially if non-linearities are present. Often times, this is far beyond the scope of the researchers' objectives and that is why they tend to use significantly simpler analysis methods. These involve asking the participants to do simple control tasks and just running an error analysis on the time traces of their outputs. This can be supplemented with subjective results which involve asking pilots to rate their performance and/or workload on a widely used scale, such as the HQR or the Bedford-Rating Scale. The use of such scales however, needs the participants to be experienced with the control tasks and with using the scales. The last part of the literature study to discuss is the type of helicopter dynamics model used. In general, previous researchers use a six degree-of-freedom model, whose states include three velocity components ( $u, v, w$ ), three attitude angles ( $\theta, \phi, \psi$ ) and three attitude rates ( $p, q, r$ ). This model can then be simplified based on however degrees-of-freedom the researchers want the participants to have for the experiment.

Based on this research, the following research questions can be formulated:

1. **What manoeuvre is most impacted by changing Field of View (FoV)?**
2. **What is the predicted pilot behaviour for the critical manoeuvre with changing FoV?**
3. **What is the actual pilot behaviour for the critical manoeuvre with changing FoV?**
4. **What is the overall effect of changing FoV on pilot performance?**
5. **What strategies do pilots employ to overcome adverse effects of changing FoV?**

It is worth noting that the first research question has already been answered. The manoeuvre most impacted by the changing FoV is the near-ground hover. The answers to the rest of the questions will be found using the visual model built, and the practical experiments.

# 3

## Visual model

2

The goal of this chapter is to develop a visual model that can explain the nature of the information one loses when peripheral vision is obstructed. It is assumed that, in the visual field of the pilot, there exists a point that can offer the maximum amount of feedback for a given manoeuvre. It is assumed that, if such a point exists and is independent of the FoV, then when the FoV is lowered, this point would get clipped out of the view. This means that the pilot would no longer see the most salient point of the environment and would need to shift their gaze to the next-most salient point. Presumably, this would result in the pilot getting feedback of their velocity being much smaller and could be the reason for why people tend to underestimate their velocity as FoV shrinks, as per the findings of the literature study in section 2.1. Additionally, as shown in chapter 2, the performance of the pilot degrades the most as FoV changes for forward translational motion. As such, it is worth analysing cases where the helicopter would move forward and backwards to see if the point of maximum feedback does exist. However, since helicopters must change their pitch to change their forward velocity, the motion of the pitch must also be considered. It was thus decided to limit the analysis to only these two degrees-of-freedom.

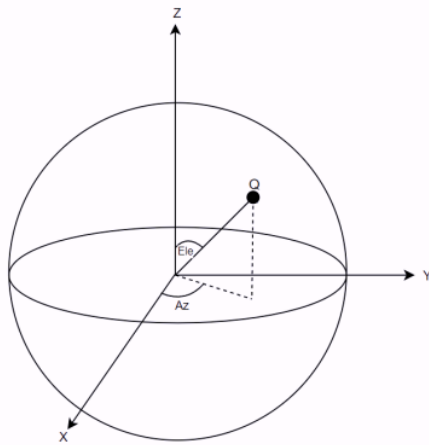
To do this, one needs to look at what type of flow is generated during motion. This flow can then be analysed to see how the human eye would see it and how this would affect their perception. Initially, an analysis was done that, among other things, focused on quantifying how this (3D) flow would look like when it was projected onto a 2D screen. This analysis did not yield tangible or useful results and thus, it was decided to ignore the effects of projecting the 3D motion onto a 2D screen. This means that the screen of the VR headset is just assumed to act as a "window to the real world" (much like the human eye) and the only projection effects that will be considered, are those that are related to projecting objects onto the curved retina of human eyes. The alternate analysis is presented in Appendix A for the interested reader

106

To start the analysis, one again considers there to be a point, P in space with the coordinates  $[x,y,z]$ , i.e:

$$P = [x, y, z] \quad (3.1)$$

this point will be projected onto the surface of the observer's retina at point Q as per Figure 3.1



19  
**Figure 3.1:** Figure showing the projection of point P onto the spherical retina

Here, **Az** and **Ele** refer to the azimuth and elevation angles of the point Q. To convert point P to point Q, Equation 3.2 can be used:

$$Q = \left( \frac{r}{|P|} \right) P \quad (3.2)$$

91 where r is the radius of the sphere and  $|P|$  is the magnitude of the vector P i.e.

$$|P| = \sqrt{x^2 + y^2 + z^2} \quad (3.3)$$

Assuming again that the 166 opter has only two Degrees-Of-Freedom, pitching and forward translation, the new position of P,  $P'$ , can be calculated using:

$$P' = R_Y(\theta)P - [u * dt, 0, 0] \quad (3.4)$$

where  $R_Y(\theta)$  is the orthogonal rotational matrix and dt is a small time-step.  $R_Y\theta$  is given by Equation 3.5:

$$R_Y(\theta) = \begin{bmatrix} \cos \theta & 0 & \sin \theta \\ 0 & 1 & 0 \\ -\sin \theta & 0 & \cos \theta \end{bmatrix} \quad (3.5)$$

Once  $P'$  is calculated, it is transformed into a new Q position,  $Q'$  and this is used to analyse how the motion appears on the observer's retina. This can be done for a grid of points within the observer's field of vision and can be plotted on a 3D graph to show how this changes over time. To get results representative of the actual scenario of a helicopter in hover, it is worth finding out what a realistic motion of a helicopter will look like. This involves looking at the dynamics of a helicopter and mapping out a pilot's control inputs to a pitching angle and a forward velocity. This is elaborated upon in more depth in section 4.2.

The control input simulated for this is sinusoidal and is applied to the system for a total of four seconds. The exact form of the input is given by Equation 3.6

$$\text{Input} = \frac{-1}{100} * \sin\left(\frac{3}{2}\pi t\right) \quad (3.6)$$

This input was chosen after many iterations such that the resulting pitch angle and velocity were high enough for there to be a visible change in flow, but not so high that it is no longer representative of a helicopter in a low speed hover. The control input can be seen in Figure 3.2a, while the resulting behaviour of  $\theta$  and  $u$  can be seen in Figure 3.2b and Figure 3.2c respectively:

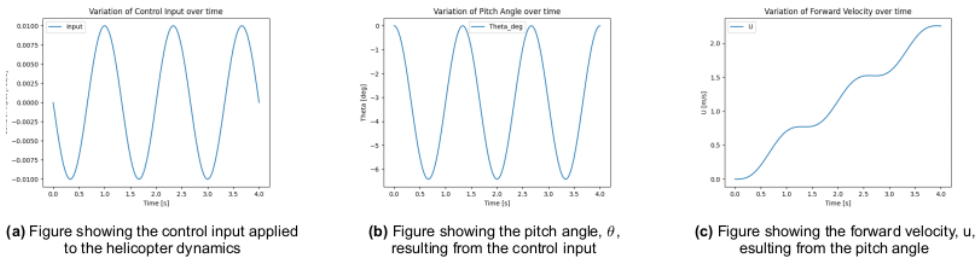


Figure 3.2: Figure showing the motion used for the analysis

**NOTE: I STILL NEED TO ADD THE GIBSON PLOTS THAT SHOW HOW THIS FLOW LOOKS ON A SCREEN**

To analytically analyse the effect of these flow vectors, one can look at the change in the Azimuth and Elevation angles that occurs due to the helicopter's motion. The Azimuth and Elevation angles can be calculated using Equation 3.7 and Equation 3.8 respectively:

$$Az = \arctan \frac{y}{x} \quad (3.7)$$

$$Ele = \arccos \frac{z}{|P|} \quad (3.8)$$

The two angles can be differentiated with respect to the pitch,  $\theta$  and the distance moved,  $u * dt$ . The partial derivative of the azimuth angle with respect to the distance moved is given by Equation 3.9:

$$\frac{\partial Az}{\partial (udt)} = \frac{y}{D^2 + y^2} \quad (3.9)$$

where

$$D = \sqrt{x^2 + y^2} \quad (189)$$

The partial derivative with respect to  $\theta$  is given by Equation 3.11:

$$\frac{\partial Az}{\partial \theta} = \frac{yx \sin \theta - yz \cos \theta}{D^2 + y^2} \quad (3.11)$$

For the elevation angle, the partial derivative with respect to the distance moved is given by Equation 3.12:

$$\frac{\partial Ele}{\partial (udt)} = \frac{-2x \cos \theta - 2z \sin \theta + 2udt}{2\sqrt{P_x^2 + y^2} \cdot \left[ C + \frac{P_x^2 + y^2}{C} \right]} \quad (3.12)$$

where

$$C = -x \sin \theta + z \cos \theta \quad (133)$$

and

$$P_x^2 = x^2 \cos^2 \theta + z^2 \sin^2 \theta + 2xz \cos \theta \sin \theta \quad (90)$$

$$- 2uxdt \cos \theta - 2uzdt \sin \theta + u^2 dt^2$$

The partial derivative with respect to  $\theta$  is given by Equation 3.15:

$$\frac{\partial Ele}{\partial \theta} = \frac{B}{2\sqrt{P_x^2 + y^2} \cdot \left[ C + \frac{P_x^2 + y^2}{C} \right]} \quad (3.15)$$

with

$$B = -x^2 \sin(2\theta) + z^2 \sin(2\theta) + 2xz \cos(2\theta) + 24xdt \sin \theta - 2uzdt \cos \theta \quad (3.16)$$

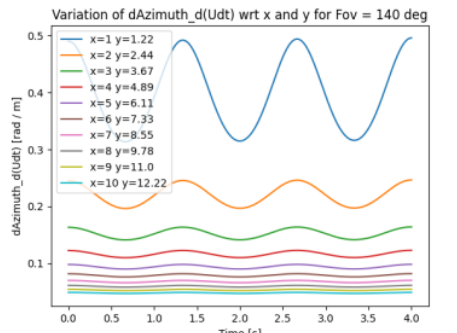
As can be seen from the equations, the partial derivatives are dependant on the position of the object, the speed and the pitch angle of the observer. To analyse the behaviour of these derivatives thus, one has to fix a few of these variables and analyse how the behaviour changes due to the remaining

variables. For this analysis, much like the flow vectors, the speed and pitch angle were determined by the example motion shown in Figure 3.2. The z-coordinate of the position was chosen to be -5 [m] as it is believed that the points an observer would see on the ground would be the most informative [29]. The remaining variables are thus  $x$  and  $y$ -coordinates of the position. Since the goal is to see the effect of FoV on these quantities, the  $x$  and  $y$ -coordinates corresponding to a specific FoV can be used. However, for any FoV, one can have an infinite number of  $x$  and  $y$ -coordinates. Thus it was decided to calculate the value of the partial derivatives for a set of  $x$  and  $y$ -coordinates (that correspond to one particular FoV) and take their average value. This value can be thought of as the value of the partial derivative for this particular FoV over the whole range of  $x$  and  $y$ -coordinates.

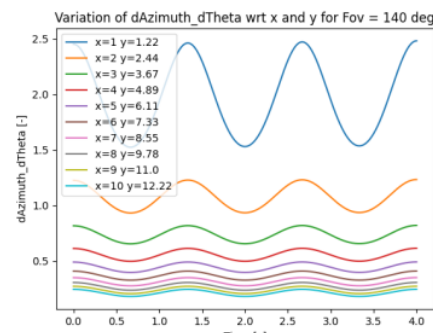
As an example, for a chosen FoV of 140 [ $^\circ$ ], a list of  $x$ -coordinates ranging from 1 [m] to 10[m] was created. Then, the corresponding  $y$ -coordinate was calculated using Equation 3.17:

$$y = x \tan(70) \quad (3.17)$$

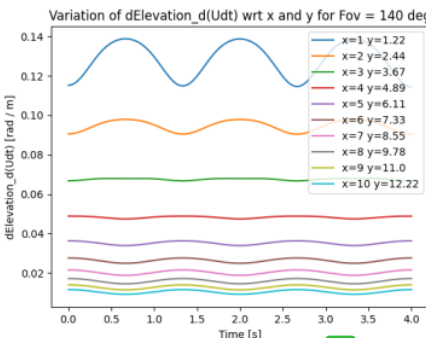
These  $x$  and  $y$ -coordinates, along with the rest of the fixed variables, were input in Equation 3.9, Equation 3.11, Equation 3.12 and Equation 3.15, and the trend was plotted. This can be seen in Figure 3.3:



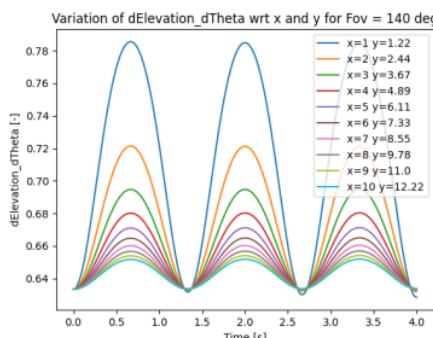
(a) Figure showing the variation of  $\frac{\partial A_z}{\partial(u dt)}$  with  $x$  and  $y$ -coordinates



(b) Figure showing the variation of  $\frac{\partial A_z}{\partial\theta}$  with  $x$  and  $y$ -coordinates



(c) Figure showing the variation of  $\frac{\partial E_z}{\partial(u dt)}$  with  $x$  and  $y$ -coordinates



(d) Figure showing the variation of  $\frac{\partial E_z}{\partial\theta}$  with  $x$  and  $y$ -coordinates

Figure 3.3: Figure showing the variation of the partial derivatives of the Azimuth and Elevation angles with  $x$  and  $y$ -coordinates

As can be seen in Figure 3.3, the value of the partial derivatives goes to zero as the distance between the observer and the object increases. As such, if one was to average the values of the partial derivatives for all the positions, the main contribution to the final value would be from the positions closest to the observer. Since the contributions of these points are what the observer will actually be able to notice or perceive, their values can be considered a good representation of what the "flow" is like

for any particular viewing angle. Therefore, going forward, whenever the value of a partial derivative of a particular angle is mentioned, the reader can assume that this means that the value is the average value of all points that lie on that viewing angle.

The procedure stated above can then be done for a wide range of FoV values to see how the partial derivatives change for points that are on the edge of the particular FoV. This is visualised in Figure 3.4:

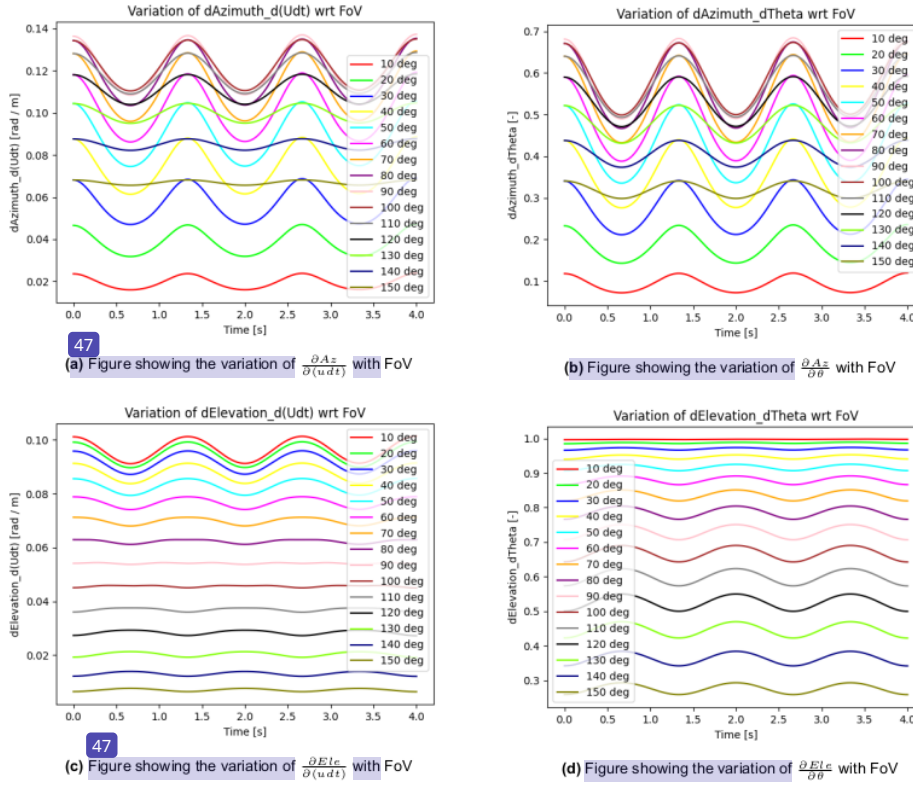


Figure 3.4: Figure showing the variation of the partial derivatives of the Azimuth and the Elevation angles with FoV

As can be seen from Figure 3.4a and Figure 3.4b, the values of the partial derivatives for the Azimuth angle on the edge of the pilot's vision increases as the FoV increases up to 90 [ $^{\circ}$ ]. After this however, the value of the partial derivative starts to decrease. This is in stark contrast to the value of the partial derivatives for the Elevation angle, which decrease as the Fov increases. This trend is visualised in Figure 3.5:

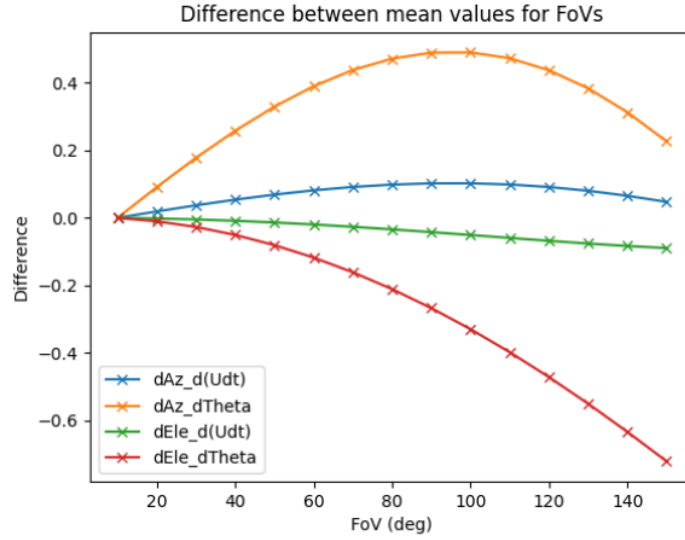


Figure 3.5: Figure showing the behaviour of the partial derivatives with respect to FoV

Figure 3.5 plots the difference between the value obtained for a particular FoV and the first value (i.e. the value for  $FoV = 10^\circ$ ). The results from Figure 3.4a, Figure 3.4b and Figure 3.5 seem to suggest that the point with the most movement in the azimuth direction, is at a horizontal viewing angle of around  $90^\circ$  from the observer. As the FoV decreases, this point would get clipped out and the next most informative point would then be on the edge of the observer's FoV. For the most informative point in terms of the elevation angle, the analysis seems to suggest that this exists right in front of the observer (i.e. at a horizontal viewing angle of  $0^\circ$ ).

To confirm these observations, one can do a grid search to find where the points with the greatest value of the derivatives are. The grid search consisted of creating points at an x-distance of between 1 [m] and 10 [m] from the observer, with 0.1 [m] increments between them. The height of the points (i.e. the z-coordinate) was set to -5 [m] which indicates that the observer is hovering 5 [m] off the ground and is looking at the ground. The y-coordinates of the points are then simply those that are visible to the observer for the particular FoV. The number of points for each FoV tested are shown in Table 3.1:

Angle [°]	Number of Points
10	386
20	749
30	1125
40	1519
50	1935
60	2390
70	2894
80	3461
90	4147
100	4902
110	5866
120	7111
130	8798
140	11267
150	15289

Table 3.1: Table showing the number of points tested for each FoV

For each of these points, the values of the four derivatives were calculated and the point with the highest value was chosen as the most informative point for that derivative. This point was expressed as a horizontal viewing angle from the observer's eye. The results for the best viewing angle to discern  $\frac{\partial A_z}{\partial(u dt)}$  and  $\frac{\partial A_z}{\partial\theta}$  are shown in Figure 3.6:

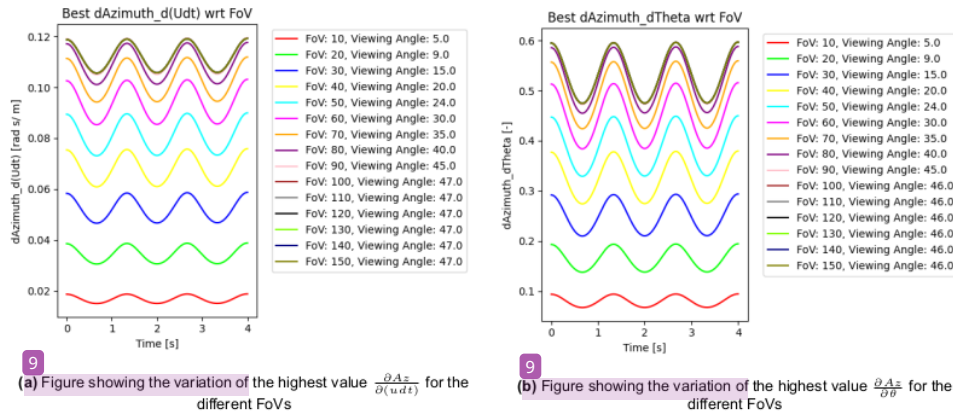
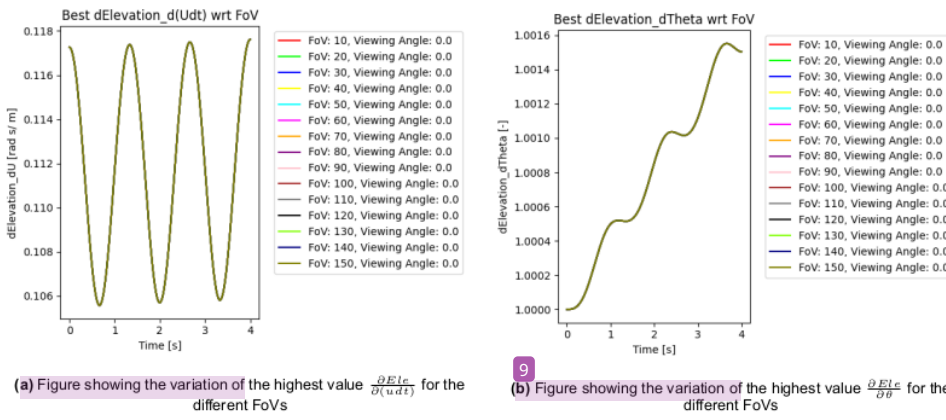


Figure 3.6: Figure showing the variation of the highest value of partial derivatives of the Azimuth angle for the different FoVs

The viewing angles in Figure 3.6a and Figure 3.6b represent the angle from the centre of the pilot's vision, their right hand side. So, an angle of 10 [°] means the point is at a 10 [°] angle to the right of the pilot's view. It is worth noting that a point at the same angle on the left hand side will also have the same value of the derivatives so it does not matter which side of the pilot's view is analysed. As can be seen from Figure 3.6, the best viewing angle to observe the change in azimuth angles due to the motion seem to lie on the edge of the pilot's FoV, for FoVs smaller than 90 [°]. For FoVs equal to and larger than 90 [°], the best point is found at a horizontal viewing angle of around 45-47 [°] left or right of the observer. This implies that the most informative point for the change in azimuth angle is located at around 45 [°] and thus, as the FoV becomes smaller, this point would get clipped out of view and the pilot would start losing information about the motion being carried out.

The results for the derivatives of the Elevation angle are given in Figure 3.7:



**9** Figure 3.7: Figure showing the variation of the highest value of partial derivatives of the Elevation angle for the different FoVs

Figure 3.7a and Figure 3.7b seem to confirm the conclusions of the numerical analysis that the most informative point for detecting changes in the elevation angle, is indeed found right in front of the pilot.

These results can be used to draw the following conclusions:

1. As the FoV decreases from 90 [ $^{\circ}$ ], the pilot's perception of how the azimuth angle changes would worsen. As the FoV increases beyond 90 [ $^{\circ}$ ], the pilot's perception of how the azimuth angle changes would remain unaffected.
2. Changing FoV has no impact on how the pilot perceives the change in elevation angles.

As Figure 3.6 show, the change in azimuth angles due to the distance moved is greater than that for a change in pitch, while the opposite is true for the change in elevation angles. This means that for a motion where there is both pitch and forward translation, one will perceive a change in both azimuth and elevation angles and so, they are likely to be affected by any changes in FoV as per the first conclusion above). Conversely, if there is only pitching motion, then the pilot will perceive mostly elevation angle changes and they may not be affected by changing FoVs. The biggest question mark with all these observations however is the level of impact it will have on the pilot perception. While the numbers conclude that, e.g., the change in azimuth angle with respect to forward motion is 10 times larger for an FoV of 90 [ $^{\circ}$ ] as compared to an Fov of 10 [ $^{\circ}$ ], it is still unknown if that will result in a large change in performance for the pilot. That makes the experiments even more important, as they will help to contextualise the impact of the values of these partial derivatives on what the pilot can actually perceive.

Keeping all of this in mind, the following hypotheses have been formulated:

1. **H1:** If a helicopter has both pitching and forward motion, decreasing the FoV to below 90 [ $^{\circ}$ ] should lower a pilot's performance significantly.
2. **H2:** If **43** helicopter has both pitching and forward motion, increasing the FoV to above 90 [ $^{\circ}$ ] should have no significant effects on a pilot's performance **43**
3. **H3:** If a helicopter has only pitching motion, changing the FoV should have no significant effect on a pilot's performance.

# 4

## Experiment Methodology

The goal of this chapter is to detail all the important aspects of the experiments that will be done to test the hypotheses created in chapter 3. The basic information about the experiment can be found in section 4.1 while details about the dynamics of the helicopter in the simulation can be found in section 4.2. Information about the forcing function is presented in section 4.3 and, lastly, information about the setup of the experimental equipment is found in section 4.4.

### 4.1. Experiment Basics

Following on from the conclusions of chapter 3, the three hypotheses need to be proven or dis-proven based on a series of practical experiments. Since the analysis focuses only on the pitching and forward velocity of the helicopter, the experiments should be set up, such that these are the only two degrees-of-freedom allowed. Additionally, since hypothesis **H3** concerns only the pitching motion, one set of experimental conditions should have only one degree-of-freedom i.e. just the pitching.

The first set of experimental conditions (aka the Velocity Disturbance Rejection Task) will involve pilots <sup>46</sup> trying to do a disturbance rejection task with changing FoVs. This means that <sup>176</sup> each FoV tested, the pilot's job is to keep the velocity of the helicopter zero, in the presence of a forcing function. This forcing function will only affect the velocity of the helicopter. The second set of experimental conditions (aka the Pitch Disturbance Rejection Task) will also be a disturbance rejection task, except this time the forcing function will affect only the pitch of the helicopter. Additionally, the velocity of the helicopter will be kept zero throughout the whole run. These two sets of experimental conditions should be sufficient to prove or dis-prove the hypotheses outlined in chapter 3.

The first thing to decide is which FoVs should be tested in the experiment phase of this project. The results of chapter 3 show that a FoV of 90 [°] needs to be included in the experiment, and that the experiments should revolve around seeing if performance is gained or lost for FoVs that are not 90 [°]. However, the analysis did not reveal specific values of FoV larger than or smaller than 90 [°] that would be worth looking at. Therefore, it is worth looking at what FoVs were tested in previous such experiments, as is detailed in chapter 2, and use those to build up the experiment matrix. This, of course, has to be done by keeping the limits of the Pimax 8K headset in mind and, as such, the maximum horizontal and vertical FoV that can be achieved are 140 ° and 102 ° respectively [30].

Keeping all of these factors in mind, the FoVs chosen to be tested are:

- 161 [°]: This is to see if performance does degrade drastically per the analysis of chapter 3 and the findings of Pretto et al and Kenyon et al [10] [11]
- 30 [°]: This is considered the minimum FoV needed to perceive the rotations efficiently according to the literature studied [10][11].
- 60 [°]: This is considered to be the optimal FoV needed to perceive forward velocities efficiently in literature [11].
- 90 [°]: This is per the results of chapter 3.

- 120 [ $^{\circ}$ ]: Literature seems to conclude that the gain in performance is minimal between 60 [ $^{\circ}$ ] and 120 [ $^{\circ}$ ] but the analysis suggests that the performance should improve until 90 [ $^{\circ}$ ]. Thus, it is worth testing this FoV
- 140[  $^{\circ}$ ]: This is the max FoV of the Pimax in normal viewing mode and this high FoV is the unique-selling-point of the Pimax. Thus, it is worth testing to see if there is indeed any benefit to having such a large FoV.

132

These FoVs will be used for the Velocity Disturbance Rejection Task. For the Pitch Disturbance Rejection Task, while the same FoVs can be used, it would be more efficient to test fewer FoVs. The reason for this is two-fold; Firstly, the analysis done in chapter 3 suggests that the performance of the pilot will remain the same for all of the listed FoVs since the most informative point will always be visible to them. Secondly, to get useful results and to get rid of errors, one would need to test each FoV at least twice, per participant. With six FoVs to test for each type of control task, each participant would have to do 24 runs in total. This can be very time-consuming and very tiring for the potential participants. Thus, it was decided that the Pitch Disturbance Rejection Task should only have two FoVs to test; 20 [ $^{\circ}$ ] and 140 [ $^{\circ}$ ]. This means that, if the hypothesis is indeed correct, one should see no change in the pilot performance for the narrowest and the widest FoV and that is enough to prove the hypothesis correct. This would also then save the participants' time and energy

## 4.2. Model structure

38

The proposed structure for the Velocity Disturbance Rejection Task consists of two loops; an inner loop and an outer loop. This is a common cascade model for pilot control and is shown in Figure 4.1[29]:

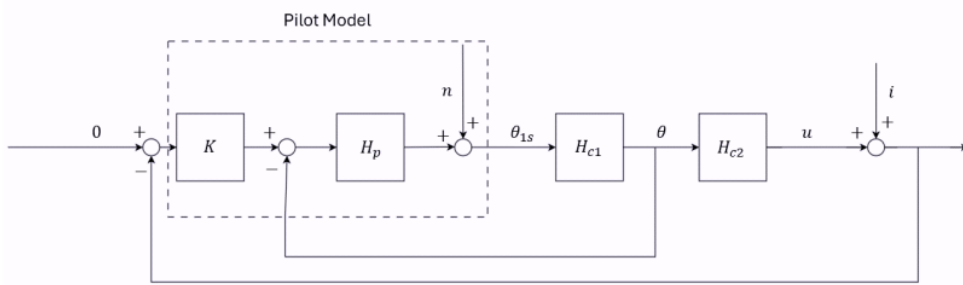


Figure 4.1: Figure showing the proposed structure for the Velocity Disturbance Rejection Task

2  
As can be seen in Figure 4.1, the inner loop consists of the pilot changing the longitudinal cyclic input,  $\theta_{1s}$  such that there is a change in the helicopter pitch angle,  $\theta$ . The outer loop is then the surge velocity,  $u$  being changed due to the change in  $\theta$ . This velocity is then compounded with the disturbance function,  $i$  which represents wind acting on the helicopter during near-ground hover maneuver. The pilot model, shown in the dashed box, consists of a simple gain for the outer loop and a transfer function,  $H_p$  for the inner loop [29]. Additionally, there is also the pilot remnant,  $n$  that must be added into the pilot model. This remnant accounts for the control inputs made that are uncorrelated with any visual cues received by the pilot throughout the experiment [23].

The blocks  $H_{c1}$  and  $H_{c2}$  represent the controlled element dynamics and they can be evaluated using

the helicopter dynamics model. Starting from the general state-space system:

$$\dot{\mathbf{x}}(t) = A\mathbf{x}(t) + B\mathbf{u}(t) \quad (4.1)$$

where

$$\begin{aligned} \mathbf{x} &= \{u, v, w, p, q, r, \theta, \phi, \psi\} \\ \mathbf{u} &= \{\theta_0, \theta_{1s}, \theta_{1c}, \theta_{0T}\} \end{aligned} \quad (4.2)$$

with the following form for the A and B matrices:

$$\mathbf{A} = \left[ \begin{array}{ccccccccc} X_u & X_w - Q_e & X_q - W_e & -g \cos \Theta_e & X_v + R_e & X_p & -g \sin \Phi_e \cos \Theta_e & X_r + V_e \\ Z_u + Q_e & Z_w & Z_q + U_e & -g \cos \Phi_e \sin \Theta_e & Z_v - P_e & Z_p - V_e & -R_e (I_{xx} - I_{zz}) I_{yy} & Z_r \\ M_u & M_w & M_q & 0 & M_v & M_p - 2P_e I_{xz} I_{yy} & 0 & M_r + 2R_e I_{xz} I_{yy} \\ 0 & 0 & 0 & 0 & 0 & 0 & 0 & -P_e (I_{xx} - I_{zz}) I_{yy} \\ Y_u - R_e & Y_w + P_e & Y_q & -g \sin \Phi_e \sin \Theta_e & Y_v & Y_p + W_e & -\Omega_a \cos \Theta_e & Y_r + U_e \\ L'_u & L'_w & L'_q + k_1 P_e - k_2 R_e & 0 & L'_v & L'_p + k_1 Q_e & -g \cos \Phi_e \cos \Theta_e & L'_r + k_2 Q_e \\ 0 & 0 & \sin \Phi_e \tan \Theta_e & \Omega_a \sec \Theta_e & 0 & 1 & 0 & \cos \Phi_e \tan \sin \Theta_e \\ N'_u & N'_w & N'_q - k_1 R_e - k_3 P_e & 0 & N'_v & N'_p + k_3 Q_e & 0 & N'_r + k_1 Q_e \end{array} \right] \quad (4.3)$$

$$\mathbf{B} = \left[ \begin{array}{cccc} X_{\theta_0} & X_{\theta_{1s}} & X_{\theta_{1c}} & X_{\theta_{0T}} \\ Z_{\theta_0} & Z_{\theta_{1s}} & Z_{\theta_{1c}} & Z_{\theta_{0T}} \\ M_{\theta_0} & M_{\theta_{1s}} & M_{\theta_{1c}} & M_{\theta_{0T}} \\ 0 & 0 & 0 & 0 \\ Y_{\theta_0} & Y_{\theta_{1s}} & Y_{\theta_{1c}} & Y_{\theta_{0T}} \\ L'_{\theta_0} & L'_{\theta_{1s}} & L'_{\theta_{1c}} & L'_{\theta_{0T}} \\ 0 & 0 & 0 & 0 \\ N'_{\theta_0} & N'_{\theta_{1s}} & N'_{\theta_{1c}} & N'_{\theta_{0T}} \end{array} \right] \quad (4.4)$$

One has to reduce them such that they represent the helicopter during hover and are expressed in terms of the relevant control input (i.e.  $\theta_{1s}$ ). For hover, the translational ( $u, v, w$ ) and angular ( $P_e, Q_e, R_e$ ) velocities are equal to 0. Furthermore, since the analysis is only for a system with two degrees of freedom (pitch and surge), height is kept fixed. Lastly, the small angle approximation is used for the attitude angles. All of this results in the following longitudinal state equation for the helicopter response to a cyclic pitch input from a trimmed hover:

$$\begin{bmatrix} u \\ 150 \\ q \\ \dot{\theta} \end{bmatrix} = \begin{bmatrix} X_u & X_w & X_q & -g \\ Z_u & Z_w & Z_q & -g\Theta_e \\ M_u & M_w & M_q & 0 \\ 0 & 0 & 1 & 0 \end{bmatrix} \begin{bmatrix} u \\ w \\ q \\ \theta \end{bmatrix} + \begin{bmatrix} X_{\theta_{1s}} \\ Z_{\theta_{1s}} \\ M_{\theta_{1s}} \\ 0 \end{bmatrix} [\theta_{1s}] \quad (4.5)$$

To derive the relevant equations for the controlled element dynamics, two further assumptions must be made. Firstly, since the height is fixed throughout the experiment and the fact that the contribution of the vertical velocity to the longitudinal motion is minimal, the second row of Equation 4.5 can be assumed to be zero. Secondly, it is assumed that the contribution of  $X_q q$  is significantly smaller than that of  $X_u u$  so  $X_q q$  is set to zero. What this means in practical terms is that the forward acceleration caused by the pitch rate is much smaller than the forward acceleration caused by the surge velocity and thus, it can be ignored completely [28]. Using these assumptions, one can derive the following equations of motion:

$$\begin{aligned} \dot{u} - X_u u + g\theta &= X_{\theta_{1s}} \theta_{1s} \\ \dot{q} - M_u u - M_q q &= M_{\theta_{1s}} \theta_{1s} \\ \dot{\theta} &= q \end{aligned} \quad (4.6)$$

182

The first part of the controlled element dynamics to analyse is the relation between  $\theta_{1s}$  and  $\theta$ . This is done by assuming the surge velocity to be 0 for hover:

$$\begin{aligned} u &= 0 \\ \dot{q} - M_q q &= M_{\theta_{1s}} \theta_{1s} \\ \dot{\theta} &= q \end{aligned} \quad (4.7)$$

substituting the fourth equation into the second gives:

$$\ddot{\theta} - M_q \dot{\theta} = M_{\theta_{1s}} \theta_{1s} \quad (4.8)$$

Taking the Laplace transform of this and rearranging shows the form of  $H_{c1}$ :

$$\frac{\Theta(s)}{\Theta_{1s}(s)} = H_{c1} = \frac{M_{\theta_{1s}}}{s(s - M_q)} \quad (4.9)$$

The moment derivatives  $M_{\theta_{1s}}$  and  $M_q$  represent how the pitching moment changes as a result of the longitudinal cyclic input and pitch rate respectively. Using data for the DRA (RAE) research Lynx helicopter, illustrated in Figure 4.2, the values of the derivatives are found to be **26.4** [1/s<sup>2</sup>] for  $M_{\theta_{1s}}$  and **-1.8955** [1/s] for  $M_q$  respectively [28].



**Figure 4.2:** Figure showing the DRA (RAE) research Lynx Helicopter [31]

The reason why this particular helicopter is chosen is due to the fact that it has been used extensively for flight tests by the British Royal Airforce (RAF) and the National Aeronautics and Space Administration (NASA), and has been used to calibrate agility standards of its successors [28]. This means that this helicopter is well suited for this research.

As is evident from Equation 4.9, the pilot will need to control a double integrator system for the inner loop. As McRuer et al have shown, this is quite a challenge for highly trained pilots and, since it is expected that the participants for the experiments for this project will not be highly trained pilots, it will be exceptionally difficult for the potential test subjects of this project [20]. Thus, it was decided to simplify the model to an integrator to facilitate the participants, i.e.:

$$\frac{\Theta(s)}{\Theta_{1s}(s)} = H_{c1} = \frac{M_{\theta_{1s}}}{s} \quad (4.10)$$

To derive the relationship between  $\theta$  and  $u$ , i.e.  $H_{c2}$ , one needs to use the first equation of Equation 4.6. Here,  $\theta_{1s}$  will be substituted such that it is expressed in terms of  $\theta$  and this will be done by analysing the steady state behaviour of Equation 4.9. This serves as a balance between the simplified version of  $H_{c1}$  used here and the actual behaviour of the system. Using the Final Value Theorem, the steady state behaviour of  $H_{c1}$  is found to be:

$$\frac{\Theta(s)}{\Theta_{1s}(s)} ss = H_{c1ss} = \frac{-M_{\theta_{1s}}}{M_q} \quad (4.11)$$

Substituting this into the first equation in Equation 4.6 and taking the Laplace transform gives:

$$sU(s) - X_u U(s) + g\Theta(s) = \frac{-X_{\theta_{1s}} M_q}{M_{\theta_{1s}}} \Theta(s) \quad (4.12)$$

Rearranging this gives the form of  $H_{c2}$ :

$$\frac{U(s)}{\Theta(s)} = \frac{\frac{-X_{\theta_{1s}} M_q}{M_{\theta_{1s}}} - g}{s - X_u} \quad (4.13)$$

The values of  $X_{\theta_{1s}}$  and  $X_u$  are **-9.280 [m/s<sup>2</sup>rad]** and **-0.02 [1/s]** respectively [28]. The bode plot for  $H_{c2}$  can be seen in Figure 4.3:

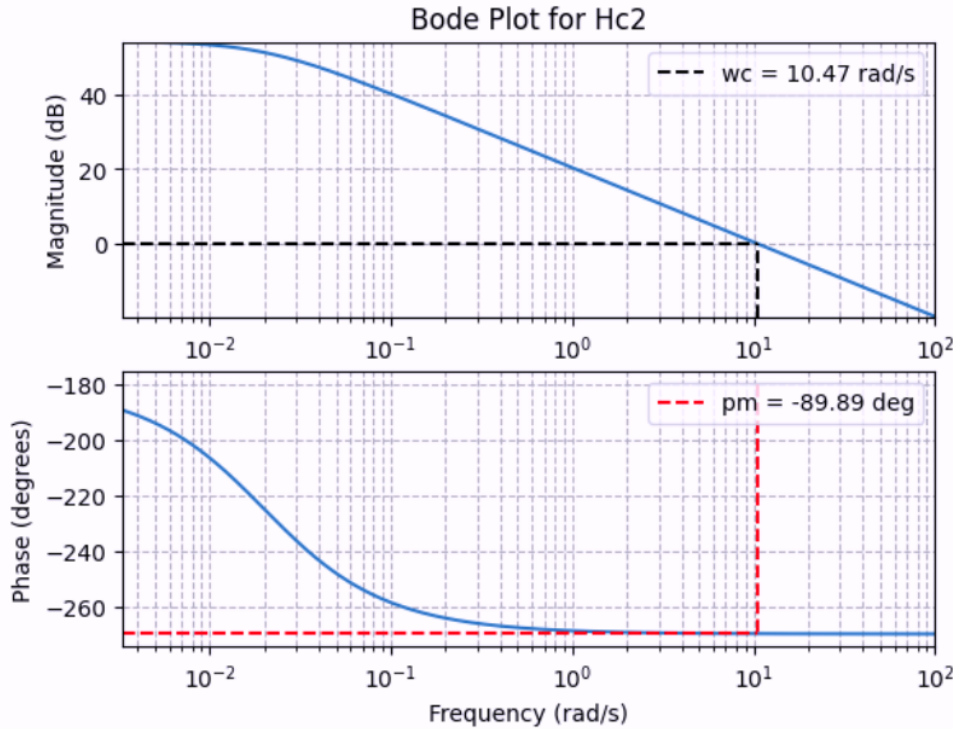


Figure 4.3: Figure showing the bode plot for  $H_{c2}$

As can be seen in Figure 4.3, the crossover frequency is 10.47 [rad/s] and the phase margin is -89.89 [deg].

For the Pitch Disturbance Rejection Task, since there is only one degree-of-freedom, the structure will only contain one loop. This is illustrated in Figure 4.4:

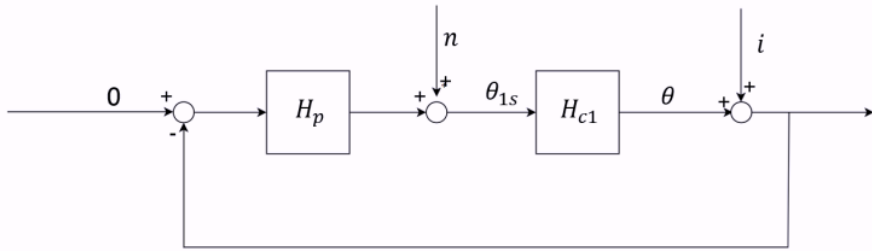


Figure 4.4: Figure showing the proposed structure for the Pitch Disturbance Rejection Task

The dynamics of  $H_{c1}$  are identical to those in Equation 4.10

68

### 4.3. Forcing Function

The forcing function is applied to the dynamics of the helicopter model [2] simulate the disturbance that the pilot has to correct. It has to appear random to the pilot such that the pilot is not able to predict the behaviour of the signal. If the pilot were to accurately predict what the signal is doing, they would change their behaviour to anticipate the signal and thus, they would no longer be doing a compensatory tracking task [14]. Additionally, the forcing function has to be repeatable such that identical tasks can be performed repeatedly. In this case, the disturbance acting on the helicopter is simulating the turbulence that the helicopter would experience due to its low altitude and proximity to other objects. Such turbulence consists of sharp "gusts" being dispersed throughout the course of the flight as a result of the wakes generated by the helicopter interacting with the ground and nearby objects.

To model such turbulence, the forcing function can be generated according to Equation 4.14:

$$f(t) = \sum_{k=1}^{N_t} A_t(k) \sin(\omega_t(k)t + \phi_t(k)) \quad (4.14)$$

119 As can be seen from Equation 4.14, the forcing function is a sum of  $N_t$  sinusoids with  $A_t(k)$ ,  $\omega_t(k)$  and  $\phi_t(k)$  being the amplitude, frequency and phase of the  $k$ th sinusoid [32]. The frequencies of the sinusoids,  $\omega_t$ , have to be in a certain range such that pilot is constantly exhibiting closed loop control [14]. If the frequency is too high, the pilot will not have enough time to change the position or attitude significantly and will thus, ignore the disturbances. If the frequency is too low, then the pilot will not be sufficiently challenged. One method of choosing  $\omega_t$  is to find the measurement time base frequency which is given by:

$$\omega_m = \frac{2\pi}{T_m} \quad (4.15)$$

where  $T_m$  is the measurement time of one experimental run. The frequency of the sinusoids can then be integer multiples of  $\omega_m$  i.e [32] [33]:

$$\omega_t(k) = n_k \omega_m \quad (4.16)$$

Lastly, the values of a particular  $\omega_t$  must not be a harmonic frequency of another  $\omega_t$  [34].

The amplitude of the sinusoids,  $A_t$ , should be large enough to displace the helicopter significantly but it should not be too large that the pilot needs very large control inputs (which would violate the linear approximation of the helicopter dynamics) [14]. For this, one can simply use a shelf for the amplitudes, where signals with a frequency higher than the bandwidth frequency have one-tenth the power of those lower than the bandwidth [34].

The final variable to determine is the phase of the sinusoids,  $\phi_t$ . This can be done by creating a random set of phases and choosing those that result in the forcing function signal having a probability closest

to a Gaussian distribution [33]. The phases chosen should be such that the final signal does not have any excessive peaks of velocity (for the velocity forcing function) and pitch angle (for the pitch forcing function). For this project, the relevant parameters of Equation 4.14 for the velocity and pitch forcing functions are given by Table 4.1 and Table 4.2 respectively:

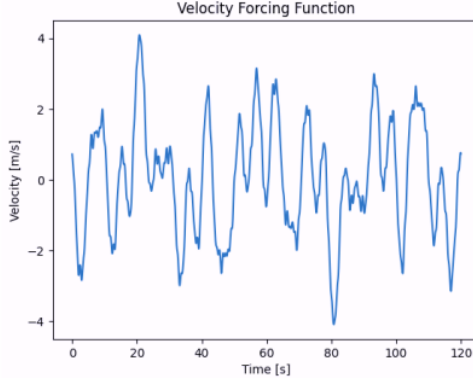
**Table 4.1:** Table showing the values of the parameters for the velocity forcing function

$n_k$	$\omega_t(k)$ [rad/s]	$A_t(k)$ [m/s]	$\phi_t(k)$ [rad]
3	0.15708	1	-1.57658
7	0.36652	1	5.66384
11	0.57596	1	2.91532
17	0.89012	0.1	1.23978
23	1.20428	0.1	-4.32260
37	1.93732	0.1	-4.32290
51	2.67035	0.1	-5.55329
73	3.82227	0.1	4.60151
103	5.39307	0.1	1.27065
139	7.27802	0.1	2.61472

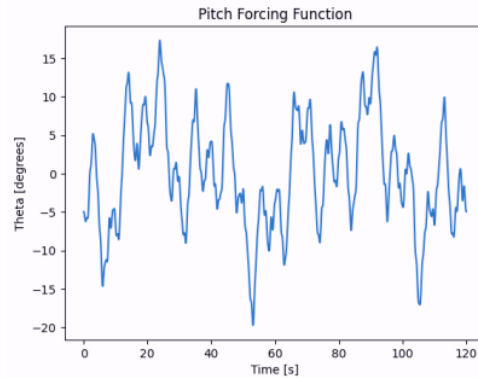
**Table 4.2:** Table showing the values of the parameters for the pitch forcing function

$n_k$	$\omega_t(k)$ [rad/s]	$A_t(k)$ [°]	$\phi_t(k)$ [rad]
2	0.10472	5	-1.04273
5	0.26179	5	2.768679
11	0.57596	5	-6.281748
23	1.20428	0.5	-2.483962
37	1.93732	0.5	-4.438996
51	2.67035	0.5	-5.122824
71	3.71756	0.5	-3.942570
83	4.34587	0.5	-1.940741
97	5.078908	0.5	-1.297258
137	7.173303	0.5	0.487785

The Velocity and Pitch forcing functions are visualised in Figure 4.5a and Figure 4.5b respectively:



(a) Figure showing the Velocity forcing function

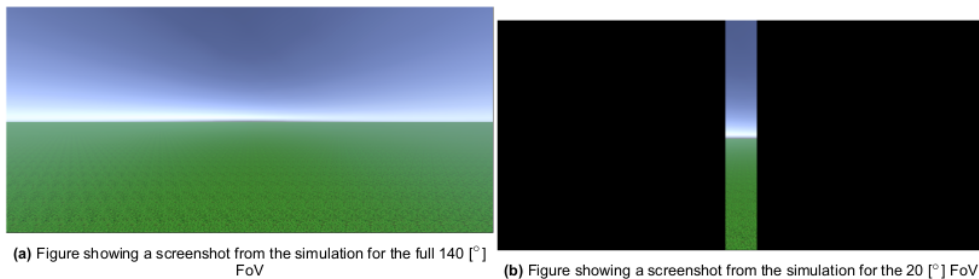


(b) Figure showing the Pitch forcing function

Figure 4.5: Figure showing the Velocity and Pitch Forcing Functions

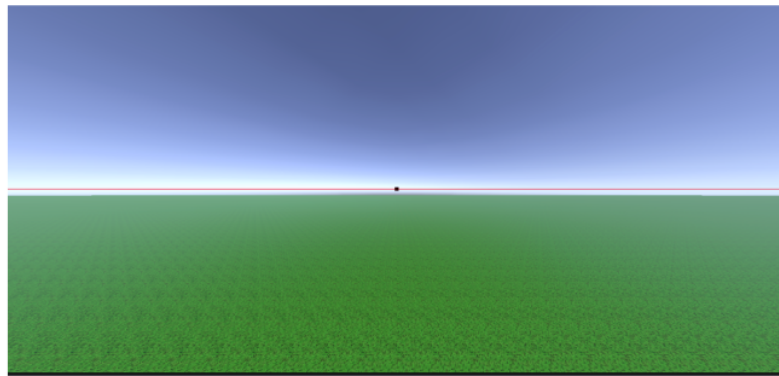
#### 4.4. Experimental setup

The experiment consists of participants using a joystick to control the pitch of the helicopter simulation to correct against the disturbance forcing function. The simulation itself was made in Unity and consists of a first-person view of a large, unending grass field. This field consists of a repeating grass texture that is used to provide the visual flow which is used by the participants to judge their velocity. A screenshot from the simulation is shown in Figure 4.6a:



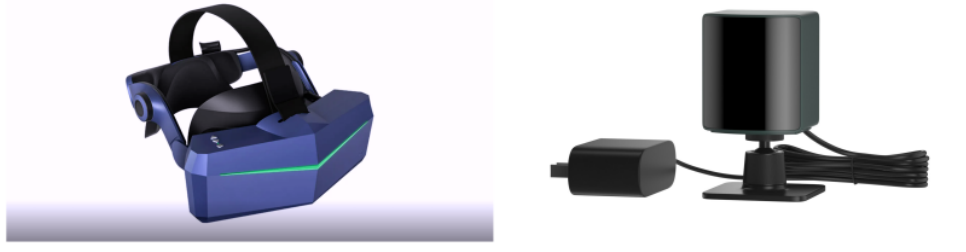
**Figure 4.6:** Figure showing two screenshots from the simulation; one for and FoV of 140 [°] and one for an FoV of [°]

Figure 4.6b shows the view for the 20 [°] FoV condition. As stated previously, the FoV was changed by adding black bars to the periphery<sup>58</sup> of the Camera object in Unity to block off the scenery that would not be visible from the chosen FoV. For the Pitch Disturbance Rejection Task, the participants<sup>113</sup> were also shown a reticle and a horizon line that allowed them to judge how their pitch changed. this is shown in Figure 4.7



**Figure 4.7:** Figure showing the pitch indicator reticle and the horizon line used for the pitch disturbance rejection task

Note, the reticle and the horizon line shown in Figure 4.7 look very small in this view, but are actually bigger when viewed through the VR headset. The simulation is viewed through the Pimax 8KX VR headset. The tracking for the headset is done using two Valve Index Base Stations which allow all the VR software<sup>28</sup> know exactly what the orientation and position of the headset is. Both these components are pictured in Figure 4.8a and Figure 4.8b:



**Figure 4.8:** Figure showing the Pimax 8KX VR headset and the accompanying base station

It is worth pointing out that the experiment was set up such that, if the participant moved their head, then the scenery would not move with them. Instead, their view would remain as them looking forward, with the grass and the horizon of Figure 4.6a. This was done to ensure that there would be no nonlinearities in what each individual participant was seeing, which aims to simplify the analysis done. If there was head tracking, i.e. the scene moved as their head did, then it would be possible to enter a situation where no participant is doing the same experiment as another.

Before the experiment had begun, participants were allowed to spend some time adjusting the VR headset such that it sat comfortably on their heads and they had a good, comfortable view of the simulation visuals. Then, they were allowed to move the helicopter in the simulation with the joystick, just so they could get a feel of the task. This was done such that the participants could get used to how sensitive the joystick was and how much they needed to pitch to get a certain velocity. Afterwards, the participants did a test run to get an idea of what the full experiment would be like. They were allowed to repeat the test runs multiple times until they were confident enough to begin the actual experiments. During the experiments, the participants would complete the disturbance rejection task for one of the FoVs and then, when it ends, they were shown an 11-point MIsery SCale (MISC). This was done to ensure that the participants were not suffering from any adverse effects which are common for VR headsets<sup>45</sup> e motion-sickness or excessive eye strain [37]. The scale that showed up in the simulation is shown in Figure 4.9

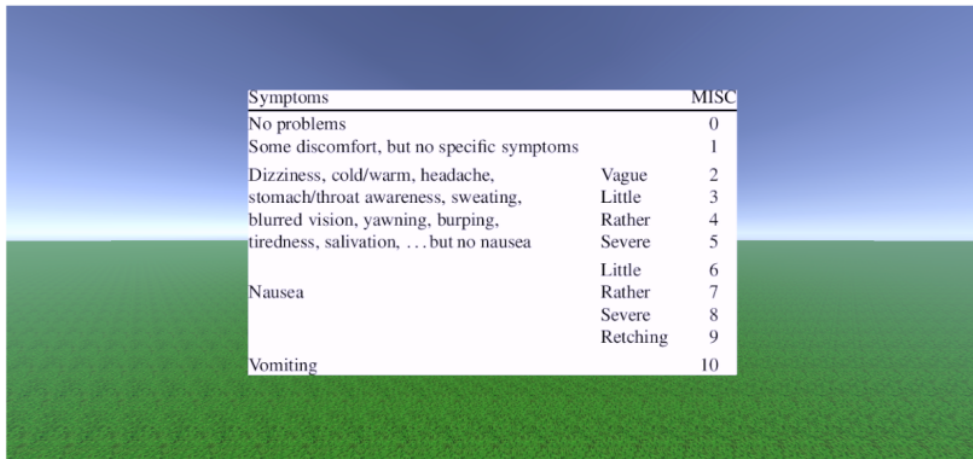


**Figure 4.9:** Figure showing the MISC scale as the participants would have seen it in the simulation [37]

The numbers on the right of the scale correspond to the symptoms on the left. If a participant indicated that the MISC score was anywhere in the 'nausea' category, the entire experiment would be immediately terminated and the necessary actions would be taken to get them feeling better. If this happens, the participant would no longer participate in the experiment.

Since there are eight different conditions to test (six FoVs for the Velocity Disturbance Rejection Task and two for the Pitch Disturbance Rejection) and each condition is tested twice, the experiment was split up into four blocks. Each block consisted of four runs after which, the participant took the headset off and took a break for about five minutes. Of course they were free to take the headset off at any point and take a break if they felt like it. Each run consisted of a 30 [s] lead in time, followed by a 120 [s] measurement time. During each run, the participants' control inputs, the helicopter's velocity, the helicopter's pitch and the value of the forcing function at that time <sup>148</sup> being recorded by Unity. This data was then exported to be used for the analysis. Additionally, the participants were asked to indicate which part of the screen their vision was focused on. They were also asked to give general comments about how hard or easy they found the task to be, compared to the previously tested condition. After the experiment had concluded, participants were asked to give feedback on general aspects of the experiment, as well as how challenging they found the task overall.

# 5

## Results and Discussion

In the end, 12 people completed the full experiment and their data is used to draw up the conclusions. To accept or reject the hypotheses, one needs to analyse the results of the experiment to see if there is indeed any performance changes across the different testing conditions. The analysis done has a subjective and an objective component. The subjective analysis relies on using the comments gathered during the experiment to get an idea of what FoV the participants thought was the most suitable. Additionally, the participants' comments about where on the screen they were looking to get the visual cues, were used to try and understand how their behaviour changed for the different FoVs. The objective analysis was done by using the 173 city and pitch data gathered in Unity to get an idea of how the pilot error changed with time. This was used as a measure of the pilot performance. Data on the pilot error for all the FoVs was then used to do a one-way Analysis of Variance (ANOVA) test and see if there was some significant difference in pilot performance for the different FoVs. If any significant difference was found, a post-hoc analysis would be done to see between which FoVs, the differences were found.

### 5.1. Subjective Results

175

Much like the objective results, the subjective results will 191 split into those for the velocity disturbance rejection task and the pitch disturbance rejection task. For the pitch disturbance rejection task, the participants claimed that they felt very little difference between the 20 [°] and 140 [°] FoV. The participants' attention was focused entirely on the reticle (shown in Figure 4.7) and the horizon line. This meant that they had no reason to look at the sides of the screen and thus, clipping those out of their view did not seem to affect the participants' behaviour. However, the participants did say that the 140 [°] view did feel more comfortable since the view looked normal and complete.

For the velocity disturbance rejection task, the participants stated that they were mostly focused on the ground texture slightly to the right of the middle of the screen. They claimed that they used this to get an idea of their velocity and would often look up at the horizon to get an idea of their pitch. This trend was present for every participant and for every FoV they tested. As the FoV increased, most participants stated that they found the view more comfortable, yet they found the system harder to control. The participants claim that they felt like they were moving faster for any given input when the FoV was larger hence they felt like the velocity was much harder to bring to zero. A few participants did express the opposite opinion though, where they stated that the higher FoVs were more distracting, due to extra activity in their peripheral vision, and thus it felt harder to focus on the task. These participants however were in the minority. Lastly, the participants stated that, when they pitched up, the ground was harder to see and they often had to pitch down again immediately afterwards. This meant that they found it harder to track parts of the forcing function that forced them to pitch up

### 5.2. Objective Results

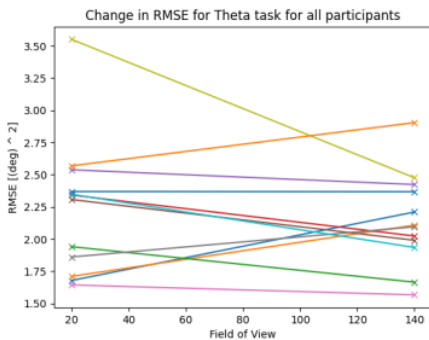
As stated before, each participant tested every 2 condition twice. The output data for each run, for the velocity disturbance rejection task, consisted of the time traces of the forcing function velocity, the

168 velocity induced due to control inputs and the overall velocity of the helicopter. The forcing function and control input velocity were used to get a visual indication of how the run had gone for the participant, and was used merely as a debugging tool to ensure no error 21 had occurred in the data-logging procedure. The overall velocity of the helicopter was used to get the Root-Mean Squared Error (RMSE), as shown in Equation 5.1

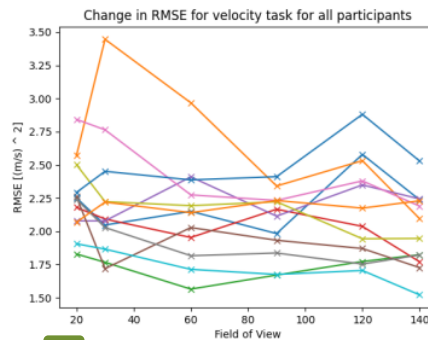
$$\text{RMSE} = \sqrt{\sum_{i=1}^n \frac{(0 - v_i)^2}{n}} \quad (5.1)$$

105 where  $v_i$  is the overall velocity at each time-step and  $n$  is the number of data-samples. For the pitch disturbance rejection task, the output data was the forcing function pitch, the pitch induced by the control inputs and the total pitch angle. Again, the RMSE was used as the performance metric for this type of task. The mean RMSE values are then used to do an ANOVA analysis to see if there were any significant differences between the mean RMSE values for each FoV. If there are significant differences, then a post-hoc analysis can be done to see 102 between which FoVs, the difference lies.

The mean RMSE values for all participants for the two types of tasks are shown in Figure 5.1:



190 (a) Figure showing the RMSE values for the Pitch Disturbance Rejection Task for all participants



(b) Figure showing the RMSE values for the Velocity Disturbance Rejection Task for all participants

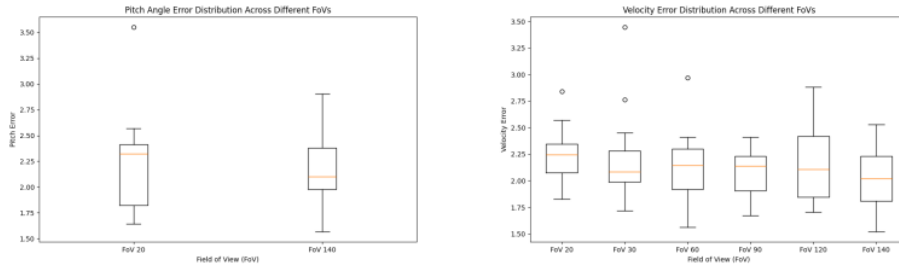
Figure 5.1: Figure showing the RMSE for the Pitch and Velocity Disturbance Rejection Tasks

As can be seen from Figure 5.1a, there does not seem to be much of a difference in performance for the two FoVs across all the participants. For the Velocity Disturbance Rejection Task, there does not seem to be a general trend in performance across the FoVs for the participants. This can be backed up by looking at the results of the ANOVA analysis which are shown in Table 5.1

	Pitch Disturbance Rejection	Velocity Disturbance Rejection
df	5,7	5,7
f-value	0.2371	0.8249
p-value	0.6311	0.5364

75 Table 5.1: Table showing the results of the one-way ANOVA analysis for the two disturbance rejection tasks

The general trend can be better visualised with the boxplots for both tasks, shown in Figure 5.2



(a) Figure showing the boxplot for the Pitch Disturbance Rejection Task (b) Figure showing the boxplot for the Velocity Disturbance Rejection Task for all participants

Figure 5.2: Figure showing the boxplots for the Pitch and Velocity Disturbance Rejection Tasks

### 5.3. Discussion

Based on the subjective results for the Pitch Disturbance Rejection Task, one can clearly see that the results match the theory outlined in chapter 3. Because the participants were looking exclusively at the pitch indicator, they were already getting the maximum amount of feedback they could get for how the pitch was changing. As shown by the visual model of chapter 3, the maximum amount of feedback on how the points in the world move is shown in the middle of the screen [57]. The ANOVA analysis has a p-value that is greater than 0.05 which means that the results fail to reject the null hypothesis that there was a statistical difference between the pilot performance for the FoVs. The lack of any significant trend, and a high p-value, shows a high probability that performance is not impacted by changing FoV for the Pitch Disturbance Rejection Task. Despite this, participants did say that the wider FoV view felt more comfortable, despite the fact that it did not impact performance. This is consistent with the research done by Podzus et al., where they found that the pilots found the larger FoV of the Pimax headset much better than the Varjo headset [6]. This was despite the fact that the pilots found the outer areas of the Pimax's FoV rather blurry. Therefore, one can conclude that, in this context, the presence of a wider FoV had no greater impact than simply providing a more 'natural' and 'comfortable view of the world'. This is especially true considering that the alternate view, the 20 [°] FoV, consisted of mostly a black screen with a small view in the centre.

Analysing the subjective results for the Velocity Tracking Task, one can see some minor correlation between the theory of the visual model and the reality. As said previously in section 5.1, the participants felt like they were moving faster as they progressed from a smaller FoV to a larger FoV. This can be linked to the fact that, in general, the change in the azimuth angles with respect to pitch angle and the distance moved is generally larger for points on the peripheries. Additionally, just the fact that the observers are getting feedback from more points within in their vision as the FoV increases can also lead to this perception of faster motion. Additionally, while it would be useful to know between which FoVs this perception was the strongest, there was no clear consensus when all the subjective comments of the participants was analysed.

Unfortunately, the general trend for the Velocity Disturbance Rejection Task that was expected based on the hypotheses could not be proven with the objective results. As can be seen from Table 5.1 and Figure 5.2b, there is no significant trend between the RMSE and the FoV of the participants. This can be explained with the fact that, for any given input, the participant is seeing more feedback due to the pitch angle rather than velocity. To show this, the output of one experiment run was analysed. This was done for one of the participants whose results were deemed to not be outliers. Their run for the Velocity Disturbance Rejection Task for an FoV of 140 [°] is shown in Figure 5.3:

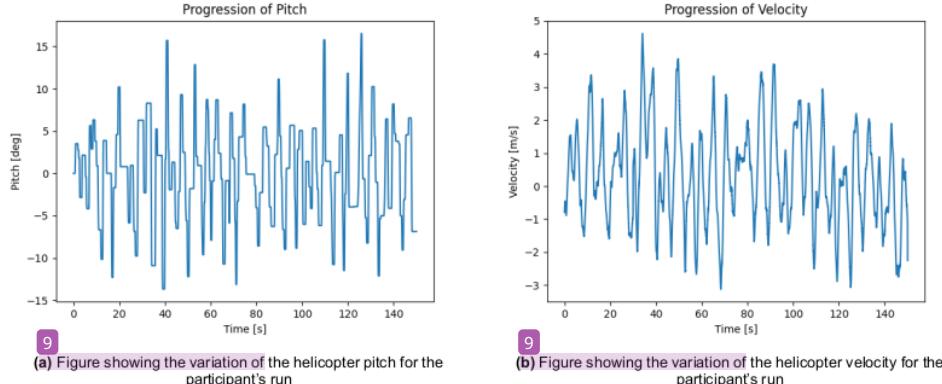


Figure 5.3: Figure showing the variation of the participant's pitch angle and velocity for the chosen run

Based on the pitch and velocity, the values of the partial derivatives of the Azimuth and Elevation angles can be calculated. The value of these derivatives with respect to  $\theta$  will give an indication of how much of the motion seen was due to the change in pitch, and the derivatives with respect to  $(udt)$  will show that with respect to the forward motion. These values can be calculated for two separate viewing angles; where the participant should theoretically have been looking and where they were actually looking.

The first set of derivatives was calculated for where the participant should have been looking i.e. 45 $^{\circ}$  to the left or right. Much like Figure 3.4, the values for the partial derivatives were calculated for all points that lie on this viewing angle, and their values were averaged. The results are shown in Figure 5.4b

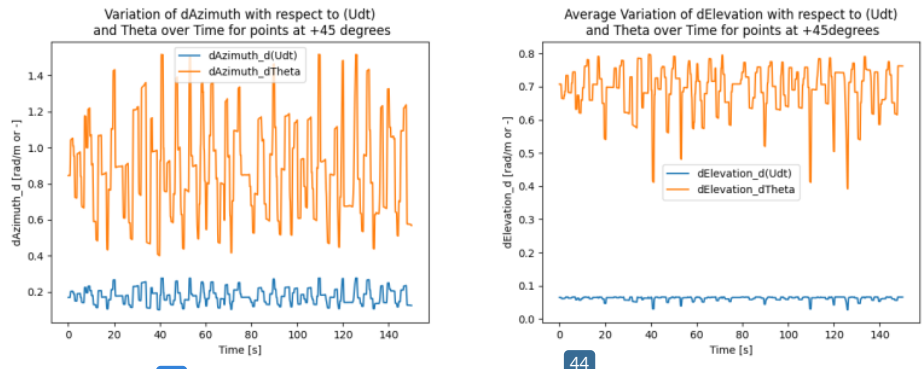
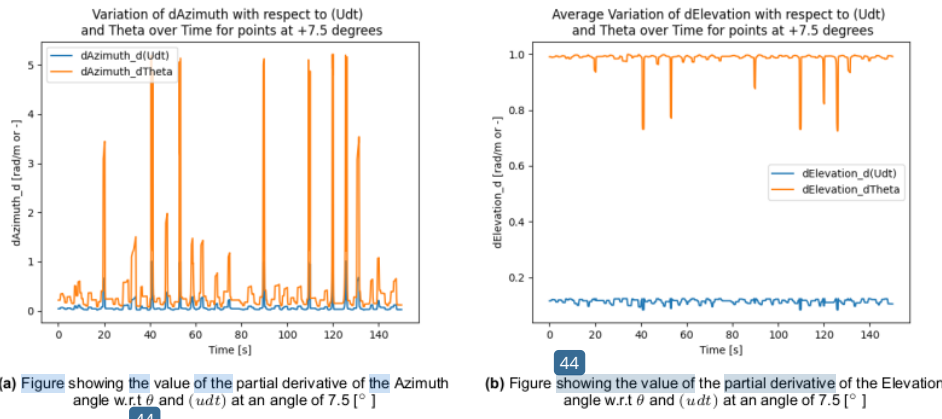


Figure 5.4: Figure showing the value of the partial derivative of the Azimuth and Elevation angles w.r.t  $\theta$  and  $(udt)$  at an angle of 45 $^{\circ}$

As can be seen from Figure 5.4a and Figure 5.4b, the magnitude of the movement caused due to the pitch angle is always magnitudes greater than that caused by the forward motion. This means that at every point on this viewing angle, the observer is likely just seeing more pitch movement than they are forward velocity movement. This is even more clear when one analyses the viewing angle where the participants were actually looking. This angle can be located from the subjective comments where all participants stated that, for the majority of the time, their gaze was focused solely on the ground texture in front, and slightly to the right of them. Now since the participants' comments could not be used to

pinpoint the exact viewing angle where their gaze was fixed, one needs to make a few assumptions. In general, the participants stated that they were always looking at the same general place regardless of the viewing angle; on the ground and slightly to the right. Since this did not change, even for the smallest FoVs, one can assume that this was at a viewing angle  $\leq 10 [^\circ]$  to the right. Therefore, one can analyse the ground points at a viewing angle of  $7.5 [^\circ]$  to the right which means that the effective FoV analysed is  $15 [^\circ]$ . For this, the behaviour of the partial derivatives can be seen in Figure 5.5



**Figure 5.5:** Figure showing the value of the partial derivative of the Azimuth and Elevation angles w.r.t  $\theta$  and  $(udt)$  at an angle of  $7.5 [^\circ]$

As can be seen from Figure 5.5, the difference between the values of the partial derivatives with respect to theta and with respect to forward motion is even greater for this angle. It can thus be theorised that the reason why the participants were looking so close to the centre of the screen, was to get better feedback for how their pitch changed since the feedback for their forward motion stays relatively the same throughout their vision. Indeed, if one compares the values of the partial derivatives with respect to  $(udt)$  for the two viewing angles, it can be seen that the magnitude is almost the same for both cases. For the partial derivatives with respect to the pitch angle however, there is a massive difference in the values of  $\frac{\partial A_z}{\partial \theta}$  for a viewing angle of  $45 [^\circ]$  and  $7.5 [^\circ]$  as per Figure 5.4a and Figure 5.5a. This means that, to an observer, if they shift their gaze from the centre of the screen to  $45 [^\circ]$  to the right, there is very little difference in how much forward motion feedback they are getting. However, there is a significant difference in how much pitch feedback they are getting and thus, they would rather look at the centre of the screen to improve their pitch tracking. This means that the participant can get enough information about their velocity and motion from the centre of the screen, instead of looking at the peripheries (or at a viewing angle of  $45 [^\circ]$  right or left). This is backed up by the comments made by some the participants. They claimed that the presence of a grass texture was enough of a velocity feedback, that they did not feel like they needed to shift their gaze anywhere else. Based on all of this, one can not accept Hypotheses H1 and H2.

The last factor to consider in the experiments, is the potential training effect that could have crept in. This is an effect whereby the participants may end up getting better at doing the tasks, the longer the experiment goes on as they are getting more and more practice. This means that, the participants' performance may be better for the final few conditions tested and this may have no relation with what the condition was. To avoid this, an experiment matrix was created which ensured that each participant did the experiments in a unique order to the participants before them. This matrix is shown and explained in Appendix C. However, some participants did mention that they felt like they were getting better the more runs they did so it is still worth checking if this effect did in fact impact the results. To do this, the participants' run data was organised by run order and an ANOVA analysis was done to see if there was a significant difference between the runs done at the start of the experiment and the runs done at the end. The run-order performance and the boxplot for this, are shown in Figure 5.6a and Figure 5.6b respectively:

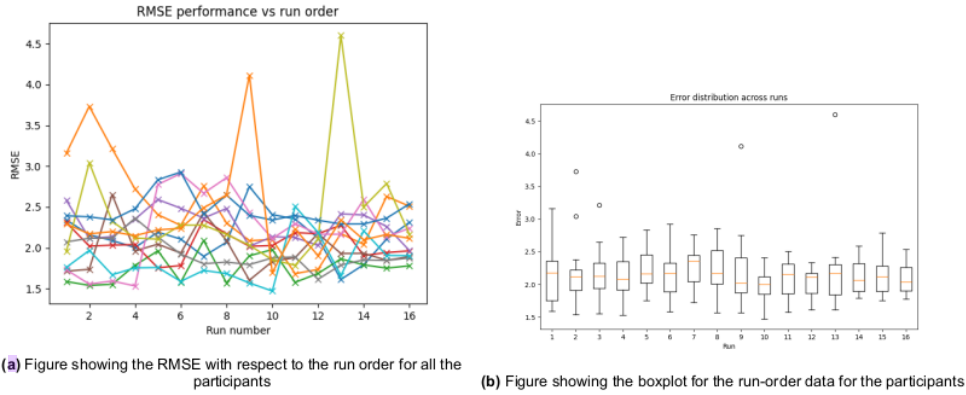


**Figure 5.6:** Figure showing the run order data and the boxplot for this run order data for all the participants

The ANOVA results show an F-statistic value of **0.4262** and a p-value of **0.9699**. Based on this and Figure 5.6b, it can be concluded that there is no significant trend between the run order and performance.

## 5.4. Recommendations

Based on the work done so far, one can outline a few recommendations that can help future researchers obtain more insight into the subject. The broad set of recommendations revolve around the idea that future experiments should be done to a higher fidelity than the one carried out in this project. The main aspect of this would be allowing more degrees-of-freedom in the helicopter, such that the pilot can control the pitch, yaw and roll of the helicopter. The reason why this might produce better results has to do with information found by previous researchers, and information given by a few of the participants of this experiment. Chung et al, during their research, asked participants why they preferred a wider FoV when flying and the pilots stated that a wider FoV helped improve their perception of roll attitude control and longitudinal velocity [7]. This sentiment was backed up by a couple of the experiment participants, who have had some flight experience in either real helicopters, or in helicopter simulators. They stated that, in a normal helicopter with six degrees-of-freedom, they would have used their peripheral vision to decouple their pitch rate from their forward velocity. In this experiment, with the simplified dynamics, that is no longer a factor and so, all they really need to see how fast they are going is any part of the ground texture. Therefore, it is recommended that any further experiments conducted allow for more degrees-of-freedom. Of course, this would require the participants to be trained pilots, or those with some flight experience, but this also opens up the opportunity to use some of the advanced subjective testing techniques mentioned in chapter 2.

The second recommendation is to make use of the head-tracking provided by VR headsets such that the scenery of the simulation moves as the participant moves their head. As stated previously, in this experiment, the participants could only see the scenery present directly in front of them, no matter where they were looking. This was done to ensure that there were no non-linearities with the experiment setup and every participant was essentially doing the same experiment. However, as the subjective comments of the participants revealed, there were some issues associated with this setup. Firstly, whenever participants pitched up, they would often lose sight of the ground texture. In a normal setup with head tracking active, a participant would simply tilt their head downwards and regain sight of the ground, but this was not possible here. As a result, the participants would often pitch back down immediately afterwards to try and regain sight of the ground, making their tracking performance worse whenever they had to correct for a positive velocity disturbance. Additionally, some participants found it uncomfortable and disorientating whenever they moved their head, with the VR headset on, and the scenery did not move. Fortunately, this was mitigated if they kept their head very still throughout the entire run, but that was not always comfortable or natural for them to do. That is why it is recommended to enable head tracking for any future experiments on a similar topic.

The final recommendation has to do with the analysis done in chapter 3. As was mentioned previously, the analysis focused on finding the most salient point in the view, and analysing what happens when this gets clipped out. However, one aspect that this analysis does not take into account is the simple fact that, as the FoV gets wider, the observer is getting information from a larger and larger number of points. Indeed, this can be seen in Table 3.1, where the number of visible points on the ground increases drastically as the FoV increases. While the analysis of chapter 3 shows that all of these points are not necessarily providing the *most* amount of feedback, it does not factor in the fact that they are still providing *some* feedback. Therefore, it is worth investigating in the future, how the increased number of points factors into the feedback one gets from the visual scene, and how it can be used to predict pilot performance.

# 6

## Conclusion

The research objective for this thesis was to investigate how using VR headsets to perform visual cueing can affect the performance of helicopter pilots flying a helicopter simulation. While previous research has done a good job of documenting what changes in a pilot's perception and performance when they use VR headsets in the simulations, one large research gap still exists. This is, namely, on explanation of why these changes occur. Since VR headsets have a near-infinite Field of Regard (FoR) as compared to standard projection systems, they can bypass any FoV restrictions that standard projection systems impose on a simulation. That is why the scope of the research was narrowed to focus on how changing FoV can impact pilot performance. Previous research done into this topic revealed that restricting a pilot's FoV has a generally negative impact on their performance. As FoV is reduced, pilots see less activity in their peripheral vision, which can lead to them underestimating their forward velocity. This leads to them having a harder time in controlling their velocity and position, which can be an extreme detriment in near-ground hover maneuvers where position and velocity control is crucial. This restricted FoV can also start clipping out key features in the out-of-window scene which forces pilots to rely on their instruments more than the out-of-window cues in such maneuvers. This makes pilots uncomfortable since they are trained to rely more on the out-of-window cues for near-ground maneuvers. All of this results in the pilots' effective time delay increasing, and performance worsening.

Armed with this knowledge, one can now look into developing a visual model that tries to investigate what is special about the cues in the peripheral vision. This can attempt to explain why losing peripheral vision view leads to pilots underestimating their speed and just generally having worse performance. To this end, the following research questions were formulated:

1. **What manoeuvre is most impacted by changing Field of View (FoV)?**
2. **What is the predicted pilot behaviour for the critical manoeuvre with changing FoV?**
3. **What is the actual pilot behaviour for the critical manoeuvre with changing FoV?**
4. **What is the overall effect of changing FoV on pilot performance?**
5. **What strategies do pilots employ to overcome adverse effects of changing FoV?**

Based on the literature studied, it was apparent that the motion that would be most impacted by changes in FoV would be the forward/backward motion of the helicopter. As this motion is induced<sup>[137]</sup> by the pilot by pitching forward/backward, the visual model and subsequent experiments were done for a system with two degrees-of-freedom; Pitch and Roll<sup>[147]</sup>. To build up the visual model, the two important features of the visual scene to analyse were the changes in the Azimuth and Elevation Angles of the points in the scene. By calculating how these angles would change for a given motion, one can predict what type of feedback the pilot is getting. This would then be used to try and find the most Salient Viewing Angle, i.e. the horizontal angle at which the pilot can look to get the maximum amount of feedback on how the azimuth and elevation angles change. It was found that, for the Elevation Angle, this was at a viewing angle of  $0 [^{\circ}]$  (i.e. right in front of the observer) and for the Azimuth Angle<sup>[185]</sup> this was at a viewing angle of  $45 [^{\circ}]$  left or right of the observer. Based on these observations, the following Hypotheses were formulated and tested in the Experiment phase:

1. **H1:** If a helicopter has both pitching and forward motion, decreasing the FoV to below 90 [°] should lower a pilot's performance significantly.
2. **H2:** If **43** helicopter has both pitching and forward motion, increasing the FoV to above 90 [°] should have no significant effects **on a pilot's performance** **43**
3. **H3:** If a helicopter has only pitching motion, changing the FoV should have no significant effect **on a pilot's performance.**

The experiments done consisted of participants doing two types of tasks; A Velocity Disturbance Rejection Task<sup>164</sup> (with six different FoVs) and a Pitch Disturbance Rejection Task (with two different FoVs). They took control of a two degree-of-freedom helicopter model and did the tasks while a Pimax 8K-X VR headset was used to do the **57** visual cueing. The pilots' outputs were used to calculate the Root-Mean-Squared-Errors (RMSE) and a one-way ANOVA analysis **was done to see if there was any significant trend in the performance with respect to FoV.**

**58** In 12 participants in total doing the experiments, the results of the ANOVA analysis were **58** follows. For the Pitch Disturbance Rejection Task, the f-statistic had a value of **0.2371** and a p-value of **0.6311**, and for the Velocity Disturbance Rejection Task, the f-statistic had a value of **0.8249** and a p-value of **0.5364**. Based on this, no significant trend can be proven to exist between FoV and pilot performance for both types of Disturbance Rejection Tasks. For the Pitch Disturbance Rejection Task, the participants' subjective comments showed that for both FoVs, their gaze was fixed on the pitch indicator reticle in the middle of the screen. The wider FoV did feel a bit more comfortable to them, but they stated that they did not feel like their performance was affected in any way. This is consistent with the results of the visual model which stated that they should be getting the most feedback from the centre of the screen, and thus would focus on that area the most.

For the Velocity Disturbance Rejection Task, the participants stated that their gaze was always on the ground texture found towards the centre of the screen. This is a departure from what was predicted since the predictions said that they would look at the edge of their vision cone, until an FoV of 90 [°]. For FoVs greater than this, they would keep looking at a viewing angle 45 [°] to **104** right or left of them. They did state that a wider FoV, in general, felt more comfortable and natural **to look at**. To rationalise **the results**, the **values of the derivatives of the Azimuth and Elevation angles with respect to pitch and forward motion for one of the runs a participant did**. This showed that the values of the angles with respect to forward motion were not that different for a viewing angle of 7.5 [°] and 45 [°]. Conversely however, the value of  $\frac{\partial A_z}{\partial \theta}$  had very high peaks at 7.5 [°], which were absent for a viewing angle of 45 [°]. This leads to the conclusion that shifting gaze from the centre of the screen (i.e approximately 7.5 [°]) to the right would have offered no change in the velocity feedback the participants got, however, it would have significantly reduced the pitch feedback they got. That is why, they chose to keep looking **2**wards the centre of the screen instead of shifting their gaze as FoV increased.

The goal of this thesis was to try and find a link between the FoV and the pilot performance, and it was chosen that this would be done by looking at how losing information in your peripheries affects the performance. Based on the research questions stated above, this goal was accomplished to a satisfactory level. The visual model made, showed that the pilot was at the risk of losing the feedback of the most salient point, when it comes to velocity feedback, if their FoV was reduced by a significant degree. The biggest question mark surrounding the visual model however, was the idea that even if this point gets clipped out, how much would this actually impact pilot perception. In the end, the results showed that the answer to that question is that the pilot perception remains somewhat the same. Regardless, the experiments and the visual model are an excellent starting point for future researchers, and the following recommendations can certainly help them learn more in this field. The first among them, is the idea that such experiments should be re-done, but with a higher fidelity when it comes to the degrees-of-freedom of the helicopter. Previous research, and comments made by some of the participants who had significant flight experience, shows that peripheral vision may be crucial for pilots to decouple different modes of motion and rotation in a helicopter. This means that, for any experiment that wishes to investigate impact of peripheral vision on flight, the helicopter model and subsequent experimental task done with it, must allow for multiple degrees-of-freedom in motion and rotation. Secondly, any experiments involving VR headsets should enable head tracking on the headsets. This was disabled in this project to simplify the analysis, but enabling it offers a more in-depth look into the impact of VR headsets and offers a more comfortable experience to the pilots. Last, but

not least, any visual model that aims to achieve the same goals as this thesis, should try and account for how the number of visible points can affect pilot perception. In the analysis done for this thesis, the fact that as FoV increases, the pilots just see more points and get feedback from more points, was not really taken into account. Therefore, it is recommended that future visual models try and incorporate this factor into their analysis.

## References

- [1] LT Adam T Biggs, Daniel J Geyer, Valarie M Schroeder, F Eric Robinson, and John L Bradley. "Adapting Virtual Reality and Augmented Reality Systems for Naval Aviation Training". en. In: (Oct. 2018). 59
- [2] Y. Çetin, E. Yilmaz, and Y.Y. Çetin. "Evaluation of visual cues of three-dimensional virtual environments for helicopter simulators". English. In: *Journal of Defense Modeling and Simulation* 9.4 (2012), pp. 347–360. ISSN: 1557380X (ISSN). DOI: 10.1177/1548512911422240. URL: <https://www.scopus.com/inward/record.uri?eid=2-s2.0-84869804421&doi=10.1177/2f1548512911422240&partnerID=40&md5=9654d90ee440c5962edc8bf59abf243e>. 31
- [3] Eric D. Ragan. "The Effects of Higher Levels of Immersion on Procedure Memorization Performance and Implications for Educational Virtual Environments". en. In: *Presence: Teleoperators and Virtual Environments* 19.6 (Dec. 2010), pp. 527–543. ISSN: 1054-7460. DOI: 10.1162/pres\_a\_00016. URL: <https://direct.mit.edu/pvar/article/19/6/527-543/18782> (visited on 02/16/2024). 8
- [4] R. A. Hess and W. Siwakosit. "Assessment of Flight Simulator Fidelity in Multitask Tasks Including Visual Cue Quality". en. In: *Journal of Aircraft* 38.4 (July 2001), pp. 607–614. ISSN: 0021-8669, 1533-3868. DOI: 10.2514/2.2836. URL: <https://arc.aiaa.org/doi/10.2514/2.2836> (visited on 03/04/2024). 34
- [5] R.A. Hess. "Application of a model-based flight director design technique to a longitudinal hover task". English. In: *Journal of Aircraft* 14.3 (1977), pp. 265–271. ISSN: 00218669 (ISSN). DOI: 10.2514/3.44590. URL: <https://www.scopus.com/inward/record.uri?eid=2-s2.0-0017471090&doi=10.2514/3.44590&partnerID=40&md5=31029c8c59603239bfeeedd44a159bbf>.
- [6] Philipp Podzus, Michael Jones, Royal Netherlands Aerospace Centre (NLR), Jur Crijnen, Stefan van't Hoff, and Paul Breed. "Evaluation of Simulator Cueing Fidelity for Rotorcraft Certification by Simulation". en. In: *Proceedings of the Vertical Flight Society 78th Annual Forum*. Fort Worth, Texas: The Vertical Flight Society, May 2022, pp. 1–11. DOI: 10.4050/F-0078-2022-17572. URL: <https://vtol.org/store/product/evaluation-of-simulator-cueing-fidelity-for-rotorcraft-certification-by-simulation-17572.cfm> (visited on 02/09/2024). 63
- [7] William Chung, Barbara Sweet, Mary Kaiser, and Emily Lewis. "Visual Cueing Effects Investigation for a Hovering Task". en. In: *AIAA Modeling and Simulation Technologies Conference and Exhibit*. Austin, Texas: American Institute of Aeronautics and Astronautics, Aug. 2003. ISBN: 978-1-62410-091-8. DOI: 10.2514/6.2003-5524. URL: <https://arc.aiaa.org/doi/10.2514/6.2003-5524> (visited on 02/19/2024). 61
- [8] Sheldon Baron, Roy Lancraft, and Greg Zacharias. "PILOT/VEHICLE MODEL ANALYSIS OF VISUAL AND MOTION CUE REQUIREMENTS IN FLIGHT SIMULATION." undefined. In: *NASA Contractor Reports* 3312 (1980). ISSN: 05657059 (ISSN). URL: <https://ntrs.nasa.gov/citations/19800020900>. 66
- [9] Adolph Atencio Jr. *Fidelity Assessment of a UH-60A Simulation on the NASA Ames Vertical Motion Simulator.pdf*. English. Tech. rep. California, USA: NASA, 1993, p. 324.
- [10] R.V. Kenyon and E.W. Kneller. "The effects of field of view size on the control of roll motion". In: *IEEE Transactions on Systems, Man, and Cybernetics* 23.1 (Feb. 1993), pp. 183–193. ISSN: 00189472. DOI: 10.1109/21.214776. URL: <http://ieeexplore.ieee.org/document/214776/> (visited on 02/29/2024). 40
- [11] P. Pretto, M. Ogier, H.H. Bülthoff, and J.-P. Bresciani. "Influence of the size of the field of view on motion perception". en. In: *Computers & Graphics* 33.2 (Apr. 2009), pp. 139–146. ISSN: 00978493. DOI: 10.1016/j.cag.2009.01.003. URL: <https://linkinghub.elsevier.com/retrieve/pii/S0097849309000132> (visited on 03/08/2024).

- [12] H.B.-L. Duh, J.W. Lin, R.V. Kenyon, D.E. Parker, and T.A. Furness. "Effects of field of view on balance in an immersive environment". en. In: *Proceedings IEEE Virtual Reality 2001*. Yokohama, Japan: IEEE Comput. Soc, 2001, pp. 235–240. ISBN: 978-0-7695-0948-8. DOI: 10.1109/VR.2001.913791. URL: <http://ieeexplore.ieee.org/document/913791/> (visited on 02/16/2024).
- [13] R.H. Hoh, Inc Hoh Aeronautics, United States Federal Aviation Administration Research, and Development Service. *The Effects of Degraded Visual Cueing and Divided Attention on Obstruction Avoidance in Rotorcraft*. DOT/FAA/90/40. U.S. Federal Aviation Administration, Research and Development Service, 1990. URL: <https://apps.dtic.mil/sti/pdfs/ADA380260.pdf>.
- [14] Helen Marie Baker. *AN INVESTIGATION OF PILOT MODELLING FOR HELICOPTER HANDLING QUALITIES ANALYSIS*. English. 2010. URL: <https://livrepository.liverpool.ac.uk/317402/1/539469.pdf>.
- [15] L. Iseler. "Piloted simulator investigation of category A civil rotorcraft terminal area cockpit displays". English. In: *Journal of the American Helicopter Society* 43.3 (1998). Publisher: American Helicopter Society, pp. 185–193. ISSN: 00028711 (ISSN). DOI: 10.4050/jahs.43.185. URL: <https://www.scopus.com/inward/record.uri?eid=2-s2.0-0032118508&doi=10.4050%2fjahs.43.185&partnerID=40&md5=c3843e777cb4a6df3137ff7c2c729dde>.
- [16] F. Erazo, S. Jennings, K. Ellis, and J. E. "Effects of Hover Symbology Display Scaling on Performance and Workload". English. In: *Journal of the American Helicopter Society* 66.2 (2021). Publisher: American Helicopter Society. ISSN: 00028711 (ISSN). DOI: 10.4050/JAHS.66.022002. URL: <https://www.scopus.com/inward/record.uri?eid=2-s2.0-85158890400&doi=10.4050%2fJAHS.66.022002&partnerID=40&md5=590e1feb8e37c135492944847765c14b>.
- [17] J. Moon, J.C. Domercant, and D. Mavris. "A simplified approach to assessment of mission success for helicopter landing on a ship". English. In: *International Journal of Control, Automation and Systems* 13.3 (2015). Publisher: Institute of Control, Robotics and Systems, pp. 680–688. ISSN: 15986446 (ISSN). DOI: 10.1007/s12555-013-0092-y. URL: <https://www.scopus.com/inward/record.uri?eid=2-s2.0-84930091516&doi=10.1007%2fs12555-013-0092-y&partnerID=40&md5=313d12bcf83aed90dd3a29da6e8a2e17>.
- [18] E. Bachelder and D. McRuer. "Perception-based synthetic cueing for night-vision device rotorcraft hover operations". English. In: *Proceedings of SPIE-The International Society for Optical Engineering* 4711 (2002), pp. 377–388. ISSN: 0277786X (ISSN). DOI: 10.1117/12.478888. URL: <https://www.scopus.com/inward/record.uri?eid=2-s2.0-0036029916&doi=10.1117/12.478888&partnerID=40&md5=904e88c9c3bdb9670cafe61372ac6486>.
- [19] W.A. Memon, M.D. White, G.D. Padfield, N. Cameron, and L. Lu. "Helicopter Handling Qualities: A study in pilot control compensation". English. In: *Aeronautical Journal* 116.1295 (2022). Publisher: Cambridge University Press, pp. 152–186. ISSN: 00019240 (ISSN). DOI: 10.1017/aer.2021.87. URL: <https://www.scopus.com/inward/record.uri?eid=2-s2.0-85119505269&doi=10.1017%2faer.2021.87&partnerID=40&md5=bca175eea89c05ae83d683e9096ac907>.
- [20] Duane McRuer and Ezra Krendel. "Mathematical Models of Human Pilot Behavior". en. In: (Jan. 1974), p. 83.
- [21] Francesca Roncolini and Giuseppe Taranta. "Virtual pilot: a review of the human pilot's mathematical modeling techniques". Eng. In: (2023). Artwork Size: 14 pages Medium: PDF Publisher: Proceedings of the Aerospace Europe Conference - EUCASS - CEAS - 2023, 14 pages. DOI: 10.13009/EUCASS2023-589. URL: <https://www.eucass.eu/doi/EUCASS2023-589.pdf> (visited on 09/11/2024).
- [22] D.M. Pool, P.M.T. Zaal, H.J. Damveld, M.M. Van Paassen, and M. Mulder. "A Cybernetic Approach to Assess Flight Simulator Motion Fidelity". en. In: *IFAC Proceedings Volumes* 41.13 (2010), pp. 380–385. ISSN: 14746670. DOI: 10.3182/20100831-4-FR-2011.00067. URL: <https://linkinghub.elsevier.com/retrieve/pii/S1474667015325623> (visited on 02/28/2024).
- [23] D.M. Pool and P.M.T. Zaal. "A Cybernetic Approach to Assess the Training of Manual Control Skills". en. In: *IFAC-PapersOnLine* 49.19 (2016), pp. 343–348. ISSN: 24058963. DOI: 10.1016/j.ifacol.2016.10.588. URL: <https://linkinghub.elsevier.com/retrieve/pii/S2405896316321796> (visited on 02/20/2024).

- [24] P. M. T. Zaal, D. M. Pool, Q. P. Chu, M. M. Van Paassen, M. Mulder, and J. A. Mulder. "Modeling Human Multimodal Perception and Control Using General Maximum Likelihood Estimation". en. In: *Journal of Guidance, Control, and Dynamics* 32.4 (July 2009), pp. 1089–1099. ISSN: 0731-5090, 1533-3884. DOI: 10.2514/1.42843. URL: <https://arc.aiaa.org/doi/10.2514/1.42843> (visited on 02/28/2024).
- [25] Marinus M. Van Paassen and Max Mulder. "Identification of Human Control Behavior". In: *International Encyclopedia of Ergonomics and Human Factors*. Jan. 2006, pp. 400–407. ISBN: ISBN 041530430X.
- [26] George E Cooper and P Harper. "THE USE OF PILOT RATING IN THE EVALUATION OF AIRCRAFT HANDLING QUALITIES". en. In: *NASA Technical Note* (Apr. 1969). URL: <https://ntrs.nasa.gov/citations/19690013177>.
- [27] A.H. Roscoe, G.A. Ellis, Royal Aerospace Establishment (Great Britain), and Great Britain Ministry of Defence Procurement Executive. *A Subjective Rating Scale for Assessing Pilot Workload in Flight: A Decade of Practical Use*. Technical report Royal Aerospace Establishment (Great Britain)). Procurement Executive, Ministry of Defence, 1990. URL: [https://books.google.nl/books?id=0\\_eJXwAACAAJ](https://books.google.nl/books?id=0_eJXwAACAAJ).
- [28] Gareth D. Padfield. *Helicopter Flight Dynamics: The Theory and Application of Flying Qualities and Simulation Modelling*. en. 1st ed. Wiley, Jan. 2007. ISBN: 978-1-4051-1817-0 978-0-470-69184-7. DOI: 10.1002/9780470691847. URL: <https://onlinelibrary.wiley.com/doi/book/10.1002/9780470691847> (visited on 03/28/2024).
- [29] 10. Mulder and J. A. Mulder. "Cybernetic Analysis of Perspective Flight-Path Display Dimensions". en. In: *Journal of Guidance, Control, and Dynamics* 28.3 (May 2005), pp. 398–411. ISSN: 0731-5090, 1533-3884. DOI: 10.2514/1.6646. URL: <https://arc.aiaa.org/doi/10.2514/1.6646> (visited on 02/29/2024).
- [30] Richard Musil. *HMD Geometry Database*. en. Dec. 2023. URL: <https://risa2000.github.io/hmdgdb/> (visited on 04/22/2024).
- [31] Appendix 4B The Three Case Helicopters: Lynx 530105 and Puma | Helicopters & Aircrafts. en-US. URL: <http://heli-air.net/2016/03/26/appendix-4b-the-three-case-helicopters-lynx-bo105-and-puma/> (visited on 08/25/2024).
- [32] P. M. T. Zaal, D. M. Pool, J. De Bruin, M. Mulder, and M. M. Van Paassen. "Use of Pitch and Heave Motion Cues in a Pitch Control Task". en. In: *Journal of Guidance, Control, and Dynamics* 32.2 (Mar. 2009), pp. 366–377. ISSN: 0731-5090, 1533-3884. DOI: 10.2514/1.39953. URL: <https://arc.aiaa.org/doi/10.2514/1.39953> (visited on 03/28/2024).
- [33] Teerd Groot, Herman Damveld, M. Mulder, and M. Van Paassen. "Effects of Aeroelasticity on the Pilot's Psychomotor Behavior". en. In: *AIAA Atmospheric Flight Mechanics Conference and Exhibit*. Keystone, Colorado: American Institute of Aeronautics and Astronautics, Aug. 2006. ISBN: 978-1-62410-045-1. DOI: 10.2514/6.2006-6494. URL: <https://arc.aiaa.org/doi/10.2514/6.2006-6494> (visited on 03/29/2024).
- [34] Waldemar Karwowski, ed. *International encyclopedia of ergonomics and human factors*. Vol. 3. 2. ed. Vol. 3. Boca Raton, Fla.: CRC Press/Taylor & Francis, 2006. ISBN: 978-0-415-30430-6.
- [35] Pimax "8K" X 3D Update Enables 90Hz Refresh Rate With Max Resolution on GeForce 30-series GPUs. URL: <https://www.roadtovr.com/pimax-8k-x-90hz-refresh-rate-native-mode-firmware/> (visited on 05/28/2024).
- [36] Valve Index Base 3D Model - TurboSquid 1670059. en. URL: <https://www.turbosquid.com/3d-models/valve-index-base-3d-model-1670059> (visited on 05/28/2024).
- [37] Jelte E. Bos. "Less sickness with more motion and/or mental distraction". en. In: *Journal of Vestibular Research* 25.1 (Mar. 2015), pp. 23–33. ISSN: 18786464, 09574271. DOI: 10.3233/VES-150541. URL: <https://www.medra.org/servlet/aliasResolver?alias=iopspress&doi=10.3233/VES-150541> (visited on 08/29/2024).
- [38] Max Mulder. *Cybernetics of tunnel-in-the-sky displays*. en. Delft: Delft Univ. Press, 1999. ISBN: 978-90-407-1963-9.

# A

## Alternate Visual Model

### 2.1. Background

The goal of this chapter is to create a visual model to try and predict how pilot behaviour will change as the FoV is changed. The literature study has shown that the pilot performance does indeed degrade but the goal is to try and find if the exact nature and extent of the degradation can be predicted. As the FoV decreases, it can be intuited that the pilot's perception of velocity also decreases. Duh et al and Pretto et al found out that this was due to the fact that there is less motion in the pilot's peripheries which degrades their immersion and performance [12][11]. To this end, one can try and quantify how this velocity perception degradation occurs by looking at how perspective projection occurs. This is outlined in Figure A.1:

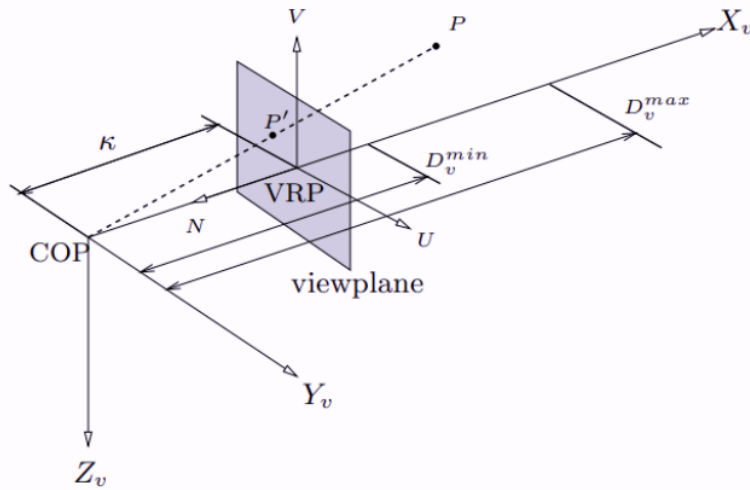


Figure A.1: Figure showing the perspective projection method [38]

where HSC and VSC are the horizontal and vertical screen size, and HGFOV and VGFOV are the horizontal and vertical FoV. Here, the COP is the Centre of Projection with  $X_v$ ,  $Y_v$  and  $Z_v$  being the viewing axis. A point P is projected onto the viewplane at position,  $P'$ . The viewplane has the vertical axis, V and horizontal axis, U. The viewplane is a distance  $\kappa$  away from the COP.  $D_v^{min}$  and  $D_v^{max}$  are the minimum and maximum viewing distances and they represent the front and back planes of the viewing frustum. That means that any point not within these two planes gets clipped out.

$\kappa$  can be calculated using Equation A.1[38]:

$$\kappa = \frac{HSC}{2 \tan(HGFOV/2)} = \frac{VSC}{2 \tan(VGFOV/2)} \quad (\text{A.1})$$

Using this, the position  $P'$  of an object,  $P$  in the viewing plane can be given by [38]:

$$\begin{aligned} u_p &= \kappa \left( \frac{y_p^v}{x_p^v} \right) \\ v_p &= -\kappa \left( \frac{z_p^v}{x_p^v} \right) \end{aligned} \quad (\text{A.2})$$

where  $x_p^v$ ,  $y_p^v$  and  $z_p^v$  are the x, y and z coordinates of point  $P$  in the Viewing axis. Do note that the Viewing axis is aligned with the helicopter's body axis. These positions can be calculated using Equation A.3 [38]:

$$\underline{x}_p^v = [x_p^v, y_p^v, z_p^v] = R_X(\phi)R_Y(\theta)R_Z(\psi) \cdot (\underline{x}_p^w - \underline{x}_{COP}^w), \quad (\text{A.3})$$

where  $\underline{x}_p^w$  are the coordinates of point  $P$  in the World axis and  $\underline{x}_{COP}^w$  are the coordinates of the COP in the World axis. The orthogonal rotation matrices  $R_X(\phi)$ ,  $R_Y(\theta)$  and  $R_Z(\psi)$  are given by [38]:

$$\underbrace{\begin{pmatrix} 1 & 0 & 0 \\ 0 & \cos \phi & \sin \phi \\ 0 & -\sin \phi & \cos \phi \end{pmatrix}}_{R_X} \underbrace{\begin{pmatrix} \cos \theta & 0 & -\sin \theta \\ 0 & 1 & 0 \\ \sin \theta & 0 & \cos \theta \end{pmatrix}}_{R_Y} \underbrace{\begin{pmatrix} \cos \psi & \sin \psi & 0 \\ -\sin \psi & \cos \psi & 0 \\ 0 & 0 & 1 \end{pmatrix}}_{R_Z}. \quad (\text{A.4})$$

with  $\theta$  being the pitch angle,  $\phi$  being the roll angle and  $\psi$  being the yaw angle.

All of this can be used to then see how the velocity of  $P$  in the viewing plane changes for a discrete motion. This is done using the image field equations [38]:

$$\begin{aligned} \dot{u}_p &= \underbrace{(-\kappa v^b + u_p u^b) / x_p^b}_{\dot{u}_p^T} + \underbrace{(-\kappa^2 r^b - \kappa v_p p^b - u_p v_p q^b - u_p^2 r^b) / \kappa}_{\dot{u}_p^R}; \\ \dot{v}_p &= \underbrace{(+\kappa w^b + v_p u^b) / x_p^b}_{\dot{v}_p^T} + \underbrace{(-\kappa^2 q^b + \kappa u_p p^b - u_p v_p r^b - v_p^2 q^b) / \kappa}_{\dot{v}_p^R}. \end{aligned} \quad (\text{A.5})$$

The image field equations allows the calculation of the velocity of point  $P$  on the wplane by taking into account the helicopter's body velocity in all three axes ( $u^b$ ,  $v^b$  and  $w^b$ ) and its attitude rates ( $p^b$ ,  $q^b$  and  $r^b$ ). Additionally, it can be seen that the velocity components of point  $P$  are split into translational components ( $\dot{u}_p^T$  and  $\dot{v}_p^T$ ) and rotational components ( $\dot{u}_p^R$  and  $\dot{v}_p^R$ )

60

The goal of this analysis is to try and find a point in the world that offers the maximum amount of velocity feedback to the pilot. It is assumed that, if such a point exists and is independent of the FoV, then when the FoV is lowered, this point would get clipped out of the view. This means that the pilot would no longer see the most salient point of the environment and would need to shift their gaze to the next-most salient point. Presumably, this would result in the pilot getting feedback of their velocity being much smaller and could be the reason for why people tend to underestimate their velocity as FoV shrinks, as per the findings of Pretto et al and others [11][12]. To quantify how much velocity feedback the pilot is getting, it was decided that the key parameter to analyse would be the ratio of the velocity of point  $P$  on the viewing plane (i.e. the on-screen velocity) and the actual velocity of the observer (or helicopter). Thus, the greater the ratio, the greater the velocity feedback. The reason why the ratio was chosen as a metric instead of the on-screen velocity is because it allows one to normalise velocity and allow for comparison between the values obtained for different observer velocities and attitude rates. Lastly, this can also be useful in providing some key FoVs that can be used for the experiment phase. The first step in this analysis is to simplify Equation A.5. As shown in chapter 2, the performance of the pilot degrades the most as FoV changes for forward translational motion. As such, it is worth analysing cases where the helicopter would move forward and backwards to see if the point of maximum feedback

does exist. However, since helicopters must change their pitch to change their forward velocity, it is also worth considering the impact of the pitching motion. Thus, for this analysis, the helicopter motion to investigate involves only forward velocity,  $u^b$  and pitch (which results in a pitch rate,  $q^b$ ). This means that one can remove the other velocity and attitude rate terms from Equation A.5 to give:

$$\begin{aligned}\dot{u}_p &= \underbrace{\frac{u_p u^b}{x_p^b}}_{\dot{u}_p^T} + \underbrace{\frac{-u_p v_p q^b}{\kappa}}_{\dot{u}_p^R} \\ \dot{v}_p &= \underbrace{\frac{v_p u^b}{x_p^b}}_{\dot{v}_p^T} + \underbrace{\frac{-\kappa^2 q^b - v_p^2 q^b}{\kappa}}_{\dot{v}_p^R}.\end{aligned}\quad (\text{A.6})$$

The ratio of on-screen velocity to actual velocity, henceforth called  $\Delta$  is given by:

$$\Delta = \frac{\sqrt{(\dot{u}_p^T)^2 + (\dot{v}_p^T)^2}}{u^b} + \frac{\sqrt{(\dot{u}_p^R)^2 + (\dot{v}_p^R)^2}}{\sqrt{(q z_p^v)^2 + (q x_p^v)^2}}\quad (\text{A.7})$$

As can be seen in Equation A.7, the ratio is calculated by first getting the magnitude of the velocities caused by the translations and rotations, and then dividing by the corresponding motion that caused the velocities. For the rotational components, the divisor is the magnitude of the cross product between the rotational rate of the helicopter in all three axis, and the 3D-coordinate<sup>67</sup> the position  $\underline{x}_p^v$ . This is done because the numerator of the expression is linear velocity in [m/s] while the pitch rate is an angular velocity in [rad/s]. Thus, the angular velocity<sup>85</sup> needs to be converted to a linear velocity. Since there is only rotation in one axis, the cross product is given by:

$$\begin{aligned}\vec{v} &= \vec{\omega} \times \vec{r} \\ \vec{v} &= \begin{pmatrix} 0 \\ 0 \\ 160 \end{pmatrix} \times \begin{pmatrix} x \\ y \\ z \end{pmatrix} \equiv \begin{vmatrix} \hat{i} & \hat{j} & \hat{k} \\ 0 & q & 0 \\ x & y & z \end{vmatrix} \\ \vec{v} &= \hat{i}(q \cdot z - 0) - \hat{j}(0 \cdot z - 0 \cdot x) + \hat{k}(0 \cdot y - q \cdot x) = \begin{pmatrix} qz \\ 0 \\ -qx \end{pmatrix}\end{aligned}\quad (\text{A.8})$$

It is now apparent that  $\dot{u}_p$  and  $\dot{v}_p$  are affected by changes in two main categories:

- **Changes in FoV:** This can either mean a change in the value of  $\kappa$  as per Equation A.1 or can mean keeping  $\kappa$  the same and simply making the view frustum smaller.
- **Change in helicopter motion:** This means that  $u^b$  and  $q^b$  change

Therefore, one can analyse what the affect is on the ratio of on-screen velocity to helicopter body velocity of these two categories. The individual conditions to analyse are:

1. Change the FoV in Equation A.1 to change the value of  $\kappa$
2. Use the same value of  $\kappa$  for all FoVs but analyse only the positions of P that would be visible for this FoV.
3. Analyse the change in on-screen velocity for 1 Degree-of-Freedom (DOF) by only changing  $u^b$
4. Analyse the change in on-screen velocity for 1 DOF by only changing  $q^b$
5. Analyse the change in on-screen velocity for 2 DOF by changing both  $u^b$  and  $q^b$

The difference between the first and second condition is simply the fact that the first condition takes into account the projection effects of changing FoV, while the second condition ignores the projection effects and simply focuses on the changes in how much can be seen with changing FoVs. This is highlighted by the examples shown in Figure A.2:

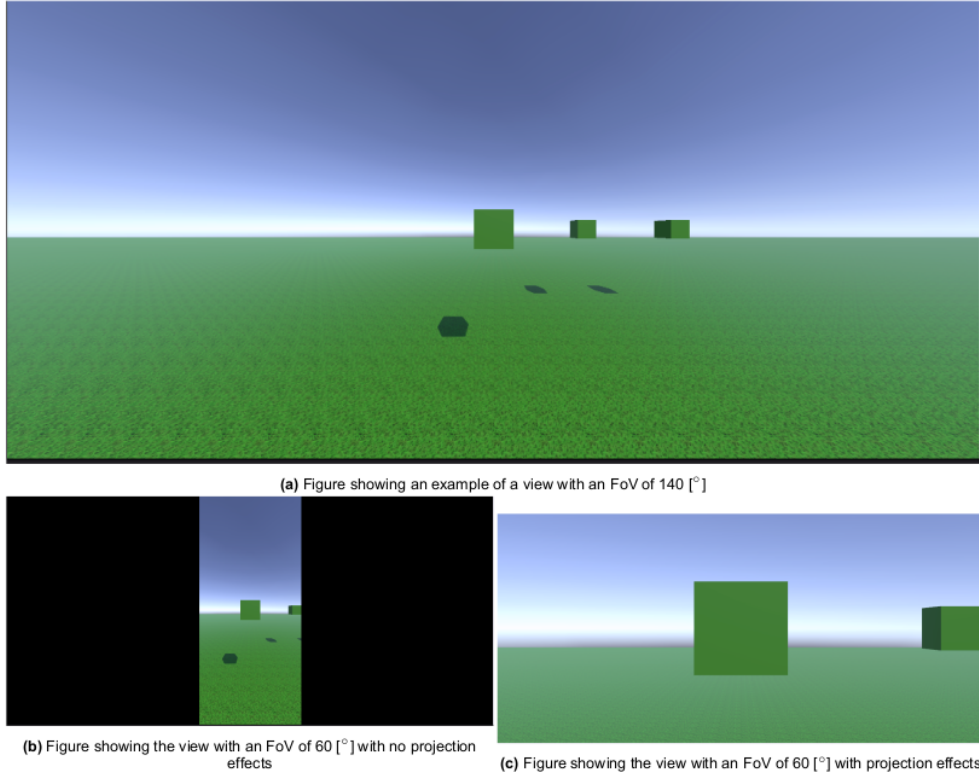


**Figure A.2:** Figure showing the difference in projection effects and no projection effects on the view

The standard view with an FoV of 140 [ $^{\circ}$ ] can be seen in Figure A.2a. If one was to restrict the FoV by keeping  $\kappa$  constant (no projection effects), then the view would look like Figure A.2b. As is apparent, some parts of the scenery get clipped out but the objects seem to be at the same distance as before. Conversely, if projection effects were taken into account, like in Figure A.2c, then the objects appear much closer than they actually are.

Since the changes in on-screen velocity can only be analysed if the helicopter is moving, there are six cases to analyse which can be seen in Table A.1:

**Table A.1:** Table showing the six cases to analyse

	94°s constant	$\kappa$ changes
1 DOF ( $u^b$ )	Case 1	Case 4
1 DOF ( $q^b$ )	Case 2	Case 5
2 DOF	Case 3	Case 6

For each of the cases, seven FoVs were tested: **20, 40, 60, 80, 100, 120 and 140 [deg]**. For each case, the values of  $D_v^{min}$  and  $D_v^{max}$  were set to **1 [m]** and **10 [m]** respectively and a list of  $X_v$  values in this range (in increments of 0.1 [m]) were generated. Using these values and each of the FoVs, a full list of  $Y_v$  and  $Z_v$  values were generated which resulted in all possible permutations of coordinates for a point P within the view frustum for each FoV. The number of possible positions to analyse for each FoV is shown in Table A.2:

**Table A.2:** Table showing the number of positions to analyse for each FoV

FoV [deg]	Number of positions
20	74401
40	150677
60	237039
80	343186
100	485900
120	704947
140	116708

For each case, the value of the ratio of on-screen velocity and actual velocity was calculated for all the possible positions and the position which gave the highest ratio was chosen. The horizontal and vertical viewing angle ( $VA_H$  and  $VA_V$ ) for this optimal position was then calculated, based on Equation A.9, to see where in the pilot's FoV this was located:

$$\begin{aligned} VA_H &= 2 \arctan \frac{Y_{optimal}}{X_{optimal}} \\ VA_V &= 2 \arctan \frac{Z_{optimal}}{X_{optimal}} \end{aligned} \quad (A.9)$$

The values of the free variables in Equation A.6 for each of the cases are presented in Table A.3:<sup>123</sup>

**Table A.3:** Table showing the values of the parameters used for each Case

Case	$u^b$ [m/s]	$\theta$ [deg]	$q^b$ [rad/s]	HSC [m]	$\kappa$ [m]
1	<b>2</b>	0	0	0.4878	0.088
2	0	-5	<b>-0.087</b>	0.4878	0.088
3	<b>2</b>	-5	<b>-0.087</b>	0.4878	0.088
4	<b>2</b>	0	0	0.4878	<b>Variable</b>
5	0	-5	<b>-0.087</b>	0.4878	<b>Variable</b>
6	<b>2</b>	-5	<b>-0.087</b>	0.4878	<b>Variable</b>

The value of  $\kappa$  for the first three cases is calculated using the horizontal screen size and the horizontal FoV. The reason this was done is because the end goal is to do experiments to accept or reject any hypotheses this analysis presents. The experiments will be done using a Pimax 8KX VR headset that has a maximum horizontal FoV of 140 [ $^\circ$ ] and a maximum vertical FoV of 100 [ $^\circ$ ] [35]. Additionally, the vertical FoV does not change when one changes the FoV settings on the actual headset which is why it was decided that, for this analysis and the experiments,  $\kappa$  will be calculated using the horizontal screen size of the Pimax (**0.4878** [m]) and the max horizontal FoV (140 [ $^\circ$ ]). Lastly, the different positions generated in Table A.2 were generated by looking at the view frustums achieved with a vertical FoV of 100 [ $^\circ$ ] and the horizontal FoVs given in the table.

The values of  $u^b$  and  $\theta$  used in the analysis were chosen such that they would be representative of a helicopter in a hover scenario. In such a scenario, a helicopter pilot would apply small pitch angles onto the helicopter to keep it steady which would result in small velocities. However, the velocity and pitch angle should still be large enough such that there is a noticeable change in the on-screen velocities so it was decided to use the aforementioned values.

## A.2. Results

**TODO: INTRODUCE SUBSECTIONS**

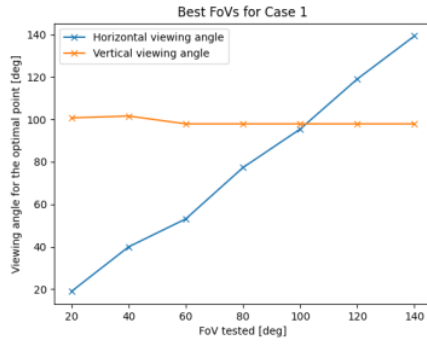
### A.2.1. Constant $\kappa$

For the first of the three cases where  $\kappa$  was kept constant, the results can be seen in Table A.4:

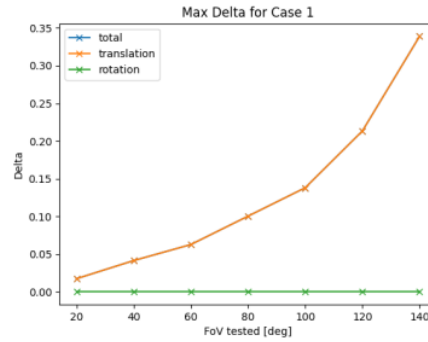
**Table A.4:** Table showing the optimal position, the horizontal and vertical viewing angle of this position and the value of  $\Delta$  for each FoV for Case 1

FoV [deg]	Optimal Position (x,y,z) [m]	Horizontal Viewing angle [deg]	Vertical Viewing Angle [deg]	$\Delta$
20	(1.20, 0.2, -1.45)	18.92	100.7	0.0174
40	(1.10, 0.4, -1.35)	39.97	101.6	0.041
60	(1.0, 0.5, -1.15)	53.13	97.93	0.063
80	(1.0, 0.8, -1.15)	77.32	97.93	0.10
100	(1.0, 1.1, -1.15)	95.45	97.93	0.14
120	(1.0, 1.70, -1.15)	119.1	97.93	0.21
140	(1.0, 2.7, -1.15)	139.3	97.93	0.34

The results can also be visualised in Figure A.3a and Figure A.3b:



(a) Figure showing the viewing angles of the optimal positions for every FoV for Case 1



(b) Figure showing the max value of  $\Delta$  for each FoV for Case 1

**Figure A.3:** Figure showing the viewing angle for the optimal positions and the max  $\Delta$  for each FoV for Case 1

As the figures show, the best horizontal viewing angle for each of the FoVs tends to be right on the edge of the FoV. This can be explained when one considers the fact that this position corresponds to the maximum possible y-coordinate in the view frustum. As can be seen by Equation A.2, the value of  $u_p$  increases as  $y_p^v$  increases. This higher  $u_p$  then accounts for a greater value of  $u_p$  (as seen by Equation A.6) which results in a higher  $\Delta$ . Keeping in mind that the Z Viewing axis is defined as positive downwards, the same logic applies to why  $\Delta$  increases for a decreasing  $z_p^v$ . Lastly, this is also why the most optimal position is one with the lowest possible X-coordinate. These findings are consistent with the findings from the literature study which suggested that, for forward motion, the most flow can be seen in the peripheries of one's vision. The value of total  $\Delta$ , shown in Figure A.3b, also increases for each FoV suggesting that the bigger the FoV, the more flow can be seen. As one would expect, the  $\Delta$  provided by the rotational components is zero since there was no rotation occurring.

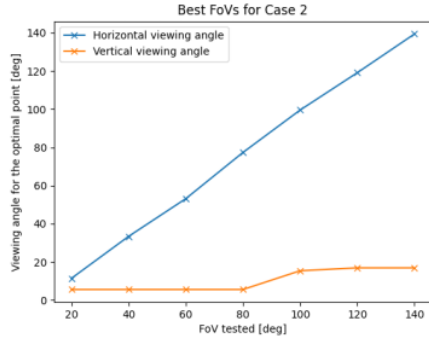
For Case 2, the results can be seen in Table A.5

**Table A.5:** Table showing the optimal position, the horizontal and vertical viewing angle of this position and the value of  $\Delta$  for each FoV for Case 2

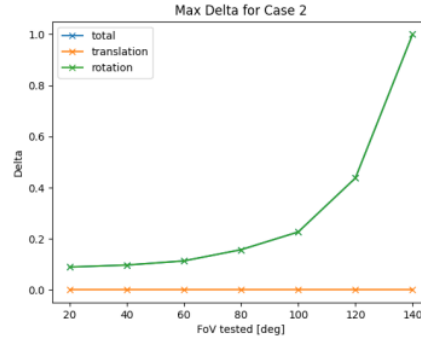
FoV [deg]	Optimal Position (x,y,z) [m]	Horizontal Viewing angle [deg]	Vertical Viewing Angle [deg]	$\Delta$
20	(1.0, 0.1, -0.05)	11.42	5.607	0.089
40	(1.0, 0.3, -0.05)	33.39	5.607	0.097
60	(1.0, 0.5, -0.05)	53.13	5.607	0.113
80	(1.0, 0.8, -0.05)	77.32	5.607	0.157
100	(1.1, 1.3, -0.15)	95.52	15.42	0.226
120	(1.0, 1.7, -0.15)	119.1	16.94	0.43
140	(1.0, 2.7, -0.15)	139.4	16.94	1.00

155

The results are visualised in Figure A.4a and Figure A.4b:



(a) Figure showing the viewing angles of the optimal positions for every FoV for Case 2



(b) Figure showing the max value of  $\Delta$  for each FoV for Case 2

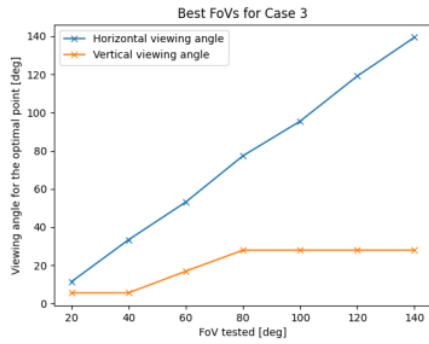
**Figure A.4:** Figure showing the viewing angle for the optimal positions and the max  $\Delta$  for each FoV for Case 2

Much like Case 1, the most optimal horizontal viewing angle continues to be on the edge of the corresponding FoV. However, the most optimal vertical FoV is now significantly lower. The reason for this comes down to the value of the Z-coordinate for the most optimal position. As can be seen in Equation A.2 and Equation A.6, a more negative value of  $z_p^v$  should result in a higher value of  $v_p$  and of the on-screen velocities  $u_p$  and  $v_p$ , which still remains true. However, the difference between Case 1 and 2 is the fact that the rotational component of  $\Delta$  (i.e. the right expression in Equation A.7) dictates the final value for all coordinates. Therefore, large values of  $z_p^v$  mean a larger denominator in Equation A.7 which results in a lower overall value of  $\Delta$ . Since there is no  $y_p^v$  term in the denominator of Equation A.7, the most optimal value of  $y_p^v$  is still one which results in the largest value of  $u_p$ , which remains to be the largest value of  $y_p^v$  for that FoV.

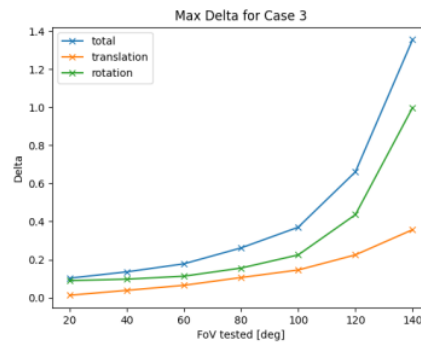
The results for the third and final case for a constant  $\kappa$  can be seen in Table A.6 and are visualised in Figure A.5a and Figure A.5b:

**Table A.6:** Table showing the optimal position, the horizontal and vertical viewing angle of this position and the value of  $\Delta$  for each FoV for Case 3

FoV [deg]	Optimal Position (x,y,z) [m]	Horizontal Viewing angle [deg]	Vertical Viewing Angle [deg]	$\Delta$
20	(1.0, 0.1, -0.049)	11.42	5.607	0.102
40	(1.0, 0.30, -0.049)	33.39	5.607	0.135
60	(1.0, 0.5, -0.15)	53.13	16.95	0.178
80	(1.0, 0.8, -0.25)	77.32	27.96	0.261
100	(1.0, 1.1, -0.25)	95.45	27.96	0.369
120	(1.0, 1.7, -0.25)	119.1	27.96	0.660
140	(1.0, 2.7, -0.25)	139.3	27.96	1.35



(a) Figure showing the viewing angles of the optimal positions for every FoV for Case 3



(b) Figure showing the max value of  $\Delta$  for each FoV for Case 3

**Figure A.5:** Figure showing the viewing angle for the optimal positions and the max  $\Delta$  for each FoV for Case 3

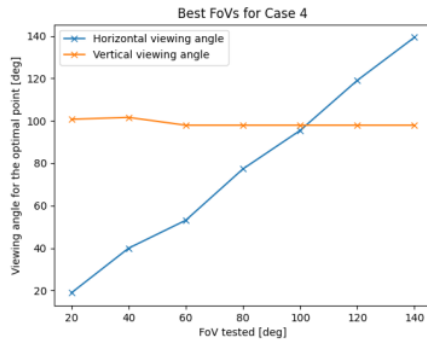
As can be expected, the results of Case 3 shadow the results of the previous two cases. Once again, the best Horizontal angle to get the most information, seems to be on the edge of the FoV. This was true for both previous cases and is, thus, true for Case 3 as well. For the vertical viewing angle, there was a mismatch between the optimal value for Case 1 and Case 2. For Case 3, it seems that the results for Case 2 are more prevalent for the optimal vertical viewing angle. This can be explained by looking at the impact of the rotational component and translational component of  $\Delta$ , shown in Figure A.5b. The value of  $\Delta$  caused by the rotation is greater than that for the translational component and that means, for each of the possible positions of P, the movement in the vertical viewing axis,  $v_p$ , is dominated by the rotational movement. Thus, the optimal Z-coordinate (which is what is used to calculate the optimal vertical viewing angle as per Equation A.9) is one that is optimal in rotation. Of course, the translational component does also have a contribution, which is why the optimal vertical viewing angles for Case 3 are higher than those for Case 2, but since the rotational component dominates this balance, they are not as high as those for Case 1.

### A.2.2. Variable $\kappa$

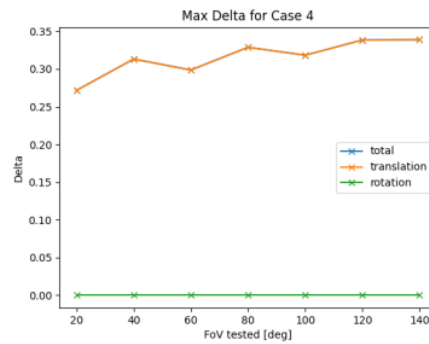
For the first of the variable  $\kappa$  cases, the results are presented in Table A.7

**Table A.7:** Table showing the optimal position, the horizontal and vertical viewing angle of this position and the value of  $\Delta$  for each FoV for Case 4

FoV [deg]	Optimal Position (x,y,z) [m]	Horizontal Viewing angle [deg]	Vertical Viewing Angle [deg]	$\Delta$
20	(1.2, 0.2, -1.45)	18.92	100.7	0.272
40	(1.1, 0.4, -1.35)	39.96	101.6	0.313
60	(1.0, 0.5, -1.15)	53.13	97.93	0.299
80	(1.0, 0.8, -1.15)	77.32	97.93	0.329
100	(1.0, 1.1, -1.15)	95.45	97.93	0.319
120	(1.0, 1.75, -1.15)	119.1	97.93	0.338
140	(1.0, 2.7, -1.15)	139.4	97.93	0.338



(a) Figure showing the viewing angles of the optimal positions for every FoV for Case 4



(b) Figure showing the max value of  $\Delta$  for each FoV for Case 4

**Figure A.6:** Figure showing the viewing angle for the optimal positions and the max  $\Delta$  for each FoV for Case 4

As can be seen from the results, the optimal viewing angles in both the horizontal and vertical case are the exact same as those for Case 1, but the values of  $\Delta$  are significantly higher and show a different pattern. As the FoV increases, the change in  $\kappa$  is shown in:

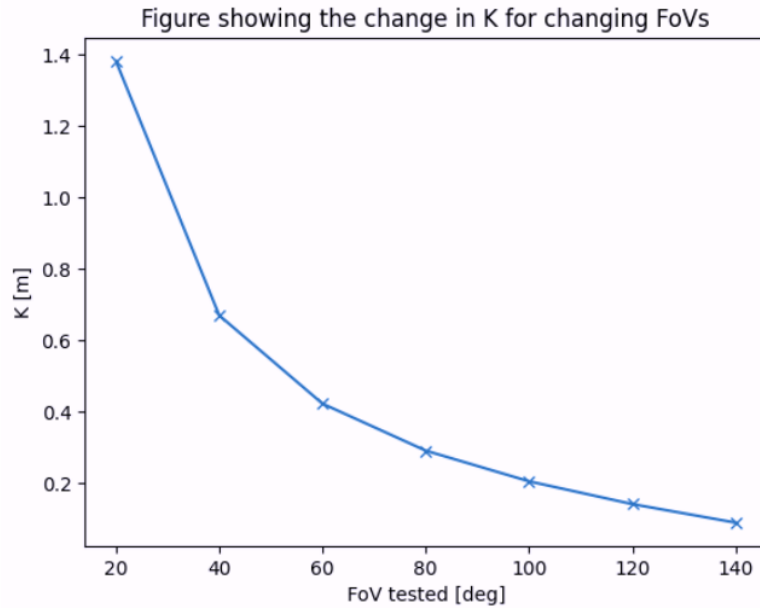


**Figure A.7:** Figure showing the change in  $\kappa$  for changing FoVs

The values for  $\kappa$  are shown in Table A.8:

**Table A.8:** Table showing the values of  $\kappa$  as FoV increases

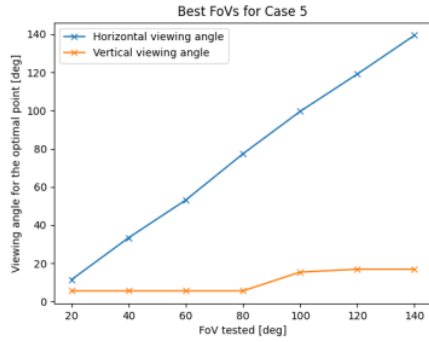
Angle [deg]	$\kappa$ [m]
20	1.38
40	0.66
60	0.42
80	0.29
100	0.20
120	0.14
140	0.088

As the FoV increases, the value of  $\kappa$  decreases tangentially. This also changes the value of  $u_p$  and  $v_p$  non-linearly since, in this case, the value of those two terms is dependant on the product of  $\kappa$  and the position coordinates of the point. Combining these effects in the final equation to calculate  $\Delta$  seems to output the result that the ratio of on-screen velocity to actual velocity remains constant for all FoVs. If this is true, then this implies that there is very little feedback lost as FoV is decreased.

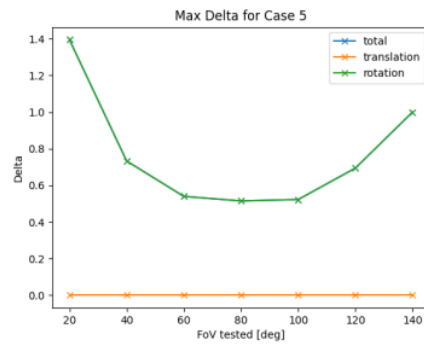
The results for Case 5 are outlined in Table A.9 and visualised in Figure A.8a and Figure A.8b:

**Table A.9:** Table showing the optimal position, the horizontal and vertical viewing angle of this position and the value of  $\Delta$  for each FoV for Case 5

FoV [deg]	Optimal Position (x,y,z) [m]	Horizontal Viewing angle [deg]	Vertical Viewing Angle [deg]	$\Delta$
20	(1.0, 0.1, -0.049)	11.42	5.607	1.39
40	(1.0, 0.3, -0.045)	33.39	5.607	0.733
60	(1.0, 0.5, -0.045)	53.13	5.607	0.539
80	(1.0, 0.8, -0.045)	77.32	5.607	0.515
100	(1.1, 1.3, -0.15)	99.53	15.43	0.522
120	(1.0, 1.7, -0.15)	119.07	16.95	0.694
140	(1.0, 2.7, -0.15)	139.35	16.95	1.00



(a) Figure showing the viewing angles of the optimal positions for every FoV for Case 5



(b) Figure showing the max value of  $\Delta$  for each FoV for Case 5

**Figure A.8:** Figure showing the viewing angle for the optimal positions and the max  $\Delta$  for each FoV for Case 5

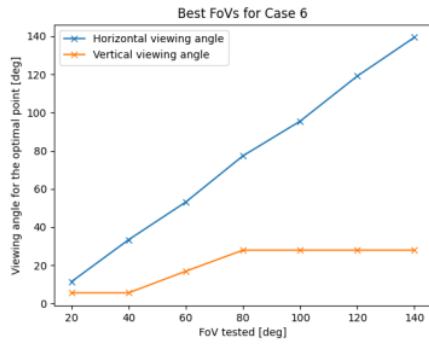
The results for this case, in terms of the optimal viewing angles, are the same as those for the previous cases. However, the values and behaviour of  $\Delta$  is significantly different from any previous case. The analysis suggests that the greatest amount of feedback is received from the lowest FoV, and that the feedback gained plateaus and then rises again. Mathematically, this can be explained with the idea that the rotational component of  $u_p$  and  $v_p$  have a non-linear relationship with  $\kappa$ . This combines with the non-linearities which results from the multiplication of a variable  $\kappa$  and variable position coordinates to create a highly non-linear relationship.

In practical terms it can be explained when one considers the projection effects that arise due to a variable  $\kappa$ . For small FoVs, the observer feels as if they've "zoomed in" on the view, which means that the movements they observe are exaggerated. This can account for the high value of  $\Delta$  for the lower FoVs. However, this does not account for why the values increase again after 100 [ $^\circ$ ].

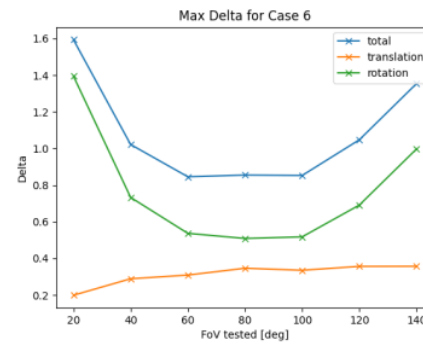
Finally, the results for Case 6 are outlined in Table A.10 and visualised in Figure A.9a and Figure A.9b

**Table A.10:** Table showing the optimal position, the horizontal and vertical viewing angle of this position and the value of  $\Delta$  for each FoV for Case 6

FoV [deg]	Optimal Position (x,y,z) [m]	Horizontal Viewing angle [deg]	Vertical Viewing Angle [deg]	$\Delta$
20	(1.0, 0.1, -0.049)	11.42	5.607	1.59
40	(1.0, 0.3, -0.045)	33.40	5.607	1.02
60	(1.0, 0.5, -0.15)	53.13	16.94	0.846
80	(1.0, 0.8, -0.25)	77.32	27.96	0.855
100	(1.0, 1.1, -0.25)	95.45	27.96	0.853
120	(1.0, 1.7, -0.25)	119.1	27.96	1.05
140	(1.0, 2.7, -0.25)	139.3	27.96	1.35



(a) Figure showing the viewing angles of the optimal positions for every FoV for Case 6



(b) Figure showing the max value of  $\Delta$  for each FoV for Case 6

**Figure A.9:** Figure showing the viewing angle for the optimal positions and the max  $\Delta$  for each FoV for Case 6

As one would expect<sup>84</sup> the results for Case 6 follow the same pattern as those for Case 3. The final values of  $\Delta$  are simply the sum of the rotational and translational components of  $\Delta$  which can be seen in Case 4 and Case 5. As mentioned previously, the rotational components have a stronger influence on the final value than the translational components.

### A.3. Sensitivity Analysis

To test if the velocities and pitch angles used to do the analysis have any impact on the optimal viewing angles or the  $\Delta$  values, a sensitivity analysis was done. This involved:

- **For Case 1 and 4:** The velocity,  $u^b$  was varied from 1 [m/s] to 6 [m/s]
- **For Case 3 and 5:** The pitch angle,  $\theta$  was varied from  $-6 [^\circ]$  to  $-1 [^\circ]$
- **For Case 3 and 6:** Each combination of the previously mentioned velocities and pitch angles were used.

For each of these sensitivity cases, the best horizontal viewing angle, the best vertical viewing angle and the maximum value of  $\Delta$  for all positions was calculated. The best horizontal viewing angles for each cases are shown in Figure A.10:

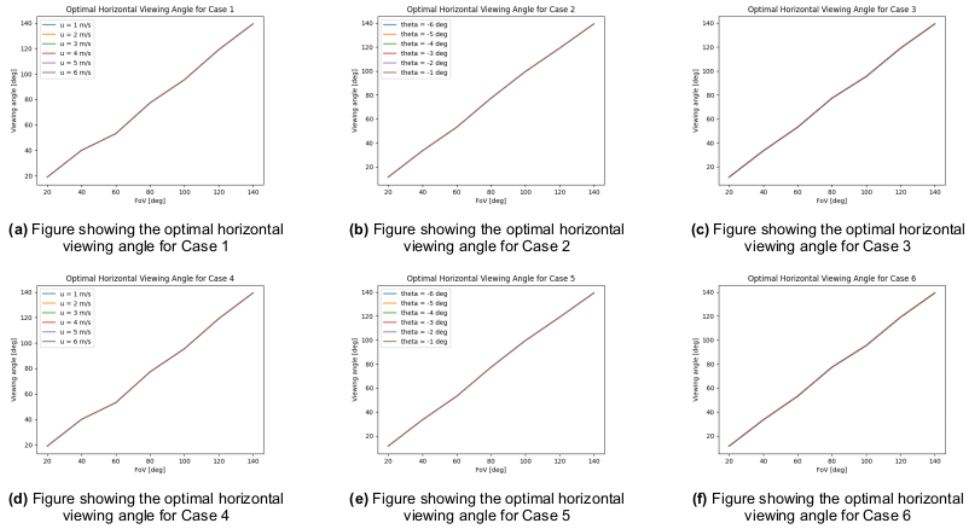


Figure A.10: Figure showing the optimal horizontal viewing angle for all six Cases

As can be seen in Figure A.10, the optimal horizontal viewing angles for all combinations tend to stay on the edge of a pilot's FoV. This seems to suggest that the most amount of feedback for such low speeds and small pitching motions will be gotten from the peripheries of one's vision.

A similar trend can be seen for the optimal vertical viewing angles shown in:

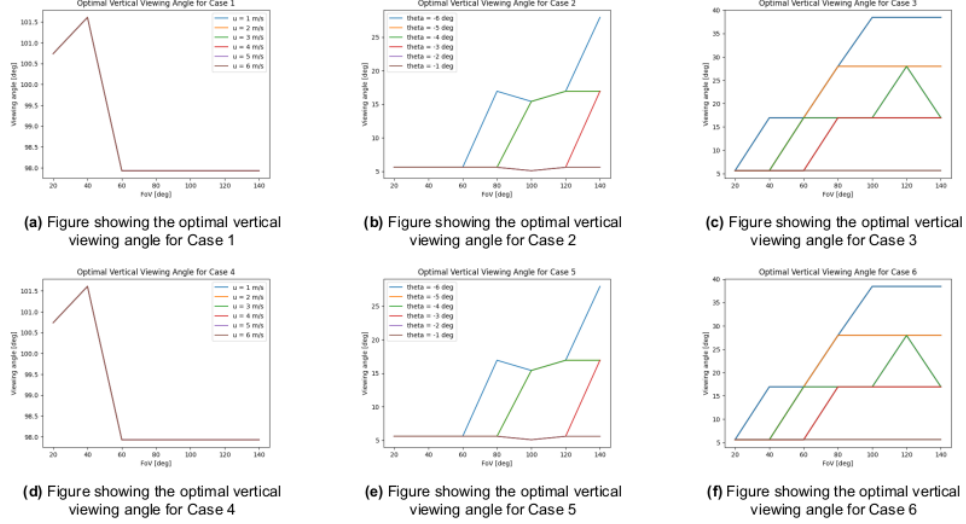
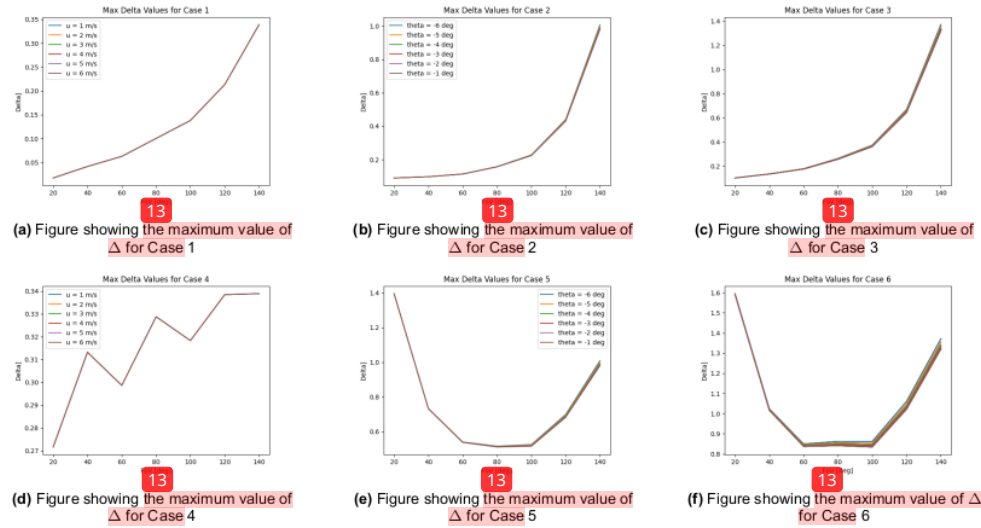


Figure A.11: Figure showing the optimal vertical viewing angle for all six Cases

2 As can be seen from Figure A.11a and Figure A.11d, the optimal vertical angle is the same for all translations within this range. However, this is not the case for purely rotational motion. For Case 2 and Case 5, there are some variations in what the most optimal vertical viewing angle is and this can be down to the fact that the  $\Delta$  values for some adjacent positions were very similar. That means that the

code would have chosen an adjacent position to the one for a previous sensitivity case. For Case 3 and Case 6, the conditions for which the values of the optimal viewing angle were different than the rest are shown in the legends of Figure A.11c and Figure A.11f. A similar explanation can be used to explain this deviance even though the difference in angles is very different. This can be confirmed if one looks at the trend of the maximum value of  $\Delta$  for all cases as shown in Figure A.12



**Figure A.12:** Figure showing the maximum value of  $\Delta$  for all six Cases

As one would expect, the differences in maximum  $\Delta$  for the cases with only translation or only rotation are negligible. However, even though there are visible differences for Case 3 and Case 6, the absolute values of the differences never exceed 0.1. If one was to consider this in percentage terms, then the difference in the on-screen velocity seen by the pilot for different conditions is less than 10 [%]. Additionally, the optimal vertical viewing angles are never high enough for any given FoV such that they can be clipped out, which means that the optimal point will always be in the pilot's view. This combined with the low change in  $\Delta$  means that the pilot would not be missing out on any information

#### A.4. Discussion

The goal of this analysis was to try and find an FoV-invariant point, that provides the greatest amount of velocity feedback to the pilot. While the analysis did not successfully deliver the required point, there is still some use that can be derived from it. Firstly, the analysis shows that for a two DOF system, the greatest amount of feedback is being gathered from the peripheries of a pilot. This means that, in theory, should the FoV be lowered, the pilot would lose out on a lot of velocity feedback and their performance would worsen. Additionally, using the metric of the ratio on-screen velocity to the actual velocity,  $\Delta$  reveals that the change in feedback for each FoV is largely invariant of the motion. This means that if one analyses the percentage decrease in  $\Delta$  for each FoV, then the loss in velocity feedback can potentially be quantified.

The percentage decrease, PD for each FoV can be calculated using Equation A.10:

$$PD = \frac{\Delta_{140} - \Delta_{FoV}}{\Delta_{140}} * 100 \quad (\text{A.10})$$

The results for each case are shown in Table A.11:

**Table A.11:** Table showing the Percentage decrease for all six Cases

FoV [deg]	Percentage decrease [%]					
	Case 1	Case 2	Case 3	Case 4	Case 5	Case 6
20	94.86	91.05	92.45	19.85	-39.51	-17.68
40	87.76	90.29	90.01	7.58	26.72	24.57
60	81.48	88.66	86.88	11.87	46.03	37.57
80	70.37	84.28	80.72	2.98	48.52	36.88
100	59.26	77.34	72.69	6.08	47.75	37.05
120	37.04	56.24	51.24	0.12	30.59	22.65
140	0.00	0.00	0.00	0.00	0.00	0.00

As can be seen in Table A.11, for the cases with a fixed  $\kappa$ , there is a large decrease in information between the smallest and largest FoV. For Case 3, which can be considered the most realistic case, there is already a 51 [%] decrease in feedback from 140 [ $^{\circ}$ ] to 120 [ $^{\circ}$ ]. This is already the largest decrease from one FoV to another but the decrease does taper off. This may mean that the pilot may not perceive much difference as they transition from FoVs of 120 [ $^{\circ}$ ] to a lower one, but theoretically their performance should degrade. For the Cases with the variable  $\kappa$

While the analysis does provide meaningful results, it is important to consider what assumptions were made to come to the conclusions. The first big assumption is the idea that one can quantify the amount of feedback being received by the pilot using the velocity seen on-screen. It is assumed that, for a simple one or two degree-of-freedom motion, the more velocity the pilot sees on screen, the better their perception of speed will be which would allow them to better control the helicopter. While literature has indeed stated that, as FoV decreases and the pilot sees less, their performance degrades, it is a big assumption to make that this performance degradation will occur because the pilot is seeing lower velocity components on their screen. It may well be the case that the pilot's performance is independent of how fast the on-screen velocity is and it simply depends on the presence of on-screen velocity. This of course, is a hypothesis that can be tested during the experimentation phase.

Another major assumption made while doing the analysis was that the optimal position for each case and each FoV, remains on screen for the entirety of the motion. In a real world case, as the helicopter moves forward, all points close to the helicopter would get clipped out of view. This is mitigated slightly in the analysis by the fact that the velocity and pitch of the helicopter are kept small. This is exactly why emphasis is put on the viewing angle of the optimal points instead of their exact coordinates. For a simple visual scene that consists only of a ground and a sky, as the helicopter moves through the scene, all points on one specific viewing angle will behave the exact same way regardless of their exact coordinate. If that scene were to have distinct scenery such as trees or other objects however, then the exact coordinate of those objects plays a part in how much feedback the pilot is getting in the sense that they are now getting both position and velocity feedback. If one considers only an experiment where velocity feedback is provided, then this analysis provides good results on what can be expected.

# B

## Experiment Procedure

### B.1. General Procedure

Each experiment itself took around 1.5 hours, which includes the time taken for explaining the experiment and the training run. When the participant first enters the room, they are asked to take a seat so the experiment details can be explained to them. They are told that they will put on a VR headset and use a joystick to control a simulation of a helicopter in near-ground hover. Then the two types of tasks that they will do, namely the Velocity Disturbance and Pitch Disturbance Rejection Tasks, are explained to them. Then, they are asked to sign the Informed Consent Form. During this time, the researcher can change the ID field in the Unity simulation to the ID that is designated for the participant. This allows the researchers to identify which dataset belongs to which participant. After this, the participant is asked to put the VR headset on and adjust it such that it sits comfortably on their head. They are free to change the settings of the headset such that they can see the scenery, shown in Figure 4.6a, clearly. They are then shown the MISC scale to make sure that they can read the scale properly. If not, the scale is moved closer or further away from them until they feel comfortable. This distance between the observer and the scale is then recorded in Unity, such that the scale always shows up in that exact same position. They then get to use the joystick to move the helicopter around such that they get used to the motion. This also serves to check whether or not the participants feel any adverse effects of motion sickness already.

The experiment begins with one or more training runs of the Velocity Disturbance Rejection Task with an FoV of  $140 [{}^{\circ}]$ . Before the run is started, the participants are told that, during the run, the researcher will ask them the following three questions:

- Which part of the screen are their eyes mostly focused on?
- Do they feel like they are doing better for this experimental condition compared to the previous one (if applicable)?
- Do they feel more comfortable with this view compared to the previous one (if applicable)?

These questions are usually asked around the 40-50 second mark. This ensures that they have made it past the lead-in phase of the run and are fully focused and comfortable with the control strategy they are employing for the task. After the run is over, they are asked to use the MISC scale to give a rating corresponding to their condition. The name of the CSV file that contains the output of the run is then entered into the Python code (either `errorAnalysisSpeed.py` or `errorAnalysisTheta.py`), such that their RMSE can be checked. In general, if the RMSE is below  $2.5 - 3.0 [(m/s)^2]$ , the participants are ready to continue with the actual experimental runs. If the RMSE is higher than  $3.0 [(m/s)^2]$ , more training runs should be conducted.

The simulation is set up such that the entire simulation can be controlled by using certain keybinds. These are detailed in Table B.1:

**Table B.1:** Table showing the commands and the associated keybinds for the simulation

Command	Keybind
Start training forcing function	T
Start Velocity or Pitch forcing function	Space
Show pitch reticle and horizon line  (If this is activated then pressing Space will start the Pitch Forcing Function)	P
Reset	R
Show MISC Scale	H
Change FoV to 20 degrees	Z
Change FoV to 30 degrees	X
Change FoV to 60 degrees	C
Change FoV to 90 degrees	V
Change FoV to 120 degrees	B
Change FoV to 140 degrees	N

Note that pressing **P** switches the simulation to Pitch Mode, which means that forward/backward movement is disabled and pressing **Space** will start the Pitch Forcing Function (i.e. Figure 4.5b) instead of the Velocity Forcing Function (i.e. Figure 4.5a).

The procedure for the experimental runs is as follows:

1. Use the Key Commands, shown in Table B.1, to set up the correct FoV for the run
2. Confirm with the participants if the view is correct
3. Begin the run
4. At around the 40-50 second mark, ask them the aforementioned questions and record their responses
5. When the run ends, ask them for their MISC rating and record this
6. Use the Python script to check their RMSE and the time traces of their control activity, to ensure that the data was recorded properly.
7. Repeat the previous steps for the second run for this experimental condition

Every four runs, the participant should be asked to take the headset off, such that they get a little break and their eyes can reset. At any point, if the participant wants to stop, the simulation should be immediately terminated and they should take the headset off. Depending on how severe the participants' symptoms are, the experiment should be terminated entirely or it should continue. This is explained in the next section.

## B.2. Terminating Experiment Due To Motion Sickness

If at any point the participant indicates a MISC score of 6 or higher (i.e. Nausea or Vomiting), the experiment must be terminated. **UNDER NO CIRCUMSTANCE MUST THE PARTICIPANT BE ALLOWED TO CONTINUE THE EXPERIMENT!** The participant should take the headset off and sit down until they stop feeling nauseous. This can be helped by giving them fizzy drinks which induce burping and help settle the stomach. Until the participant feels good enough to stand up and walk around, they must not be allowed to leave the room. It is generally advised to wait up to an hour before the participant is allowed to drive or cycle.

# C

## Experiment Matrix

Since there are eight conditions to test, the minimum number of participants needed is also eight. This ensures that the results have no order effects since each participant will test the different conditions in different orders. This is why an experiment matrix is used to determine in which order a participant does the experiment. This is shown in Table C.1

<sup>2</sup>  
Table C.1: Table showing the Experiment Matrix used to determine the order in which the participants do the experiments

Participant number	Experiment Condition							
	1	2	3	4	5	6	7	8
1	V20	V30	V60	V90	V120	V140	P20	P140
2	V30	V60	V90	V120	V140	P20	P140	V20
3	V60	V90	V120	V140	P20	P140	V20	V30
4	V90	V120	V140	P20	P140	V20	V30	V60
5	V120	V140	P20	P140	V20	V30	V60	V90
6	V140	P20	P140	V20	V30	V60	V90	V120
7	P20	P140	V20	V30	V60	V90	V120	V140
8	P140	V20	V30	V60	V90	V120	V140	P20

In Table C.1, the condition **V20** refers to a Velocity Disturbance Rejection task with an FoV of 20 [°], **V30** refers to a Velocity Disturbance Rejection task with an FoV of 30 [°] and so on. **P20** refers to a Pitch Disturbance Rejection Task with an FoV of 20 [°] and so on. The table is created such that each condition appears only once per column and once per row. This ensures that nobody in the group of participants does the experiments in the same order as another. If there are more than eight participants, then the ninth participant does the order in the first column, the second does the order in the second column and so on.

# D

## Human Research Ethics Committee Documents

To be able to do the experiments, the potential participants had to sign an Informed Consent Form. This is shown below.

## Opening Statement

You are being invited to participate in a Masters research study titled "Testing Pilot Behaviour for Helicopter flight using VR headsets". This study is being done by Sheharyar Ali from the TU Delft

The purpose of this research study is to see how a pilot's performance changes when they are using VR headsets for visual cueing. The goal is to change the Field Of View (FoV) of the headset and test what happens to the performance of the pilot. The experiment will take you approximately 120 minutes to complete. The data will be used for a Master's thesis researching how control behaviour is affected by such a task. We will be asking you to use a joystick to control a simulation of a helicopter and your task will be to keep the helicopter stationary in the face of a disturbance. You will do this while wearing a VR headset which will be used to show you the simulation. Please note: wearing a VR headset can cause motion sickness so please only participate if you have no previous history of motion sickness.

1 As with any online activity the risk of a breach is always possible. To the best of our ability your answers in this study will remain confidential. We will minimize any risks by anonymising all data collected. Data such as your name and email addresses will not be published in any way and the published data will only consist of performance parameters of the participant. This data will be published with no reference to who the participant was.

1 Your participation in this study is entirely voluntary and you can withdraw at any time. You are free to omit any questions. Should you wish to withdraw your consent to publish the data from your experiment, we will happily remove all of the requested data from storage and your results will not be published.

2 If you have any questions or complaints, feel free to email me at

1 PLEASE TICK THE APPROPRIATE BOXES		Yes	No
<b>A: GENERAL AGREEMENT – RESEARCH GOALS, PARTICPANT TASKS AND VOLUNTARY PARTICIPATION</b>			
1. I have read and understood the study information dated _____, or it has been read to me. I have been able to ask questions about the study and my questions have been answered to my satisfaction.		<input type="checkbox"/>	<input type="checkbox"/>
2. I consent voluntarily to be a participant in this study and understand that I can refuse to answer questions and I can withdraw from the study at any time, without having to give a reason.		<input type="checkbox"/>	<input type="checkbox"/>
3. I understand that taking part in the study involves:		<input type="checkbox"/>	<input type="checkbox"/>
• Using a VR headset and a joystick to control the simulation of a helicopter			

<b>PLEASE TICK THE APPROPRIATE BOXES</b>		<b>Yes</b>	<b>No</b>
<ul style="list-style-type: none"> <li>Collecting data on how well a participant does by collecting data on control input and errors</li> <li>A small discussion about how the experiment went after the experiment has finished</li> </ul>			
4. I understand that the study will end around the end of September 2024		<input type="checkbox"/>	<input checked="" type="checkbox"/>
<b>B: POTENTIAL RISKS OF PARTICIPATING (INCLUDING DATA PROTECTION)</b>			
<p>5. I understand that taking part in the study involves the use of VR headsets which may cause motion sickness or dizziness. I understand that these will be mitigated by:</p> <ul style="list-style-type: none"> <li><b>Doing the experiment in a well-ventilated room</b></li> <li><b>Stopping the experiment at any point if any sign of discomfort is shown by the participant or if the participant wants to stop</b></li> <li><b>Taking frequent breaks to let the participant rest</b></li> </ul>		<input type="checkbox"/>	<input type="checkbox"/>
6. I understand that taking part in the study also involves collecting specific personally identifiable information (PII) and associated personally identifiable research data (PIRD) with the potential risk of my identity being revealed. The PII and PIRD collected is limited to the participant's name, email address, age and gender		<input type="checkbox"/>	<input type="checkbox"/>
<p>8. I understand that the following steps will be taken to minimise the threat of a data breach, and protect my identity in the event of such a breach</p> <ul style="list-style-type: none"> <li>Data is only accessible by the researcher, Sheharyar Ali and their supervisor, Olaf Stroosma</li> <li>The data is stored in encrypted storage locations like the TU Delft Surf Drive and TU Delft One drive</li> <li>The non-anonymised data will be deleted upon the completion of this study</li> <li>All data can be removed at the request of the participant</li> </ul>		<input type="checkbox"/>	<input type="checkbox"/>
9. I understand that personal information collected about me that can identify me, such as my name and email address, will not be shared beyond the study team.		<input type="checkbox"/>	<input type="checkbox"/>
10. I understand that the (identifiable) personal data I provide will be destroyed once the thesis is published at the end of September, or when I request for it to be deleted		<input type="checkbox"/>	<input type="checkbox"/>
<b>C: RESEARCH PUBLICATION, DISSEMINATION AND APPLICATION</b>			
<p>11. I understand that after the research study the de-identified information I provide will be used for:</p> <ul style="list-style-type: none"> <li><b>Analysing the trends in pilot control behaviour for different testing conditions</b></li> <li><b>Publishing the general trend shown by the participants in how their control behaviour changed</b></li> <li><b>Publishing the general findings of the study in a final thesis report</b></li> </ul>		<input type="checkbox"/>	<input type="checkbox"/>

**1**  
**Signatures**

Name of participant [printed]

Signature

Date

I, as researcher, have accurately read out the information sheet to the potential participant and, to the best of my ability, ensured that the participant understands to what they are freely consenting.

**Sheharyar Ali**

Researcher name [printed]

Signature

Date

Study contact details for further information:

[Back to text](#)

# E

## Analysing Effectiveness of VR Headsets to Jumpscare Participants

When VR headsets first entered commercial use, they were advertised as the next generation of video game consoles. At the start, the most popular type of media that was available for VR headsets was the "interactive horror experience". This type of game made use of the headsets' infinite FoR to jumpscare the players, as they were escorted through a linear maze of horror set pieces. To show homage to the early days of VR, and because it is just objectively funny to scare people, an Easter egg was programmed into the Unity Simulation for the experiments. This Easter egg had a 1 in 30 chance to trigger every time a participant finished a run and would swap the view to an image [82] for 0.2 [s] that would startle the participant. The image chosen to do this is the portrait of the character [Freddy Fazbear](#) from the popular horror game [Five Nights at Freddy's](#). This is shown in Figure E.1



Figure E.1: Figure showing the jumpscare image of Freddy Fazbear from Five Nights at Freddy's

The reason why the chance of it occurring is so low, is because if it occurs too frequently, the participant's performance may be affected for the rest of the experiment. Since this is undesirable, albeit very funny, the chance of it triggering was kept to a minimum.

Regardless, the actual effect triggered at least once for 5 out of 12 participants. However, only two of the participants acknowledged that it did while the other three were oblivious to the fact that it had happened. Even those that did notice it were not scared or startled by its appearance, they were merely confused. When asked why they did not find it scary, one of them claimed that they had no

idea what they were looking at since it was only on screen for a short time. The other participant did recognise the character from the games, but they claimed that seeing it pop up was more confusing than scary. Based on this, the following recommendations can be made to future researchers who wish to jump-scare participants using VR headsets:

1. Make sure the jumpscare happens more often
2. Make sure the image is on-screen for a longer period of time
3. Add a sound effect that plays through the VR headset's speaker to add to the scariness factor of the jumpscare
4. When a participant does get startled or scared by the jumpscare happening, vehemently deny the fact that there was any jumpscare at all. This adds more anxiety to the participant as they feel like they are imagining things and will be on edge for when they next jumpscare occurs.

**N.B: The author of this thesis feels obligated to add that this should be done sparingly since it may, under some legal definitions, count as psychological torture**

# Thesis\_GL\_draft.pdf

## ORIGINALITY REPORT



## PRIMARY SOURCES

1	<b>Submitted to TU Delft</b> Student Paper	2%
2	<b>repository.tudelft.nl</b> Internet Source	1 %
3	<b>elib.dlr.de</b> Internet Source	1 %
4	<b>docplayer.net</b> Internet Source	<1 %
5	<b>Gareth D. Padfield. "Helicopter Flight Dynamics", Wiley, 2007</b> Publication	<1 %
6	<b>v1.overleaf.com</b> Internet Source	<1 %
7	<b>Submitted to University of Canterbury</b> Student Paper	<1 %
8	<b>www.iris.unict.it</b> Internet Source	<1 %
9	<b>Ndibatya, I., M.J. Booysen, and J. Quinn. "An adaptive transportation prediction model for</b>	<1 %

the informal public transport sector in Africa",  
17th International IEEE Conference on  
Intelligent Transportation Systems (ITSC),  
2014.

Publication

10	<a href="http://hanspeterschaub.info">hanspeterschaub.info</a>	<1 %
11	<a href="http://pure.tudelft.nl">pure.tudelft.nl</a>	<1 %
12	<a href="http://tuprints.ulb.tu-darmstadt.de">tuprints.ulb.tu-darmstadt.de</a>	<1 %
13	"Helicopter Flight Dynamics", Wiley, 2018	<1 %
14	Submitted to University of Sydney	<1 %
15	<a href="http://arc.aiaa.org">arc.aiaa.org</a>	<1 %
16	<a href="http://crest.science">crest.science</a>	<1 %
17	<a href="http://etd.auburn.edu">etd.auburn.edu</a>	<1 %
18	<a href="http://publikationen.uni-tuebingen.de">publikationen.uni-tuebingen.de</a>	<1 %
19	Sue Looney. "Same But Different Math - Helping Students Connect Concepts, Build	<1 %

Number Sense, and Deepen Understanding",  
Routledge, 2022

Publication

---

- |    |   |      |
|----|---|------|
| 20 | <a href="http://etheses.whiterose.ac.uk">etheses.whiterose.ac.uk</a>  | <1 % |
|    | Internet Source   |      |
| 21 | <a href="http://ntnuopen.ntnu.no">ntnuopen.ntnu.no</a>  | <1 % |
|    | Internet Source   |      |
| 22 | William Chung, Barbara Sweet, Mary Kaiser,<br>Emily Lewis. "Visual Cueing Effects<br>Investigation for a Hovering Task", AIAA<br>Modeling and Simulation Technologies<br>Conference and Exhibit, 2003 | <1 % |
|    | Publication   |      |
| 23 | <a href="#">Submitted to University of Leicester</a>  | <1 % |
|    | Student Paper   |      |
| 24 | <a href="http://livrepository.liverpool.ac.uk">livrepository.liverpool.ac.uk</a>  | <1 % |
|    | Internet Source   |      |
| 25 | <a href="http://data-science.meduniwien.ac.at">data-science.meduniwien.ac.at</a>  | <1 % |
|    | Internet Source   |      |
| 26 | <a href="http://theses.gla.ac.uk">theses.gla.ac.uk</a>  | <1 % |
|    | Internet Source   |      |
| 27 | Rebecca Lim, Gregory P. Penoncello, Dean<br>Hobbis, Daniel P. Harrington1, Yi Rong.<br>"Technical Note: Characterization of novel<br>iterative reconstructed cone beam CT images                      | <1 % |

for dose tracking and adaptive radiotherapy  
on L-shape linacs", Medical Physics, 2022

Publication

---

- 28 acikbilim.yok.gov.tr <1 %  
Internet Source
- 29 Martin Rosenberger, Manfred Pichl, Klaus Six, Johannes Edelmann. "The Dynamics of Vehicles on Roads and Tracks - Proceedings of the 24th Symposium of the International Association for Vehicle System Dynamics (IAVSD 2015), Graz, Austria, 17-21 August 2015", CRC Press, 2019 <1 %  
Publication
- 30 "Mobile Displays", Wiley, 2008 <1 %  
Publication
- 31 Yangming Shi, Jing Du, Darrell A. Worthy. "The impact of engineering information formats on learning and execution of construction operations: A virtual reality pipe maintenance experiment", Automation in Construction, 2020 <1 %  
Publication
- 32 d-nb.info <1 %  
Internet Source
- 33 P. Pretto, M. Ogier, H.H. Bülthoff, J.-P. Bresciani. "Influence of the size of the field of <1 %

view on motion perception", Computers & Graphics, 2009

Publication

---

34	<a href="http://apps.dtic.mil">apps.dtic.mil</a>	<1 %
35	<a href="http://www.aees.be">www.aees.be</a>	<1 %
36	<a href="http://core.ac.uk">core.ac.uk</a>	<1 %
37	<a href="http://www.roadtovr.com">www.roadtovr.com</a>	<1 %
38	<a href="http://dspace.lib.cranfield.ac.uk">dspace.lib.cranfield.ac.uk</a>	<1 %
39	<a href="http://semarakilmu.com.my">semarakilmu.com.my</a>	<1 %
40	<a href="http://sites.cs.ucsb.edu">sites.cs.ucsb.edu</a>	<1 %
41	<a href="http://easychair.org">easychair.org</a>	<1 %
42	Edward N. Bachelder, Jeffrey Lusardi, Bimal Aponso, Martine Godfroy-Cooper. "Estimating Handling Qualities Ratings from Hover Flight Data Using SCOPE", AIAA Scitech 2021 Forum, 2021	<1 %

Publication

---

- 43 P. M. T. Zaal, D. M. Pool, J. de Bruin, M. Mulder, M. M. van Paassen. "Use of Pitch and Heave Motion Cues in a Pitch Control Task", Journal of Guidance, Control, and Dynamics, 2009 <1 %
- Publication
- 
- 44 Vincent J. Parks. "A method for directly determining surface strain fields using diffraction gratings", Experimental Mechanics, 1972 <1 %
- Publication
- 
- 45 [citeseerx.ist.psu.edu](http://citeseerx.ist.psu.edu) <1 %
- Internet Source
- 
- 46 [5dok.net](http://5dok.net) <1 %
- Internet Source
- 
- 47 Submitted to Imperial College of Science, Technology and Medicine <1 %
- Student Paper
- 
- 48 Submitted to Politecnico di Milano <1 %
- Student Paper
- 
- 49 [coek.info](http://coek.info) <1 %
- Internet Source
- 
- 50 [ebin.pub](http://ebin.pub) <1 %
- Internet Source
- 
- 51 [www2.inf.h-brs.de](http://www2.inf.h-brs.de) <1 %
- Internet Source
-

52	Submitted to University of Southampton Student Paper	<1 %
53	Submitted to Utah Education Network Student Paper	<1 %
54	open.uct.ac.za Internet Source	<1 %
55	ris.utwente.nl Internet Source	<1 %
56	corescholar.libraries.wright.edu Internet Source	<1 %
57	essay.utwente.nl Internet Source	<1 %
58	A. R. Valente Pais, D. M. Pool, A. M. de Vroome, M. M. Van Paassen, M. Mulder. "Pitch Motion Perception Thresholds During Passive and Active Tasks", Journal of Guidance, Control, and Dynamics, 2012 Publication	<1 %
59	Submitted to Embry Riddle Aeronautical University Student Paper	<1 %
60	T. Adachi, K. Tateyama, M. Kimura. "Modern Tunneling Science and Technology", A.A. Balkema Publishers, 2020 Publication	<1 %

61	archive.org Internet Source	<1 %
62	doczz.net Internet Source	<1 %
63	www.grafiasi.com Internet Source	<1 %
64	David A. Bies, Colin H. Hansen, Carl Q. Howard, Kristy L. Hansen. "Engineering Noise Control", CRC Press, 2023 Publication	<1 %
65	pure.mpg.de Internet Source	<1 %
66	Amanda Lampton, David Klyde. "Power Frequency - A New Metric for Analyzing Pilot-in-the-Loop Flying Tasks", AIAA Atmospheric Flight Mechanics Conference, 2011 Publication	<1 %
67	Ranjan Vepa. "Flight Dynamics, Simulation, and Control - For Rigid and Flexible Aircraft", CRC Press, 2019 Publication	<1 %
68	T Dehouck, M Mulder, M Van Paassen. "The Effects of Simulator Motion Filter Settings on Pilot Manual Control Behaviour", AIAA Modeling and Simulation Technologies Conference and Exhibit, 2006 Publication	<1 %

69	Submitted to Universidade Nova De Lisboa Student Paper	<1 %
70	vtechworks.lib.vt.edu Internet Source	<1 %
71	Caroline Desgranges, Jerome Delhommelle. "Molecular Networking - Statistical Mechanics in the Age of AI and Machine Learning", CRC Press, 2024 Publication	<1 %
72	George C. Christodoulou, Anastasios I. Stamou. "Environmental Hydraulics", CRC Press, 2010 Publication	<1 %
73	Kirill Zaychik, Frank Cardullo, Gary George. "A Conspectus on Operator Modeling: Past, Present and Future", AIAA Modeling and Simulation Technologies Conference and Exhibit, 2006 Publication	<1 %
74	Masaru Ito, Yusuke Funahara, Seiji Saiki, Yoichiro Yamazaki, Yuichi Kurita. "Development of a Cross-Platform Cockpit for Simulated and Tele-Operated Excavators", Journal of Robotics and Mechatronics, 2019 Publication	<1 %
75	research.tue.nl Internet Source	<1 %

76	<a href="http://www.politesi.polimi.it">www.politesi.polimi.it</a> Internet Source	<1 %
77	<a href="http://eucass-ceas-2023.eu">eucass-ceas-2023.eu</a> Internet Source	<1 %
78	<a href="http://www2.ulb.ac.be">www2.ulb.ac.be</a> Internet Source	<1 %
79	R.V. Kenyon, E.W. Kneller. "The effects of field of view size on the control of roll motion", IEEE Transactions on Systems, Man, and Cybernetics, 1993 Publication	<1 %
80	Submitted to University of Queensland Student Paper	<1 %
81	Xufei Yan, Renliang Chen. "Augmented flight dynamics model for pilot workload evaluation in tilt-rotor aircraft optimal landing procedure after one engine failure", Chinese Journal of Aeronautics, 2018 Publication	<1 %
82	Submitted to CSU, Stanislaus Student Paper	<1 %
83	Submitted to Cranfield University Student Paper	<1 %
84	Hassen Fourati, Djamel Eddine Chouaib Belkhiat. "Multisensor Attitude Estimation -	<1 %

Fundamental Concepts and Applications",  
CRC Press, 2019

Publication

---

- 85 James K. Peterson. "Basic Analysis II - A Modern Calculus in Many Variables", CRC Press, 2020 <1 %
- 86 Peter Zaal, Daan Pool, Max Mulder, Marinus van Paassen, Jan Mulder. "Multimodal Pilot Model Identification in Real Flight", AIAA Modeling and Simulation Technologies Conference, 2009 <1 %
- 87 m.moam.info <1 %
- Internet Source
- 88 sahris.sahra.org.za <1 %
- Internet Source
- 89 Submitted to <1 %
- Student Paper
- 90 Submitted to Manchester Metropolitan University <1 %
- Student Paper
- 91 N.P. Sobenin, B.V. Zverev. "Electrodynamical Characteristics of Accelerating Cavities", Routledge, 2020 <1 %
- Publication
- Submitted to University of Leeds

93

Usama Bin Khalid. "Numerical and Optical Assessment of Different Solutions for Pollutant Emission Reduction in Compression Ignition Engines", Universitat Politecnica de Valencia, 2024

&lt;1 %

Publication

94

etd.lib.metu.edu.tr

&lt;1 %

Internet Source

95

Peter M.T. Zaal. "Manual Control Adaptation to Changing Vehicle Dynamics in Roll–Pitch Control Tasks", Journal of Guidance, Control, and Dynamics, 2016

&lt;1 %

Publication

96

Peter Zaal, Daan Pool, Jaap de Bruin, M. Mulder, M. van Paassen. "Pilots' Use of Pitch and Heave Motion Cues in a Pitch Control Task", AIAA Modeling and Simulation Technologies Conference and Exhibit, 2008

&lt;1 %

Publication

97

W.A. Memon, M.D. White, G.D. Padfield, N. Cameron, L. Lu. "Helicopter Handling Qualities: A study in pilot control compensation", The Aeronautical Journal, 2021

&lt;1 %

Publication

98	bora.uib.no Internet Source	<1 %
99	dokumen.pub Internet Source	<1 %
100	m.vtol.org Internet Source	<1 %
101	pure.coventry.ac.uk Internet Source	<1 %
102	www.promoldingshanghai.com Internet Source	<1 %
103	www.research.unipd.it Internet Source	<1 %
104	C. Marjolein Dohmen-Janssen, Suzanne J.M.H. Hulscher. "River, Coastal and Estuarine Morphodynamics: RCEM 2007", CRC Press, 2019 Publication	<1 %
105	Clarence W. de Silva. "Vibration - Fundamentals and Practice, Second Edition", CRC Press, 2019 Publication	<1 %
106	Pankaj Jain. "An Introduction to Astronomy and Astrophysics", CRC Press, 2019 Publication	<1 %

- 107 Srinivasan Gopalakrishnan. "Wave Propagation in Materials and Structures", CRC Press, 2019 **<1 %**  
Publication
- 
- 108 [bicycle.tudelft.nl](http://bicycle.tudelft.nl) **<1 %**  
Internet Source
- 
- 109 [c.coek.info](http://c.coek.info) **<1 %**  
Internet Source
- 
- 110 [www.scribd.com](http://www.scribd.com) **<1 %**  
Internet Source
- 
- 111 [www2.mdpi.com](http://www2.mdpi.com) **<1 %**  
Internet Source
- 
- 112 [5dok.org](http://5dok.org) **<1 %**  
Internet Source
- 
- 113 [9pdf.net](http://9pdf.net) **<1 %**  
Internet Source
- 
- 114 D.M. Pool, P.M.T. Zaal. "A Cybernetic Approach to Assess the Training of Manual Control Skills", IFAC-PapersOnLine, 2016 **<1 %**  
Publication
- 
- 115 Haym Benaroya, Mark Nagurka, Seon Han. "Mechanical Vibration - Analysis, Uncertainties, and Control", CRC Press, 2017 **<1 %**  
Publication
-

- 116 Linghai Lu, Michael Jump. "Multiloop Pilot Model for Boundary-Triggered Pilot-Induced Oscillation Investigations", Journal of Guidance, Control, and Dynamics, 2014 <1 %  
Publication
- 
- 117 Petar Georgiev, C. Guedes Soares. "Sustainable Development and Innovations in Marine Technologies", CRC Press, 2019 <1 %  
Publication
- 
- 118 Peter R. Grant, Bonnie Yam, Ruud Hosman, Jeffery A. Schroeder. "Effect of Simulator Motion on Pilot Behavior and Perception", Journal of Aircraft, 2006 <1 %  
Publication
- 
- 119 Vincent G. Duffy. "Handbook of Digital Human Modeling - Research for Applied Ergonomics and Human Factors Engineering", CRC Press, 2019 <1 %  
Publication
- 
- 120 Yannick Sauer, Malte Scherff, Markus Lappe, Katharina Rifai, Niklas Stein, Siegfried Wahl. "Self-motion illusions from distorted optic flow in multifocal glasses", iScience, 2022 <1 %  
Publication
- 
- 121 [publicaciones.uci.cu](http://publicaciones.uci.cu) <1 %  
Internet Source
- 
- 122 [scholarscompass.vcu.edu](http://scholarscompass.vcu.edu)

Internet Source

<1 %

---

123 shodh.inflibnet.ac.in:8080 <1 %  
Internet Source

---

124 vbn.aau.dk <1 %  
Internet Source

---

125 vdoc.pub <1 %  
Internet Source

---

126 www.bozpinfo.cz <1 %  
Internet Source

---

127 www.dalrrd.gov.za <1 %  
Internet Source

---

128 www.e-education.psu.edu <1 %  
Internet Source

---

129 www.mycopter.eu <1 %  
Internet Source

---

130 www.pinterest.com.mx <1 %  
Internet Source

---

131 www.researchgate.net <1 %  
Internet Source

---

132 A. M. de Vroome, A. R. Valente Pais, D. M. <1 %  
Pool, M. M. van Paassen, M. Mulder.  
"Identification of Motion Perception  
Thresholds in Active Control Tasks", AIAA

# Modeling and Simulation Technologies Conference, 2009

Publication

---

- 133 A. V. Anisovich, V. Kleber, E. Klempert, V. A. Nikonov, A. V. Sarantsev, U. Thoma. "Baryon resonances and polarization transfer in hyperon photoproduction", *The European Physical Journal A*, 2007 <1 %
- Publication
- 
- 134 Capustiac, Alina(Banabic, Dorel, Berce Petru, Kowalczyk, Wojciech, Schramm, Dieter and Staicu Stefan). "Development and application of smart actuation methods for vehicle simulators", DuEPublico: University of Duisburg-Essen Publications Online, 2013. <1 %
- Publication
- 
- 135 Carlo Gualtieri, Dragutin T. Mihailovic. "Fluid Mechanics of Environmental Interfaces", Taylor & Francis, 2018 <1 %
- Publication
- 
- 136 Charles S. Hynes, James A. Franklin, Gordon H. J. Hardy, James L. Martin, Robert C. Innis. "Flight evaluation of pursuit displays for precision approach of powered-lift aircraft", *Journal of Guidance, Control, and Dynamics*, 1989 <1 %
- Publication
-

- 137 Christian Reschke. "Flight Loads Analysis with Inertially Coupled Equations of Motion", AIAA Atmospheric Flight Mechanics Conference and Exhibit, 2005 <1 %  
Publication
- 
- 138 Clayton T. Crowe, Clayton T. Crowe. "Multiphase Flow Handbook", CRC Press, 2019 <1 %  
Publication
- 
- 139 D. M. Pool, P. M. T. Zaal, M. M. van Paassen, M. Mulder. "Effects of Heave Washout Settings in Aircraft Pitch Disturbance Rejection", Journal of Guidance, Control, and Dynamics, 2010 <1 %  
Publication
- 
- 140 Hugo Zolner, Daan Pool, Herman Damveld, Marinus van Paassen, Max Mulder. "The Effects of Controlled Element Break Frequency on Pilot Dynamics During Compensatory Target-Following", AIAA Modeling and Simulation Technologies Conference, 2010 <1 %  
Publication
- 
- 141 Johannes Edelmann, Manfred Plöchl, Peter E. Pfeffer. "Advanced Vehicle Control AVEC'16", CRC Press, 2016 <1 %  
Publication
-

- 142 Kiyotaka Kimura, Yuki Tamatsukuri, Hideaki Shishido, Hidetomo Kobayashi et al. " P-6: 2731ppi OLED Display with Low Power Consumption and Wide Viewing Angle Using OS/Si VLSI Process Technology ", SID Symposium Digest of Technical Papers, 2022 <1 %  
Publication
- 
- 143 Kristen Grinyer, Robert J. Teather. "Effects of Field of View on Dynamic Out-of-View Target Search in Virtual Reality", 2022 IEEE Conference on Virtual Reality and 3D User Interfaces (VR), 2022 <1 %  
Publication
- 
- 144 Manfred Ploechl. "Road and Off-Road Vehicle System Dynamics Handbook", CRC Press, 2014 <1 %  
Publication
- 
- 145 Peter Grant, Jeffery Schroeder. "Modeling Pilot Control Behaviorfor Flight Simulator Design and Assessment", AIAA Modeling and Simulation Technologies Conference, 2010 <1 %  
Publication
- 
- 146 Qiushi Zhou, Difeng Yu, Martin N. Reinoso, Joshua Newn, Jorge Goncalves, Eduardo Velloso. "Eyes-free Target Acquisition During Walking in Immersive Mixed Reality", IEEE Transactions on Visualization and Computer Graphics, 2020 <1 %

- 
- 147 R. LANCRAFT, G. ZACHARIAS, S. BARON. <1 %  
"Pilot/vehicle model analysis of visual and motion cue requirements in flight simulation", Flight Simulation Technologies Conference, 1981
- Publication
- 
- 148 Sjoerd Breur, Daan Pool, Marinus van Paassen, Max Mulder. "Effects of Displayed Error Scaling in Compensatory Roll-Axis Tracking Tasks", AIAA Modeling and Simulation Technologies Conference, 2010 <1 %
- Publication
- 
- 149 Soňa Molčíková, Viera Hurčíková, Peter Blišťan. "Advances and Trends in Geodesy, Cartography and Geoinformatics II", CRC Press, 2020 <1 %
- Publication
- 
- 150 Yves Chauvin, David E. Rumelhart. "Backpropagation - Theory, Architectures, and Applications", Psychology Press, 2013 <1 %
- Publication
- 
- 151 Zaal, Peter M. T., Frank M. Nieuwenhuizen, Marinus M. van Paassen, and Max Mulder. "Modeling Human Control of Self-Motion Direction With Optic Flow and Vestibular Motion", IEEE Transactions on Systems Man and Cybernetics Part B (Cybernetics), 2012. <1 %

152	Zhiyun Shen. "The Dynamics of Vehicles on Roads and on Tracks", CRC Press, 2021	<1 %
153	api.crossref.org	<1 %
154	aristotel-project.eu	<1 %
155	digitalscholarship.unlv.edu	<1 %
156	elibrary.kaznu.kz	<1 %
157	escholarship.mcgill.ca	<1 %
158	escholarship.org	<1 %
159	etda.libraries.psu.edu	<1 %
160	folk.ntnu.no	<1 %
161	kipdf.com	<1 %
162	mafiadoc.com	<1 %

163	onlinebooks.library.upenn.edu	<1 %
Internet Source		
164	pdfcookie.com	<1 %
Internet Source		
165	plato.ea.ugent.be	<1 %
Internet Source		
166	pt.scribd.com	<1 %
Internet Source		
167	rafael-ayala.r-universe.dev	<1 %
Internet Source		
168	schematicsforfree.com	<1 %
Internet Source		
169	theses.eurasip.org	<1 %
Internet Source		
170	uavbook.byu.edu	<1 %
Internet Source		
171	uwspace.uwaterloo.ca	<1 %
Internet Source		
172	vigir.missouri.edu	<1 %
Internet Source		
173	worldwidescience.org	<1 %
Internet Source		
174	www.kyb.tuebingen.mpg.de	<1 %
Internet Source		

- 175 D. M. Pool, M. Mulder, M. M. Van Paassen, J. C. Van Der Vaart. "Effects of Peripheral Visual and Physical Motion Cues in Roll-Axis Tracking Tasks", Journal of Guidance, Control, and Dynamics, 2008 <1 %
- Publication
- 
- 176 Herman Damveld, David Abbink, Mark Mulder, Max Mulder, Marinus van Paassen, Frans van der Helm, Ruud Hosman. "Measuring the Contribution of the Neuromuscular System During a Pitch Control Task", AIAA Modeling and Simulation Technologies Conference, 2009 <1 %
- Publication
- 
- 177 Honglei Ji, Linghai Lu, Mark D. White, Renliang Chen. "Advanced Pilot Modeling for Prediction of Rotorcraft Handling Qualities in Turbulent Wind", Aerospace Science and Technology, 2022 <1 %
- Publication
- 
- 178 Linda Daniela. "New Perspectives on Virtual and Augmented Reality - Finding New Ways to Teach in a Transformed Learning Environment", Routledge, 2020 <1 %
- Publication
- 
- 179 Mark S. Young, Michael G. Lenné. "Simulators for Transportation Human Factors - Research and Practice", Routledge, 2017 <1 %

- 180 Mulder, Max, and M Paassen. "Identification of Human Control Behavior", International Encyclopedia of Ergonomics and Human Factors Second Edition - 3 Volume Set, 2006. <1 %
- Publication
- 
- 181 R A Hess. "Simplified approach for modelling pilot pursuit control behaviour in multi-loop flight control tasks", Proceedings of the Institution of Mechanical Engineers Part G Journal of Aerospace Engineering, 04/01/2006 <1 %
- Publication
- 
- 182 Vincent A. Laurensen, Daan M. Pool, Herman J. Damveld, Marinus Rene M. van Paassen, Max Mulder. "Effects of Controlled Element Dynamics on Human Feedforward Behavior in Ramp-Tracking Tasks", IEEE Transactions on Cybernetics, 2015 <1 %
- Publication
- 
- 183 William S. Levine. "Control System Applications", CRC Press, 2018 <1 %
- Publication
- 
- 184 research-information.bris.ac.uk <1 %
- Internet Source
- 
- 185 "Engineering Psychology and Cognitive Ergonomics", Springer Science and Business Media LLC, 2023 <1 %
- Publication
-

- 186 C. Venkatesan. "Fundamentals of Helicopter Dynamics", CRC Press, 2019 <1 %  
Publication
- 
- 187 G. C. Beerens, H. J. Damveld, M. Mulder, M. M. Van Paassen, J. C. Van Der Vaart. "Investigation into Crossover Regression in Compensatory Manual Tracking Tasks", Journal of Guidance, Control, and Dynamics, 2009 <1 %  
Publication
- 
- 188 Jitendra R. Raol, Ajith K. Gopal. "Mobile Intelligent Autonomous Systems", CRC Press, 2016 <1 %  
Publication
- 
- 189 K. Kong Wan. "Quantum Mechanics - A Fundamental Approach", CRC Press, 2019 <1 %  
Publication
- 
- 190 Marisa K Heckner, Edna C Cieslik, Kaustubh R Patil, Martin Gell, Simon B Eickhoff, Felix Hoffstädter, Robert Langner. "Predicting executive functioning from functional brain connectivity: network specificity and age effects", Cerebral Cortex, 2023 <1 %  
Publication
- 
- 191 P. M. T. Zaal, D. M. Pool, M. Mulder, M. M. Van Paassen. "Multimodal Pilot Control Behavior in Combined Target-Following Disturbance- <1 %

## Rejection Tasks", Journal of Guidance, Control, and Dynamics, 2009

Publication

- 
- 192 P. M. T. Zaal, D. M. Pool, Q. P. Chu, M. M. Van Paassen, M. Mulder, J. A. Mulder. "Modeling Human Multimodal Perception and Control Using Genetic Maximum Likelihood Estimation", Journal of Guidance, Control, and Dynamics, 2009 <1 %

Publication

- 
- 193 S. Konishi, J. Chikazoe, K. Jimura, T. Asari, Y. Miyashita. "Neural mechanism in anterior prefrontal cortex for inhibition of prolonged set interference", Proceedings of the National Academy of Sciences, 2005 <1 %

Publication

- 
- 194 Shuting Xu, Wenqian Tan, Alexander V. Efremov, Liguo Sun, Xiangju Qu. "Review of control models for human pilot behavior", Annual Reviews in Control, 2017 <1 %

Publication

---

Exclude quotes Off  
Exclude bibliography Off

Exclude matches Off